Contemporary Conflicts and Crises

A mathematical approach

Brethouwer, J.F.

DOI
10.4233/uuid:617757b7-32d2-4bac-8be3-5a6a13e6e710

Publication date
2024

Document Version
Final published version

Citation (APA)
Brethouwer, J. F. (2024). *Contemporary Conflicts and Crises: A mathematical approach*. [Dissertation (TU Delft), Delft University of Technology]. https://doi.org/10.4233/uuid:617757b7-32d2-4bac-8be3-5a6a13e6e710

CONTEMPORARY CONFLICTS AND CRISES

A MATHEMATICAL APPROACH

CONTEMPORARY CONFLICTS AND CRISES

A MATHEMATICAL APPROACH

Dissertation

for the purpose of obtaining the degree of doctor
at Delft University of Technology
by the authority of the Rector Magnificus, prof. dr. ir. T.H.J.J. van der Hagen,
chair of the Board for Doctorates
to be defended publicly on
Tuesday 25 June 2024 at 15:00 o'clock

by

Jan-Tino Fier BRETHOUWER

Master of Science in Applied Mathematics, Universiteit Twente, The Netherlands,
born in Deventer, The Netherlands

This dissertation has been approved by the promotors.

Composition of the doctoral committee:

Rector Magnificus	Chairperson
Prof. dr. F.H.J. Redig	Delft University of Technology, *promotor*
Prof. dr. ir. R.H.A. Lindelauf	Tilburg University, *promotor*
Dr. ir. R.J. Fokkink	Delft University of Technology, *copromotor*
Independent members:	
Dr. C. Kraaikamp	Delft University of Technology
Prof. dr. H.M. Schuttelaars	Delft University of Technology
Prof. dr. H. Monsuur	Nederlandse Defensie Academie
Prof. dr. M. Postma	Tilburg University
Prof. dr. ir. M.B. van Gijzen	Delft University of Technology, reserve member

The research in this dissertation was funded by the Dutch Ministry of Defence.

Printed by: Gildeprint

Cover by: Anouk Heitink | another view

ISBN 978-94-6496-144-7

An electronic copy of this dissertation is available at
https://repository.tudelft.nl/.

An innocent looking problem often gives no hint as to its true nature. It might be like a marshmallow, serving as a tasty tidbit supplying a few moments of fleeting enjoyment. Or it might be like an acorn, requiring deep and subtle new insights from which a mighty oak can develop.

Paul Erdős

CONTENTS

SUMMARY

In this thesis, we use mathematical models to assist the Dutch Ministry of Defence with understanding and decision-making within contemporary conflicts and crises. We explore ways to reduce the spread of COVID-19, study dynamics in the Sino-Indian border dispute, and investigate the value of scouting in conflicts involving autonomous systems.

The first two chapters of this thesis are introductory. In Chapter 1, we discuss how this thesis came to be and provide a comprehensive overview of its contents. In Chapter 2, we introduce concepts and tools from game theory, network science and uniform distribution theory, fundamental to subsequent chapters in this thesis. Specifically, we discuss the concept of discrepancy, necessary for Chapter 3, introduce small-world models, applied in Chapter 4, and present concepts from game theory, which we use in Chapters 5, 6 and 7.

Part I of the thesis involves mathematical sociology, applied to reduce the spread of COVID-19. In Chapter 3, we study the distribution of points on a circle, with the aim of maximizing the minimum distance between them. We delve into previous work and introduce an novel adaptation to finite sequences, for which we provide an optimal solution. This work has applications in optimizing social distancing. Chapter 4 focuses on modeling the spread of the COVID-19 pandemic using network science. We show that some specific social contacts are especially dangerous for virus spread. Our analysis supports strategies aimed at reducing these high-risk social interactions, thereby allowing for increased social contacts per person while still reducing the spread of the virus.

Part II of this thesis involves the application of game theory to contemporary conflicts. In Chapter 5, we study the value of manpower versus intelligence, as seen in the Russo-Ukrainian War. To model this dynamic, we introduce General Lotto games with scouts, an adaptation of the well established General Lotto game. We provide optimal solutions for this game, which leads to interesting insights about the value of manpower versus intelligence. In Chapter 6, we study the Sino-Indian Border conflict. We examine the trends of the last 15 years, and show they are not random. We use game theory to provide a possible explanation for the observed behaviour. In Chapter 7 we study search games on a partially ordered set.

SAMENVATTING

In dit proefschrift gebruiken we wiskundige modellen om Defensie te ondersteunen met het begrijpen en het nemen van beslissingen in hedendaagse conflicten en crises. We onderzoeken manieren om de verspreiding van COVID-19 te vertragen, bestuderen de dynamiek in het grensgeschil tussen China en India, en onderzoeken de waarde van verkenning in conflicten met autonome systemen.

De eerste twee hoofdstukken van dit proefschrift zijn inleidend. In Hoofdstuk 1 bespreken we hoe dit proefschrift tot stand is gekomen en geven we een uitgebreider overzicht van de inhoud. In Hoofdstuk 2 introduceren we concepten en andere hulpmiddelen uit speltheorie, netwerkwetenschap en uniforme verdelingstheorie, die gebruikt worden in de daaropvolgende hoofdstukken van dit proefschrift. We introduceren discrepantie, noodzakelijk voor Hoofdstuk 3, small-world modellen, toegepast in Hoofdstuk 4, en concepten uit speltheorie, die worden gebruikt in Hoofdstuk 5, 6 en 7.

In deel I van dit proefschrift wordt wiskundige sociologie toegepast om de verspreiding van COVID-19 te vertragen. In Hoofdstuk 3 bestuderen we de verdeling van punten op een cirkel, met als doel de minimale afstand tussen een paar punten te maximaliseren. We beschrijven eerder werk voor dit probleem en introduceren een extensie naar eindige rijen, waarvoor we de optimale oplossing vinden. Dit werk heeft toepassingen bij het optimaliseren van social distancing. Hoofdstuk 4 richt zich op het modelleren van de verspreiding van de COVID-19-pandemie met behulp van netwerk science. We tonen aan dat bepaalde sociale connecties veel meer invloed hebben op de verspreiding van het virus dan gemiddeld. Onze analyse ondersteunt strategieën gericht op het verminderen van deze hoogrisico-sociale interacties, waardoor er meer sociale connecties per persoon mogelijk zijn, terwijl de verspreiding van het virus nog steeds wordt afgeremd.

Deel II van dit proefschrift bevat de hoofdstukken waar speltheorie wordt toegepast op hedendaagse conflicten. Hoofdstuk 5 bestuderen we de waarde van mankracht versus intelligentie, zoals te zien is in de Russisch-Oekraïense oorlog. Om deze dynamiek te modelleren, introduceren we General Lotto games with scouts, een extensie van het gevestigde General Lotto spel. We vinden de optimale oplossingen van dit spel, en halen daaruit interessante inzichten over de waarde van mankracht versus intelligentie. In Hoofdstuk 6 bestuderen we het grensgeschil tussen China en India. We onderzoeken de trends van de laatste 15 jaar en tonen aan dat ze niet willekeurig zijn. We gebruiken speltheorie om een mogelijke verklaring te bieden voor het waargenomen gedrag. In Hoofdstuk 7 bestuderen we zoekspellen op een deels geordende verzameling.

1

INTRODUCTION

In this thesis, we use mathematical models to assist defence with understanding and decision-making in contemporary conflicts and crises. We explore ways to reduce the spread of COVID-19, study dynamics in the Sino-Indian border dispute, and investigate the value of scouting in conflicts involving autonomous systems. In this introductory chapter, we explain how these projects started, what mathematical models we use to solve them, and how this thesis is organized.

My PhD project is a collaboration between the Delft University of Technology and the Dutch Ministry of Defence. In the world of defence and safety, one often faces the challenge of optimizing the use of limited resources. This requires smart decision-making, and this is where mathematicians can provide invaluable support. However, there is frequently a gap between theory and practice, with those tackling real-world challenges unaware of the potential assistance mathematicians can provide, and vice versa. My PhD was established with the goal of bringing these two worlds together. The initial aim was to talk to subject-matter experts within defence, about different challenges and identify relevant mathematical models to apply to these challenges. While we did find projects this way, the unforeseen arrival of the COVID-19 pandemic caused my PhD to take a different turn.

The emergence of the COVID-19 introduced both challenges and opportunities. The existence of a pandemic made it difficult to engage with subject-matter experts, shut down large parts of society and required all work to be done at home. Being a fresh PhD student in a new city, this was quite challenging. However, COVID-19 itself also turned out to be an interesting research opportunity. The world was not prepared for a pandemic of this size, and there was an urgent need for government policy to contain the outbreak. We decided that we would do our part, and used mathematical models to determine how the spread of COVID-19 could be reduced. In the meanwhile, tensions kept rising between the West and China, as well as between the West and Russia, especially following the Russian invasion of Ukraine.

The work I did during my PhD can be divided into two parts: Work on

reducing the spread of COVID-19, and work using Game theory in contemporary conflicts. We have studied reducing the spread of COVID-19 in two different ways. Firstly, on an individual level, through ways to improve social distancing. Secondly, on a group level, using social network models to study the impact of government policies on the spread of the disease.

Part I of the thesis involves mathematical sociology. In a social experiment that was carried out in 2021, we examined social distancing in a very practical situation: a number of people enter a room, and take a seat at a round table. They don't know how many people will enter the room. Where should you take a seat to maximize social distancing? A general version of this problem is known as the stick-breaking problem. What happens if the number of people entering the room has a known maximum? The results of this experiment are reported in [1], while a broader mathematical study is presented in [2].

Furthermore, we applied a mathematical model of the spread of an infectious disease, to study the COVID-19 Pandemic on a group level. To tackle the spreading virus, people everywhere around the world had to minimize social contacts and practice social distancing. However, some social contacts might be more dangerous than others. We used simulations based on open source data and small-world models to test the effectiveness of different strategies for reducing virus spread, and published our paper [3]. This work eventually led us to compete in the COVID-19 prediction challenge, a challenge in which researchers could use a prediction model to predict the number of COVID-19 deaths. We participated in the USA category, in which our model outperformed all other participants. The challenge organisers have written a paper about the challenge and its results, of which we are co-author [4].

Part II of this thesis involves the application of game theory to contemporary conflicts. Game theory is a branch of mathematics which studies cooperation or conflict between rational decision makers. It involves the analysis of various models and scenarios to understand how players make decisions and how their choices affect the overall outcome of the game. The applications of game theory are diverse and can be found in various fields, including economics, psychology and political science. It has also been used to study many aspects of conflict and crises, from very specific situations during World War II, to broad concepts, such as the dynamics of the nuclear arms race during the Cold War.

As time has progressed, both conflicts and their associated research have evolved. For instance, the increased availability of open-source data provides new opportunities for analysis, while the use of unmanned drones can influence the dynamics of a conflict. While the game theory models developed in the past can offer valuable insights into these new conflicts, they must be adapted to suit the new situations. The aim of this research is to use game theory to help understand certain dynamics in the problems we face today.

During my PhD, we met with several subject-matter experts, to discuss if they had challenges we could tackle with Game Theory. In this thesis, we study two projects which use game theory on contemporary conflicts. Our first project followed from conversations with the Robotic Autonomous Systems (RAS) unit within the Royal Netherlands Army. They had a specific scenario, where an army unit consisting of several autonomous systems had to retake a river area with several bridges from the opposing forces. The question is: how should the troops be divided over the different bridges for the best results? Furthermore, if they could send out some scouting drones to gain some information about the distribution of the opposing troops, how would that change the problem? How valuable is this information gained by the scouts? What is the optimal mix of scouting drones and units providing firepower, for a given budget? We use game theory to find answers to these questions. The main result of this work appears in [5].

Figure 1.1.: THeMIS unmanned ground vehicles, part of the RAS unit

The second project is focused on the Sino-Indian border. This work was done together with researchers at Northwestern University, Chicago. The Sino-Indian border conflict is an ongoing conflict between China and India. Both countries disagree where their border should be, which leads to regular flare-ups of violence along the border. Many of these incidents are reported in newspapers, from which we assembled a data set about border incursions from China into India of the last 15 years. We study this new set of data using game theory models, to see if the incursions are random, or if they follow underlying mechanisms [6].

We conclude this thesis with our work on search and rescue games on a partially ordered set. A search and rescue game is a new type of game on a graph that has quickly found applications in scheduling, object detection, and adaptive search. In our research, we broaden the definition of search and rescue games by imposing a partial order on the search. This ordering means that if location A appears before location B in the imposed order, then A can no longer be searched after B has been searched. We extend known solutions of these games and pave the way to further applications. [7]

REFERENCES CHAPTER 1

[1] A. Buijsrogge, R. Lindelauf, A. van de Rijt, and J.-T. Brethouwer. “Self-Organized Social Distancing”. In: *Submitted to the Journal of Mathematical Sociology* (2023).

[2] J.-T. Brethouwer, A. Buijsrogge, and R. Fokkink. “On an equidistribution problem of De Bruijn and Erdős”. In: *Paper in preparation* (2024).

[3] J.-T. Brethouwer, A. van de Rijt, R. Lindelauf, and R. Fokkink. ““Stay nearby or get checked”: A Covid-19 control strategy”. In: *Infectious Disease Modelling* 6 (2021), pp. 36–45.

[4] M. A. Golden, T. Slough, H. Zhai, A. Scacco, M. Humphreys, E. Vivalt, A. Diaz-Cayeros, K. Y. Dionne, S. KC, E. Nazrullaeva, P. M. Aronow, J.-T. Brethouwer, A. Buijsrogge, J. Burnett, S. DeMora, J. R. Enríquez, R. Fokkink, C. Fu, N. Haas, S. V. Hayes, H. Hilbig, W. R. Hobbs, D. Honig, M. Kavanagh, R. H. A. Lindelauf, N. McMurry, J. L. Merolla, A. Robinson, J. S. Solís Arce, M. ten Thij, F. F. Türkmen, and S. Utych. “Gathering, Evaluating, and Aggregating Social Scientific Models”. In: *Available at SSRN 4570855, submitted to Political Analysis* (2023).

[5] J.-T. Brethouwer, B. Van Ginkel, and R. Lindelauf. “General Lotto Games with Scouts: Information versus Strength”. In: *preprint, arXiv:2404.05841, submitted to Dynamic Games and Applications* (2024).

[6] J.-T. Brethouwer, R. Fokkink, K. Greene, R. Lindelauf, C. Tornquist, and V. Subrahmanian. “Rising tension in the Himalayas: A geospatial analysis of Chinese border incursions into India”. In: *PloS one* 17.11 (2022), e0274999.

[7] J.-T. Brethouwer and R. Fokkink. “Search and Rescue on a Poset”. In: *preprint, arXiv:2312.06622, submitted to Naval Research Logistics* (2023).

2

MATHEMATICAL BACKGROUND

In this chapter, we establish the mathematical foundation for subsequent chapters. Each subsection starts with a specific mathematical problem. We delve into the historical context of the problem, as well as the mathematical tools necessary to solve it. For those readers already familiar with both the problem and its solution methodology, the subsection may be safely skipped.

2.1. DISCREPANCY OF A SEQUENCE

This section provides an introduction to mathematics used in Chapter 3.

> Say you want to distribute n points as equal as possible over a circle. For a given n, the optimal solution is trivial, simply divide the circle into n intervals of equal size, and place all your points at the endpoints of the intervals. However, what if you want to add the points one by one, and want to have all points to be relatively equally distributed at every step?

In 1935 J.G. van der Corput [8] asked himself this question. This problem turned out to be complicated and marked the beginning of the research field of uniform distribution theory [9]. In this section, we provide a brief introduction to uniform distribution theory and its history. We provide the definitions of discrepancy, the big O notation and the van der Corput sequence. For a more extensive description concerning discrepancy and the work of van der Corput, we refer to Tijdeman [10] and Faure, Kritzer en Pillichshammer [11].

As mentioned in the original problem, points are perfectly distributed if all intervals between two adjacent points are equal. It is easy to see from Figure 2.1 alone that achieving perfect distribution at every step is impossible. Specifically, this figure demonstrates that when perfect distribution is obtained after four points have been placed, the points cannot have been perfectly distributed when only the first three points have been placed. So while perfect is not possible, van der Corput wondered what the most equal distributed sequence possible would be. He proposed the following conjecture [12], which we explain more afterwards:

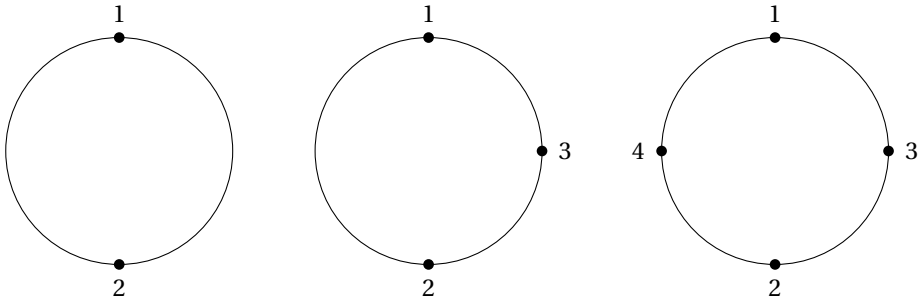

(a) After placing 2 points (b) After placing 3 points (c) After placing 4 points

Figure 2.1.: An example of placing 4 points on a circle. The points are perfectly distributed over the circle when 2 points are placed and when 4 points are placed, but are not when 3 points are placed.

Conjecture 2.1 (van der Corput, 1935)**.** *"If $w = w_1, w_2, \ldots$ is an infinite sequence of real numbers lying between 0 and 1, then corresponding to any arbitrarily large constant K, there exist a positive integer N and two subintervals, of equal length, of the interval $[0,1)$, such that the number of w_n with $n = 1,2,\ldots,N$ that lie in one of the subintervals differs from the number of such w_n that lie in the other subinterval by more than K."*

Firstly, notice that this conjecture concerns the interval $[0,1)$ instead of the circle. We can map the circle to the interval $[0,1)$ by connecting the start and end of the interval $[0,1)$, as shown in Figure 2.2a.

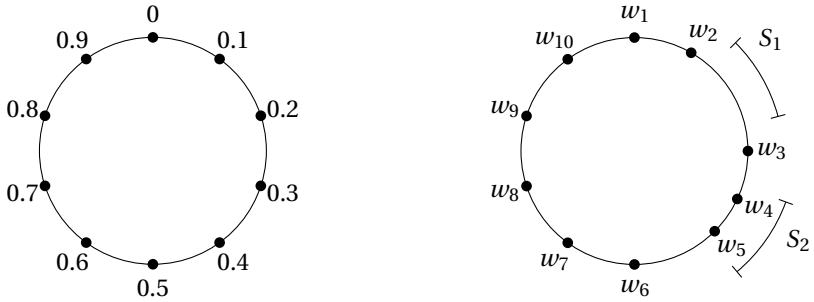

(a) Mapping the interval $[0,1)$ to a circle. (b) Two subintervals of equal length, S_1 and S_2.

Figure 2.2.: Left: How to map the circle to the interval $[0,1)$. Right: Two subintervals S_1 and S_2, after 10 points of a sequence w have been placed. The first subinterval contains no points, while the second subinterval contains two points.

In his conjecture, van der Corput compares the number of points in any two

subintervals of equal size. An example is given in Figure 2.2b, where one interval has no points, and the other interval has two points, so in this example the difference is two. The claim of the conjecture is that this difference cannot be bounded by any constant for any sequence.

To further describe this claim, we introduce the notion of *discrepancy*.

Definition 2.2 (Discrepancy)**.** *Let $N \in \mathbb{N}$. For a sequence $w = w_1, w_2, \ldots$, its discrepancy $D_N(w)$ is defined as:*

$$D_N(w) := \sup_{0 \le \alpha < \beta \le 1} \left| \frac{A_N([\alpha, \beta))}{N} - (\beta - \alpha) \right|,$$

where $A_N([\alpha, \beta))$ is the number of points w_n with $n \le N$ and $0 \le \alpha \le w_n < \beta \le 1$.

A sequence is called *equidistributed* or *uniformly distributed* if its discrepancy tends to zero for N to infinity, i.e.,

$$\lim_{N \to \infty} D_N(w) = 0.$$

This means that every subinterval of $[0,1)$ in the limit contains the fraction of the points equal to the length of the subinterval. For example, any subinterval of length 0.2 must contain 20% of all points.

We recall the following notions from asymptotic analysis:

Definition 2.3 (Big O notation)**.** *For a given function $f(x)$, we say that $g(x)$ is $O(f(x))$, denoted as $g(x) = O(f(x))$, if and only if there exist positive constants c and x_0 such that*

$$|g(x)| \le c|f(x)|$$

for all $x \ge x_0$.

Big O belongs to a set of notations collectively known as the Bachmann–Landau notation, named after the German mathematicians Paul Bachmann and Edmund Landau. Other members of this notation used in this thesis include Big Omega and Big Theta:

Definition 2.4 (Big Omega notation)**.** *For a given function $f(x)$, we say that $g(x)$ is $\Omega(f(x))$, denoted as $g(x) = \Omega(f(x))$, if and only if there exist positive constants c and x_0 such that*

$$c|f(x)| \le |g(x)|$$

for all $x \ge x_0$.

Definition 2.5 (Big Theta notation)**.** *For a given function $f(x)$, we say that $g(x)$ is $\Theta(f(x))$, denoted as $g(x) = \Theta(f(x))$, if and only if there exist positive constants c_1, c_2, and x_0 such that*

$$c_1|f(x)| \le |g(x)| \le c_2|f(x)|$$

for all $x \ge x_0$.

With the definition of discrepancy, we can restate the conjecture of van der Corput. His conjecture is equivalent to stating that

$$N \cdot D_N(w) > K, \qquad \text{for infinitely many } N$$

for any constant K, or saying $D_N(w)$ is $\Omega(\frac{1}{N})$. This conjecture turned out to be quite difficult. It would eventually be proven by Mrs van Aardenne-Ehrenfest in 1945 [13]. However, there was still a gap between the best known sequence, and the lower bound, so research continued. In 1949, van Aardenne-Ehrenfest [14] improved her result, demonstrating that

$$N \cdot D_N(w) > C \frac{\log\log N}{\log\log\log N}.$$

This result was even further improved by Roth in 1954 [12], who showed that

$$N \cdot D_N(w) > \sqrt{C \log N}.$$

Finally, in 1972, Schmidt [15] proved that

$$N \cdot D_N(w) > C \log N, \tag{2.1}$$

which matches the order of magnitude of the best known sequence. The only unknown remains the constant. Some bounds have been found, but its exact value remains an open problem.

THE VAN DER CORPUT SEQUENCE

In his 1935 paper, van der Corput also introduced a low discrepancy sequence. It is nowadays called the *van der Corput sequence (vdC-sequence)*. It is made by writing numbers down in their binary form, and then mirroring their bits around the comma.

Definition 2.6 (van der Corput sequence)**.** *Let n be any positive integer and let L be the non-negative integer such that $2^L \leq n < 2^{L+1}$. The binary representation of n is*

$$n = \sum_{k=0}^{L} d_k(n) 2^k = d_0(n)2^0 + d_1(n)2^1 + \cdots + d_L(n)2^L,$$

where $d_k(n)$ is either 1 or 0. Then the n-th number of the vdC-sequence is:

$$S_{vdC}(n) = \sum_{k=0}^{L} d_k(n) 2^{-1-k} = d_0(n)2^{-1} + d_1(n)2^{-2} + \cdots + d_L(n)2^{-L-1}.$$

As an example, take n=13. In binary notation, 13 is written as 1101, which becomes 0,1011 if mirrored around the comma. This translates back to $\frac{1}{2} + \frac{1}{8} + \frac{1}{16} = \frac{11}{16}$. Thus, the 13th number of the vdC-sequence is $\frac{11}{16}$. The first few numbers of the vdC-sequence are:

$$\frac{1}{2}, \frac{1}{4}, \frac{3}{4}, \frac{1}{8}, \frac{5}{8}, \frac{3}{8}, \frac{7}{8}, \frac{1}{16}, \frac{9}{16}, \frac{5}{16}, \frac{13}{16}, \frac{3}{16}, \frac{11}{16}, \frac{7}{16}, \frac{15}{16}, \frac{1}{32}, \cdots$$

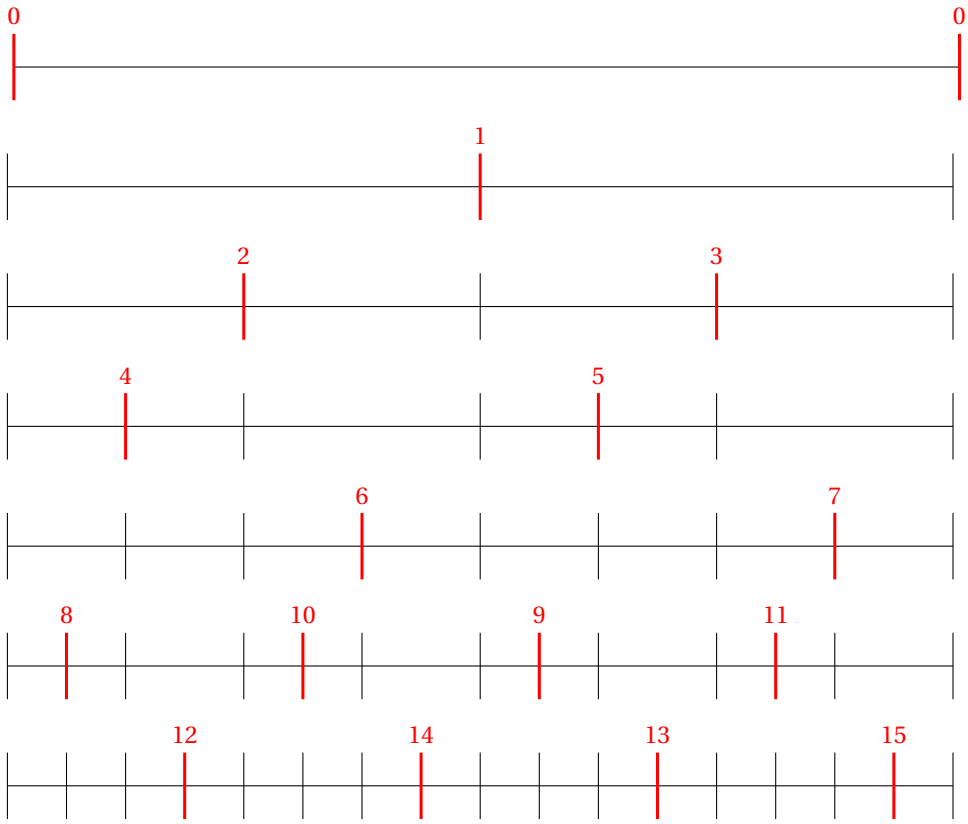

Figure 2.3.: The points of the vdC-sequence.

In Figure 2.3 the first few terms of the vdC-sequence are illustrated.

Van der Corput provided the first bound on the discrepancy of the vdC-sequence in his 1935 paper:

$$N \cdot D_N(w) \leq 1 + \frac{\log N}{\log 2}, \qquad \forall N > 2.$$

If we compare this with the result of Schmidt [15] in Equation (2.1), we see that this bound was already optimal in order of magnitude. Over time, there have been several improvements of this upper bound, often with (variants of) the vdC-sequence. Nowadays, the best known bounds are [16]:

$$D_N^*(w) \geq c_\infty \frac{\log N}{N} \qquad \text{for infinitely many } N,$$

where $0.121128\cdots < c_\infty < 0.353494\ldots$.

The vdC-sequence also has several interesting properties, such as that at every step, the intervals between points only have at maximum 2 different sizes. vdC-sequences are important for Monte Carlo methods [11]. Specifically, if many random samples are taken, it is important that every area is tested relatively equally often. This can be quite a challenge in higher dimensional spaces.

2.2. SMALL WORLD NETWORKS

This section provides an introduction to mathematics used in Chapter 4.

> In 1967, Stanley Milgram sent letters to random addresses in east USA. They were accompanied by instructions to send these letters to a target person in west USA. The information of this target person was limited to his full name and the city he lived in. If the recipient of the letter knew the target person, they were to forward the letter to him directly. If they did not know the target person, they were to forward the letter to someone who they believed had a better chance of knowing the target person. How many steps would it take before the letters reach the target person?

The experiment, now known as the "small-world experiment", was predicated on the idea that even in a vast and seemingly disconnected society, individuals could be linked through a surprisingly small number of intermediaries. As the letters traversed the expanse from the east to the west, they highlighted the concept of "degrees of separation", signifying the number of connections it would take to bridge the geographic and social gap between any two people. Milgram's experiment revealed that, on average, it took approximately six intermediaries for the letter to reach the target person. This was the basis of the "six degrees of separation" hypothesis, the idea that all people are six or fewer social connections away from each other.

In 1998, Watts and Strogatz [17] noted that small world models could be classified based on two key characteristics, namely the clustering coefficient, and average node-to-node distance. The clustering coefficient measures the degree to which nodes in a network tend to cluster together, forming tightly-knit groups. Watts and Strogatz provided an algorithm to create small world networks. Their model is now known as the Watts–Strogatz model.
The algorithm works as follows:

- First, you decide on a number of nodes N, an average degree k and a clustering coefficient $0 < p < 1$.
- Secondly, create a regular ring lattice, a graph with N nodes each connected to K neighbours
- Finally, for every edge (i, j) with $i < j$, rewire it with probability p to the edge (i, k). Here k is chosen randomly, under the condition that the (i, k) is not already present.

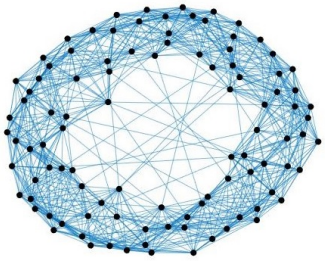

Figure 2.4.: An example of a Watts-Strogatz small-world graph with $N = 100$ nodes, each with degree $k = 20$ and clustering coefficient $p = 0.05$.

The clustering coefficient p determines how often edges get rewired. for $p = 0$, the graph remains a regular ring lattice. For large p, the graph resembles a random graph.

2.3. FINITE CONSTANT-SUM GAMES

This section provides an introduction to mathematics used in Chapters 5 and 6.

> Colonel Blotto commands four soldiers, with which to oppose an enemy Colonel with four soldiers. There are three battlefields on which the battle will take place in the morning. Whoever sends more soldiers to a battlefield wins that battlefield, and both Colonels want to win as many battlefields as possible. How should Blotto divide his troops over the battlefields?

This problem was first described by Borel in 1921, in this paper "The Theory of Play and Integral Equations with Skew Symmetric Kernels" [18]. At that time, the field of Game Theory had not yet been established, and in this paper Borel presented his ideas on how a game between two players could be mathematically modelled. The Colonel Blotto game was introduced in this paper as an example game, although it did not have this name yet. The game received the name “Colonel Blotto” and the accompanying backstory in 1924, when it appeared in The Weekend Puzzle Book by Caliban. In this section, we demonstrate how to solve this game while introducing some notions from Game Theory.

In his paper, Borel also described what a solution to this game would look like. First, he requires both players to choose a "method of play", nowadays known as a *strategy*. A strategy defines what decision a player takes for every possible situation throughout the game. In the Colonel Blotto game, there is only one decision to take, which is how to divide the soldiers over the battlefields. But in other games, there might be many different decisions to take. For example, in chess, a strategy would consist of a defined move for any possible state of the board. For any

combination of two strategies, one for each player, the payoff for each player must be defined. In the Colonel Blotto game, the payoff is measured in fields won. With any combination of two strategies, it is possible to see which player wins which battlefield, and thus calculate the payoff for each player. If both players send the same amount of soldiers to any field, then both players get half of that field.

He remarks that the game is *symmetric*, which means that both players have the same possible actions and receive the same payoffs for each combination of actions. Furthermore, the game is a *constant-sum game*, which means that all the payoff one player gets, must come as a cost to another player. The total payoff over all players must remain constant for any combination of strategies. In the Colonel Blotto game, there are three battlefields, and if a player wins one, the other player loses that field. The sum of the payoff of the players is always equal to three, the number of battlefields.

The solution to a game consists of the best possible strategies for the players. Borel states that the best strategy a player can have in a symmetric game, is a strategy that guarantees himself at least as much payoff as his opponent. In any constant-sum game, this would be half the total payoff. Better than half is not possible, since the other player can use the same strategy to guarantee themselves half. Therefore, this strategy would create an equilibrium, where both players played this strategy and can not improve by switching to other strategies. Such an equilibrium is called a *Nash Equilibrium*. In our Colonel Blotto game, the solution would be an optimal strategy that guarantees that you win 1.5 battlefields in expectation, against any possible distribution of the other player.

We can now look for the solution of the described Colonel Blotto game. In this game, there are fifteen ways a player can divide the soldiers over the battlefields. We simplify the game a bit and say the Colonels only have to divide their soldiers into three unordered groups. The groups will then be randomly assigned to different battlefields. This leaves four different strategies for both players: (4,0,0), (3,1,0), (2,2,0) and (2,1,1). We describe the payoff of the game as the expected number of battlefields that Colonel Blotto wins, in Table 2.1.

A matrix like Table 2.1, where all the strategies of the players and the payoff for every combination of strategies is described, is called the *Normal Form* of a game. Looking at this table, you might notice that if Colonel Blotto plays (2,2,0), then every possible payoff is at least 1.5. This means that both players playing (2,2,0) is a Nash equilibrium and the solution of this game.

Strategies of a player can be *pure strategies* or *mixed strategies*. The pure strategies are (4,0,0), (3,1,0), (2,2,0) and (2,1,1). A player having a pure strategy, means he chooses one of these with certainty. A mixed strategy is a probability distribution on the set of pure strategies. For instance, choosing (4,0,0) and (2,2,0) both with probability $\frac{1}{2}$. A Nash Equilibrium consisting of pure strategies, such as

		Enemy			
		(4,0,0)	(3,1,0)	(2,2,0)	(2,1,1)
Blotto	(4,0,0)	$\frac{3}{2}$	$\frac{4}{3}$	$\frac{4}{3}$	1
	(3,1,0)	$\frac{5}{3}$	$\frac{3}{2}$	$\frac{3}{2}$	$\frac{4}{3}$
	(2,2,0)	$\frac{5}{3}$	$\frac{3}{2}$	$\frac{3}{2}$	$\frac{5}{3}$
	(2,1,1)	2	$\frac{5}{3}$	$\frac{4}{3}$	$\frac{3}{2}$

Table 2.1.: The Colonel Blotto game for three fields and four soldiers on each side. The matrix describes the expected number of battlefields won by Colonel Blotto, for any chosen configuration of soldiers by Colonel Blotto and the Enemy Colonel.

we found in the Colonel Blotto game, is called a pure Nash equilibrium.

So does such a solution always exist? In his 1921 paper, Borel claims that "it is easy to see" that once a player has more than seven actions, in general no solution exists. Luckily for us, this turned out to be wrong. In 1928, von Neumann published his paper "Zur Theorie der Gesellschaftsspiele" [19], in which he proved the existence of equilibria in any finite constant-sum game, using his minimax theorem. Von Neumann's paper is widely acknowledged as the starting point of the field of Game Theory. Building upon this work, von Neumann, alongside Oskar Morgenstern, wrote the influential book "Theory of Games and Economic Behavior" in 1944 [20]. In 1951, Nash [21] extended the minimax theorem of von Neumann, by proving that mixed Nash equilibria exist in any finite game for any number of players. This is why these equilibria are now known as Nash equilibria. This work would earn Nash the Nobel Prize.

Knowing Nash equilibria exist does not necessarily make them easy to find. For finite games, the problem of finding Nash equilibria is PPAD-complete, a complexity class that is a subclass of NP [22]. When the game is also constant-sum, such as the Colonel Blotto game, it can be formulated as a linear program and therefore solved in polynomial time. However, this does not guarantee these games can be solved in a reasonable amount of time in practice. Our example game, with three fields and four soldiers, is straightforward and can be solved almost instantly. However, when the number of fields and soldiers are increased, finding Nash equilibria can quickly become computationally infeasible.

To completely solve a game, we need to find a general solution. For Colonel Blotto, that is a solution for n fields, where Blotto has B troops and the enemy Colonel has R troops. Due to the complexity of the game, such a general solution is unlikely to be found. Luckily, there exists a variant of Colonel Blotto games, which is better solvable. In his original paper, Borel introduced two versions of the Colonel Blotto game: discrete Colonel Blotto and continuous Colonel Blotto. The discrete Colonel Blotto game is the version we have studied until now, where the number of troops sent to a field has to be a non-negative integer. In the continuous Colonel Blotto game, this constraint is relaxed, and the number of troops can be any non-negative number. Contrary to the discrete version, the continuous Colonel Blotto has a known general solution.

The first solutions to the continuous Colonel Blotto game were found by Gross and Wagner in 1950 [23]. They were able to solve the game completely for two fields, for any number of troops on either side. They also provided solutions for three or more fields, under the condition that both sides have an equal number of troops. The continuous Blotto game was eventually completely solved by Roberson [24], allowing for any number of fields and asymmetric troop numbers between players. The discrete version remains a computational challenge, and algorithms to solve it keep getting refined.

REFERENCES CHAPTER 2

[8] J. v. d. Corput. "Verteilungsfunktionen i". In: *Proc. Kon. Ned. Akad. v. Wetensch.* 38 (1935), pp. 813–821.

[9] L. Kuipers and H. Niederreiter. *Uniform distribution of sequences*. Courier Corporation, 2012.

[10] R. Tijdeman. "Gelijkverdeelde rijen bestaan niet". In: *Nieuw Archief voor Wiskunde* 19.2 (2018), pp. 90–92.

[11] H. Faure, P. Kritzer, and F. Pillichshammer. "From van der Corput to modern constructions of sequences for quasi-Monte Carlo rules". In: *Indagationes Mathematicae* 26.5 (2015), pp. 760–822.

[12] K. F. Roth. "On irregularities of distribution". In: *Mathematika* 1.2 (1954), pp. 73–79.

[13] T. van Aardenne-Ehrenfest. "Proof of the impossibility of a just distribution of an infinite sequence of points over an interval". In: *Proc. Kon. Ned. Akad. v. Wetensch* 48 (1945), pp. 266–271.

[14] T. van Aardenne-Ehrenfest. "On the impossibility of a just distribution". In: *Proc. Kon. Ned. Akad. v. Wetensch* 52 (1949), pp. 734–739.

[15] W. Schmidt. "Irregularities of distribution, VII". In: *Acta Arithmetica* 21.1 (1972), pp. 45–50.

[16] G. Larcher. "On the discrepancy of sequences in the unit-interval". In: *Indagationes Mathematicae* 27.2 (2016), pp. 546–558.

[17] D. J. Watts and S. H. Strogatz. "Collective dynamics of 'small-world' networks". In: *Nature* 393.6684 (1998), p. 440.

[18] E. Borel. "La théorie du jeu et les équations intégralesa noyau symétrique". In: *Comptes rendus de l'Académie des Sciences* 173.1304-1308 (1921), p. 58.

[19] J. v. Neumann. "Zur theorie der gesellschaftsspiele". In: *Mathematische annalen* 100.1 (1928), pp. 295–320.

[20] J. Von Neumann and O. Morgenstern. *Theory of games and economic behavior (60th Anniversary Commemorative Edition)*. Princeton university press, 2007.

[21] J. Nash. "Non-cooperative games". In: *Annals of mathematics* (1951), pp. 286–295.

[22] C. Daskalakis, P. W. Goldberg, and C. H. Papadimitriou. "The complexity of computing a Nash equilibrium". In: *Communications of the ACM* 52.2 (2009), pp. 89–97.

[23] O. Gross and R. Wagner. *A continuous Colonel Blotto game*. Rand Corporation, 1950.

[24] B. Roberson. “The Colonel Blotto game”. In: *Economic Theory* 29.1 (2006), pp. 1–24.

I

COVID-19 SPREAD AND SOCIAL DISTANCING

3

A CONJECTURE BY DE BRUIJN AND ERDOS

The focus of this chapter emerged from research conducted on social distancing strategies during the COVID-19 pandemic. A research experiment asked a number of people to consecutively take a seat at a round table, such that the minimal distance between any two individuals is maximised. The catch was that none of the participants were aware of how many people would take place at the table. This created an interesting dilemma for the participants. Do you just take the best spot for yourself, or do you sit down in a way that leaves extra space for the people after you? If you are the last person to join the table, you would want to choose the best spot, but if you are not the last one, leaving extra space would be much better.

For example, consider a scenario where three individuals need to take seats at a table. Initially, the table is empty, allowing the first person the freedom to sit anywhere. The second person faces a choice: they could strategically take a seat directly opposite the first person or opt to sit slightly off-center, leaving some room persons yet to join. This would improve the outcome massively in the case that exactly three people join the table, see Figure 3.1.

It is clearly visible in this figure that the minimal distance is larger when person 2 plans one step ahead. However, if four people had to take place at the table instead of three, this changes again. In that case, not planning ahead would actually do better than planning ahead for the third person. And everything is different again if five people had to take seats, because their best distribution is very different again. This is what makes this problem so difficult, how do you plan a strategy that does reasonably well in all these scenarios?

The research primarily focused on the strategies individuals would adopt in

Parts of this chapter been submitted to Journal of Mathematical Sociology [1]. Additional work containing parts of this chapter is in preparation [2].

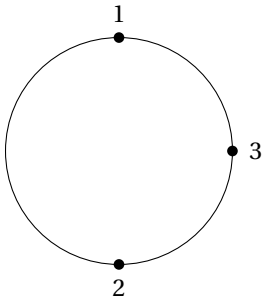

(a) Person 2 does not plan ahead.

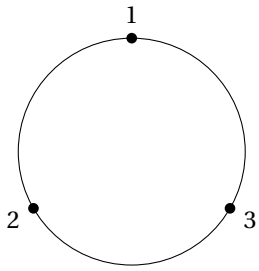

(b) Person 2 plans ahead, and leaves space for person 3

Figure 3.1.: Three people take place at the table consecutively, and want to optimize the minimal distance between any two persons.

the given scenario, but it also raised the question of what an optimal strategy would be. As more individuals join the table, the minimum distance between any two people would naturally decrease. However, we can still compare this outcome to what would have been the best possible minimum distance for the number of participants, and try to keep the ratio between the best solution and the actual outcome as close to 1 as possible. This is quite difficult, particularly when the number of individuals expected to join the table is unknown, and requires extensive foresight.

While we investigated this problem for a round table, there are many applications possible. For instance, one could also ask this same question for the square room in a cinema. During the high time of COVID-19, cinemas would use only a small part of the chairs, so that everybody was 1,5 meters removed from everybody else. At the time, there were some questions if 1,5 meters was even enough. Even with the reduced number of people allowed, these cinemas weren't always completely filled at the time, and it would therefore be possible for everybody to sit 3 meters from another, while everybody would still fit in the cinema. This leads us back to the same question of our research: How would you seat people, in such a way that the minimum distance between any two persons is as large as possible? You would not know how many people would show up to watch the movie, but you can appoint them seats as they go in. The minimum distance between people would slowly go down when more people joined, with a hard minimum of 1,5 meter, at which point no extra people would be allowed to join the cinema. A strategy like this could allow the same amount of people, just with extra safety.

Eventually this question lead us to work of de Bruijn and Erdős [25], who had looked at this problem, albeit in a different context. Their paper contained several interesting results, and also open conjectures. This specific work seemed to be mostly forgotten with time. As evidenced when several years later the same research question was asked anew by Ostrowski in 1957 [26], and was consequently

solved by Toulmin [27], independently of the work of De Bruijn and Erdős.

The problem was later studied again in 1978 by Ramshaw [28], this time under the name *Stick-Breaking*. After this it was forgotten again until in 2016 a similar problem was studied by Chung and Graham [29], who managed to strengthen a conjecture by D.J. Newman. Where we study the length of the intervals between the first n points of a sequence, they study the length of the intervals between n points of any subsequence anywhere in the sequence.

In this chapter, we first provide definitions and theory underlying the De Bruijn-Erdős paper, as well as a summary of their main results and conjectures in Section 3.1 and Section 3.2. As their focus was on infinite sequences, we expand their proofs to show what bound they provide for finite sequences. We then follow that with our experimental results about their conjecture in Section 3.3. Finally, we describe our main result, how to create optimal finite sequences, in Section 3.4. This extension to finite sequences is the solution to our original social distancing problem.

3.1. GAPS BETWEEN POINTS ON A CIRCLE

In this section, we define the problem and provide the bounds and sequence found by De Bruijn and Erdős. We follow the exposition from their paper [25].

Let $w := (w_1, w_2, \ldots)$ be a sequence of points on a circle with circumference 1, i.e., all $w_i \in [0,1)$. By connecting the start and end of the interval $[0,1)$, it is mapped to the circle, as shown in Figure 3.2a:

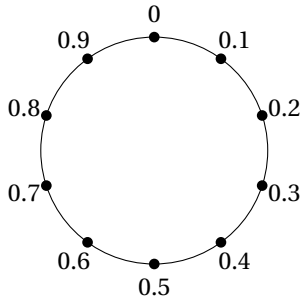

(a) Mapping the interval $[0,1)$ to a circle.

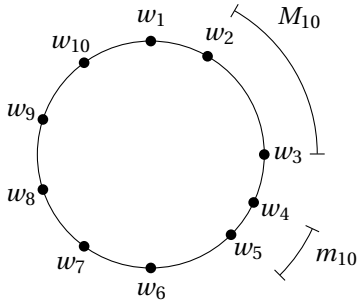

(b) M_n and m_n for a sequence with $n = 10$ points placed.

Figure 3.2.: How to map the circle to the interval $[0,1)$, and how to measure M_n and m_n.

After the first n points have been placed, the circle is divided into n intervals, which together sum up to 1. We are interested in the largest and the smallest interval. Let $M_n(w)$ denote the length of the largest interval and $m_n(w)$ denote the length of the

smallest interval after n points have been placed. Let μ_n denote the ratio between these, i.e.,

$$\mu_n = \frac{M_n(w)}{m_n(w)}.$$

Since the n intervals together sum up to one, it follows that the average length of an interval is $\frac{1}{n}$, and thus

$$M_n(w) \geq \frac{1}{n} \geq m_n(w),$$

where this would only be equality's if every interval had exactly length $\frac{1}{n}$. The main question is; How to create a sequence w such that $M_n(w)$ and $m_n(w)$ are always very close to $\frac{1}{n}$, regardless of n? To that end, we introduce $\Lambda(w)$, $\lambda(w)$ and $\mu(w)$ as

$$\begin{aligned}\limsup_{n\to\infty} n \cdot M_n(w) &= \Lambda(w)\\ \liminf_{n\to\infty} n \cdot m_n(w) &= \lambda(w)\\ \limsup_{n\to\infty} \mu_n(w) &= \mu(w)\end{aligned}$$

This means that, in the limit of n for a given sequence w, the largest interval is at most $\Lambda(w)$ times the average, the smallest interval is at least $\lambda(w)$ times the average, and the ratio between the largest and smallest interval is at most $\mu(w)$. These values might only hold in the limit, it is possible that they are larger for smaller n.

Furthermore, let Λ be the greatest lower bound on $\Lambda(w)$, let λ be the lowest upper bound on $\lambda(w)$ and let μ be the greatest lower bound on $\mu(w)$.

Determining the values of Λ, λ and μ and finding a sequence that matches these values solves the problem. First, we provide a lower bound on Λ in Section 3.1.2. Following that we provide an upper bound on λ in Section 3.1.3 In Section 3.1.5, we present the De Bruijn-Erdős sequence, which values for Λ, λ and μ match these bounds and therefore prove these bounds are sharp.

Finally, we look at an extension to consecutive intervals. Instead of looking at the maximum or minimum size of a single interval, we now look at the maximum and minimum size of r consecutive intervals.

3.1.1. HARMONIC NUMBERS

This problem turned out to have a strong connection to Harmonic Numbers. Harmonic numbers are an interesting concept in mathematics, and have uses in several parts of number theory. In this section, we introduce harmonic numbers and explain some of its interesting properties. We also provide a helpful lemma we use later.

Harmonic numbers are derived from the harmonic series, which is the infinite series formed by summing the reciprocals of all positive integers:

$$\sum_{i=1}^{\infty} \frac{1}{i} = 1 + \frac{1}{2} + \frac{1}{3} + \dots$$

The name "harmonic series" comes from the concept of harmony in music. In music theory, harmonics are the overtones or additional frequencies that are produced when a musical instrument vibrates or when a sound wave propagates through a medium. Harmonic frequencies are whole-number multiples of the fundamental frequency of a musical note, and they play a crucial role in creating the timbre or tone quality of a musical sound.

Each term in the series is the reciprocal of a positive integer, and these terms are added together, much like the harmonic frequencies in music combine to create complex sounds. The harmonic series is named in analogy to the harmonic overtones in music due to this mathematical relationship between the terms and the concept of harmonics in music.

The n-th harmonic number, denoted as H_n, is defined as the sum of the first n elements:

Definition 3.1. *For any positive integer n, the n-th harmonic number H_n is defined as:*

$$H_n = 1 + \frac{1}{2} + \frac{1}{3} + \dots + \frac{1}{n} = \sum_{i=1}^{n} \frac{1}{i}.$$

The Harmonic Series is a famous example of a divergent series. This means that as n approaches infinity, H_n becomes arbitrarily large, and grows beyond any constant. This was already proven by Oresme around 1360.

Harmonic Numbers also gained the attention of Euler, who used them for a new proof to show the existence of infinitely many prime numbers. He also studied the relation between the Harmonic Numbers and the natural logarithm, and he proved in 1734 that their difference approaches a constant, now known as the Euler–Mascheroni constant γ:

$$\lim_{n\to\infty} (H_n - \ln(n)) = \gamma,$$

with $\gamma \approx 0.5772$. It is still an unsolved problem in mathematics whether this is a rational number or not.

In this work, we have to calculate several versions of the difference $H_{2n} - H_n$. For any converging series, this would approach zero whenever n tends to infinity. However, the harmonic series is a divergent series. The difference between the harmonic numbers can be calculated in the following way:

Lemma 3.2. *The difference between the harmonic numbers H_{2n} and H_n goes to* $\ln(2)$ *in the limit, i.e.,*

$$\lim_{n\to\infty}(H_{2n}-H_n)=\ln(2).$$

Proof.

$$\begin{aligned}\lim_{n\to\infty}(H_{2n}-H_n) &= \lim_{n\to\infty}\Big(H_{2n}-\ln(2n)+\ln(2n)-H_n+\ln(n)-\ln(n)\Big)\\ &= \lim_{n\to\infty}\left(\ln\left(\frac{2n}{n}\right)+(H_{2n}-\ln(2n))-(H_n-\ln(n))\right)\\ &= \ln(2)+\gamma-\gamma=\ln(2)\end{aligned}$$

□

When we need to calculate the difference between two harmonic numbers, we refer back to Lemma 3.2 for the calculation method.

Aside from Lemma 3.2, there is another surprising property of harmonic numbers we will use. It is given by the following lemma:

Lemma 3.3. *The sequence $(H_{2n}-H_n)$ is strictly increasing, while the sequence $(H_{2n-1}-H_{n-1})$ is strictly decreasing.*

Proof. To prove $(H_{2n}-H_n)$ is strictly increasing, we need to show that for any positive integer n:

$$H_{2n}-H_n<H_{2(n+1)}-H_{n+1}.$$

Rearranging terms yields

$$H_{n+1}-H_n<H_{2(n+1)}-H_{2n}.$$

By using the definition of Harmonic numbers, this reduces to

$$\frac{1}{n+1}<\frac{1}{2n+2}+\frac{1}{2n+1},$$

which always holds. In the same way, we can prove that the sequence $(H_{2n-1}-H_{n-1})$ is strictly decreasing:

$$\begin{aligned}H_{2n-1}-H_{n-1}&>H_{2n+1}-H_n\\ H_n-H_{n-1}&>H_{2n+1}-H_{2n-1}\\ \frac{1}{n}&>\frac{1}{2n+1}+\frac{1}{2n}\end{aligned}$$

which proves the lemma. □

3.1.2. LOWER BOUND ON Λ

In this section we study the maximum sized interval between two point of the sequence, and provide a lower bound on Λ of $\frac{1}{\ln(2)}$, using the proof of De Bruijn and Erdős [25].

Theorem 3.4 (Lower bound on Λ)**.** *Let $w := (w_1, w_2, \ldots)$ be any sequence on the circle. Then for any integer $n > 0$:*

$$\sup_{n \le k < 2n} k \cdot M_k(w) \ge \frac{1}{H_{2n-1} - H_{n-1}},$$

where H_n is the n-th harmonic number. Furthermore, by letting n go to infinity it follows that

$$\Lambda \ge \frac{1}{\ln 2}.$$

Proof of Theorem 3.4. We prove this by contradiction. Assume there exists a sequence w and a positive integer n such that

$$\sup_{n \le k < 2n} k \cdot M_k(w) < \frac{1}{H_{2n-1} - H_{n-1}}. \tag{3.1}$$

Let the lengths of intervals determined by $w_1, \ldots, w_n$ be $a_1, a_2, \ldots, a_n$, sorted in descending order. We have that $M_n(w) = a_1$. Since adding any point to the sequence can only destroy one interval to create 2 new intervals, it follows that after w_{n+1} is placed, either the interval of length a_1 or the interval of length a_2 still exists. Thus, we know that $M_{n+1}(w) \ge a_2$. We can repeat this for points $w_{n+2}, \ldots, w_{2n-1}$ to derive:

$$M_n(w) = a_1, \quad M_{n+1}(w) \ge a_2, \quad \ldots, \quad M_{n+k}(w) \ge a_{k+1}, \quad \ldots, \quad M_{2n-1}(w) \ge a_n.$$

Since the entirety is a circle with a circumference of one, the sum of all intervals $a_1, \ldots, a_n$ must equal one. Therefore, we have

$$M_n(w) + M_{n+1}(w) + \cdots + M_{2n-1}(w) \ge a_1 + a_2 + \cdots + a_n = 1.$$

Furthermore, from Assumption (3.1), we know that $M_k < \frac{1}{k(H_{2n-1} - H_{n-1})}$ for all $n \le k < 2n$. From this assumption, we can derive

$$M_n(w) + \cdots + M_{2n-1}(w) < \frac{1}{H_{2n-1} - H_{n-1}} \left(\frac{1}{n} + \frac{1}{n+1} + \cdots + \frac{1}{2n-1} \right) = \frac{H_{2n-1} - H_{n-1}}{H_{2n-1} - H_{n-1}} = 1.$$

Combining these last two equations yields

$$1 \le M_n(w) + M_{n+1}(w) + \cdots + M_{2n-1}(w) < 1,$$

which is a clear contradiction, and thus proves the first part of the theorem. We now proceed to establish the limit value. Based on Lemma 3.3, we know that $(H_{2n-1} - H_{n-1})$ is strictly decreasing. Consequently, the supremum of $\frac{1}{H_{2n-1} - H_{n-1}}$ is achieved in the limit of n to infinity. Employing the approach used in the proof of Lemma 3.2, it follows that

$$\lim_{n \to \infty} (H_{2n-1} - H_{n-1}) = \ln 2.$$

□

3.1.3. UPPER BOUND ON λ

In this section, we look at the smallest interval and provide an upper bound on λ.

Theorem 3.5 (Upper bound on λ)**.** *Let $w := (w_1, w_2, \ldots)$ be any sequence on the circle, then for any integer $n > 0$:*

$$\inf_{n<k\leq 2n} k \cdot m_k(w) \leq \frac{1}{2\,(H_{2n} - H_n)},$$

where H_n is the n-th harmonic number. Furthermore, by letting n go to infinity it follows that

$$\lambda \leq \frac{1}{\ln 4}.$$

Proof of Theorem 3.5. We prove this by contradiction. Assume there exists a sequence w and a positive integer n such that

$$\inf_{n<k\leq 2n} k \cdot m_k(w) > \frac{1}{2\,(H_{2n} - H_n)}. \tag{3.2}$$

Let the length of the intervals determined by $w_1, \ldots, w_{2n}$ be $a_1, a_2, \ldots, a_{2n}$, sorted in descending order. We have that $m_{2n}(w) = a_{2n}$. We now take one step back and remove w_{2n}. Removing any point of the sequence merges two intervals into one, and doesn't change the other intervals. This means that before w_{2n} was placed, one of the intervals of length a_{2n-2}, a_{2n-1} or a_{2n} already existed. Therefore, we know that $m_{2n-1}(w) \leq a_{2n-2}$. We can continue to work backwards and repeat this for the points $w_{2n-1}, \ldots, w_{n+1}$ to derive:

$$m_{2n}(w) = a_{2n}, \quad m_{2n-1}(w) \leq a_{2n-2}, \quad \ldots, \quad m_{2n-k}(w) \leq a_{2n-2k}, \quad \ldots, \quad m_{n+1}(w) \leq a_2.$$

Since the entirety is a circle, all intervals together sum up to one. Thus, we can rewrite this as

$$1 = \sum_{i=1}^{2n} a_i \geq 2 \sum_{i=1}^{n} a_{2i} \geq 2 \sum_{i=1}^{n} m_{n+i}.$$

Furthermore, by Assumption (3.2), we know that $m_k > \frac{1}{2k(H_{2n}-H_n)}$ for all $n < k \leq 2n$. From this assumption, we can derive

$$\sum_{i=1}^{n} m_{n+i} > \frac{1}{2\,(H_{2n} - H_n)} \left(\frac{1}{n+1} + \cdots + \frac{1}{2n} \right) = \frac{H_{2n} - H_n}{2\,(H_{2n} - H_n)} = \frac{1}{2}.$$

Combining these last two equations gives

$$1 \geq 2 \sum_{i=1}^{n} m_{n+i} > 1,$$

which is a clear contradiction, and thus proves the first part of the theorem. Similarly as before, we can employ the approach used in the proof of Lemma 3.2 to show that $2(H_{2n} - H_n)$ goes to $\ln 4$ for $n \to \infty$. □

3.1.4. MAXIMUM RATIO BETWEEN LARGEST AND SMALLEST INTERVAL

In this section, we determine a lower bound on μ. It is noteworthy that while we already know that $\frac{\Lambda}{\lambda} \geq 2$, this has no implications on μ. This is because for any sequence Λ might occur after n_1 points of the sequence are placed, and λ might occur after n_2 points of the sequence are placed, where $n_1 \neq n_2$. By definition μ is the limit supremum of μ_n, which is the ratio after a fixed number of points n is placed, not the ratio between peaks for different n. Therefore, we can only conclude that $\frac{\Lambda}{\lambda} \geq \mu$, which does not yet provide a bound in this case. We do provide a bound with Theorem 3.6. In this work, we use the notation lg for $\log_2$.

Theorem 3.6. *Let $w := (w_1, w_2, \ldots)$ be any sequence on the circle, then for any integer $n > 0$:*

$$\sup_{n \leq k < 2n} \left(1 + \frac{1}{k}\right)^{1+c} \mu_k(w) \geq 2,$$

with

$$c = \frac{\lg\left(\frac{2}{1+\frac{1}{2n}}\right)}{\lg(2+\frac{1}{n})} = \frac{1+\lg\left(\frac{1}{1+\frac{1}{2n}}\right)}{1+\lg(1+\frac{1}{2n})},$$

where $0 < c < 1$. Furthermore, by letting n go to infinity, it follows that

$$\mu \geq 2.$$

Proof. We begin by proving a property necessary for the theorem. Let $n \leq k < 2n$ and let a_i be the length of the interval that w_k is placed in. Placing w_k splits this interval into two new intervals, whose lengths we denote by b_1 and b_2. It follows that

$$M_k(w) \geq a_i = b_1 + b_2 \geq 2\min(b_1, b_2) \geq 2m_{k+1}(w),$$

and consequently

$$\frac{M_k(w)}{m_{k+1}(w)} \geq 2. \tag{3.3}$$

This is a nice property, and close to the required inequality. If we had $\frac{M_k(w)}{m_k(w)} \geq 2$, we would be done. We now proceed to the statement of the theorem, proving it by contradiction. Assume there exists a sequence w and a positive integer n such that for any k with $n \leq k < 2n$ it holds that

$$\mu_k(w) = \frac{M_k(w)}{m_k(w)} < \frac{2}{\left(1+\frac{1}{k}\right)^{1+c}} = 2\left(\frac{k}{k+1}\right)^{1+c}. \tag{3.4}$$

Combining Equation (3.4) with Equation (3.3) leads to

$$\frac{m_{k+1}(w)}{m_k(w)} < \left(\frac{k}{k+1}\right)^{1+c}. \tag{3.5}$$

Using Equation (3.5) for all values of $n \leq k < 2n$ yields

$$\frac{m_{2n}(w)}{m_n(w)} = \frac{m_{2n}(w)}{m_{2n-1}(w)} \cdot \ldots \cdot \frac{m_{n+1}(w)}{m_n(w)} < \left(\frac{2n-1}{2n}\right)^{1+c} \cdot \ldots \cdot \left(\frac{n}{n+1}\right)^{1+c} = \left(\frac{n}{2n}\right)^{1+c} = \frac{1}{2^{1+c}}.$$

This can be rewritten in combination with the bound $m_n(w) \leq \frac{1}{n}$ as

$$m_{2n}(w) < \frac{1}{2^{1+c}} m_n(w) \leq \frac{1}{2^{1+c}n}. \tag{3.6}$$

3

Using Equation (3.6) and the bound $M_{2n}(w) \geq \frac{1}{2n}$, we can derive

$$\mu_{2n} = \frac{M_{2n}(w)}{m_{2n}(w)} > \frac{\left(\frac{1}{2n}\right)}{\left(\frac{1}{2^{1+c}n}\right)} = 2^c.$$

Combining this with Equation (3.4) we have

$$2^c < \mu_{2n} < \frac{2}{\left(1+\frac{1}{2n}\right)^{1+c}}$$
$$\left(2+\frac{1}{n}\right)^c < \frac{2}{\left(1+\frac{1}{2n}\right)}$$

By definition of c, the left-hand side is exactly equal to the right-hand side. This leaves us with a contradiction, and therefore the first part of the theorem must hold. For μ we have the bound

$$\mu = \limsup_{n\to\infty} \mu_n(w) \geq \frac{2}{\left(1+\frac{1}{n}\right)^2}.$$

Since $\left(1+\frac{1}{n}\right)$ is a strictly decreasing function, the right-hand side is maximized by letting n go to infinity:

$$\mu \geq \lim_{n\to\infty} \frac{2}{\left(1+\frac{1}{n}\right)^2} = 2.$$

□

3.1.5. THE DE BRUIJN-ERDŐS SEQUENCE

The bounds on Λ, λ and μ as mentioned in Theorem 3.4, Theorem 3.5 and Theorem 3.6, originate from the work of de Bruijn and Erdős [25]. In their work, they also provided a sequence to show that these bounds were tight. We refer to this sequence as the *De Bruijn-Erdős sequence* (DBE-Sequence). In this section, we describe this sequence and show that this sequence has the best Λ, λ and μ possible.

Definition 3.7 (De Bruijn-Erdős sequence)**.** *The De Bruijn-Erdős sequence is a sequence* $w := (w_1, w_2, \ldots)$ *where the points are defined as*

$$w_k = \lg(2k-1) \mod 1. \tag{3.7}$$

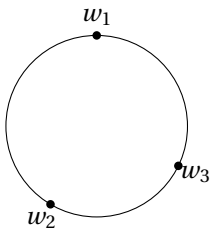

(a) The first three points of the De Bruijn-Erdős sequence on the circle.

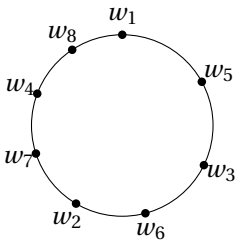

(b) The first eight points of the De Bruijn-Erdős sequence on the circle.

Figure 3.3.: The first points of the De Bruijn-Erdős sequence on the circle.

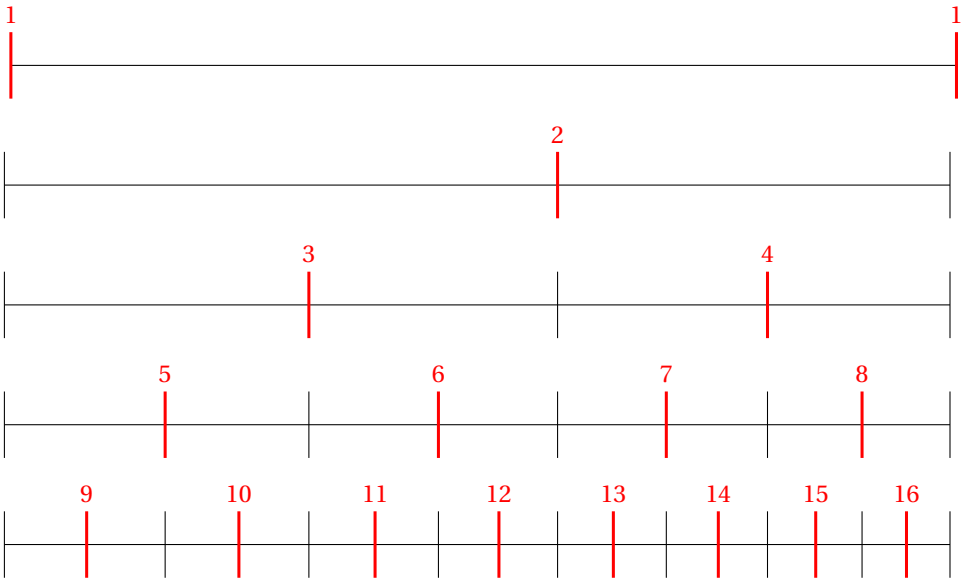

Figure 3.4.: The points of De Bruijn-Erdős sequence. Every point is placed slightly right of the middle of the largest gap available.

We show that the De Bruijn-Erdős sequence has the best $\lambda(w)$ and $\Lambda(w)$ possible by proving the following theorem:

Theorem 3.8. *For the De Bruijn-Erdős sequence w, it holds that* $\Lambda(w) = \frac{1}{\ln 2}$, $\lambda(w) = \frac{1}{\ln 4}$ *and* $\mu(w) = 2$.

Proof. Let $w_1, \dots w_n$ be the first n points from the De Bruijn-Erdős sequence, i.e.,

$$\lg(1), \lg(3), \dots, \lg(2n-1) \mod 1.$$

First we show that these points are a permutation of the points $b_1, \dots, b_n$, with

Person	Position
w_1	0
w_2	0.585…
w_3	0.322…
w_4	0.807…
w_5	0.170…
w_6	0.459…
w_7	0.700…
w_8	0.907…

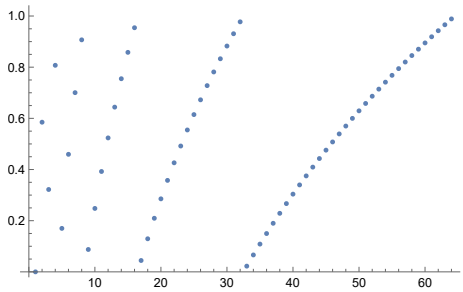

Figure 3.5.: The locations of the first points of the De Bruijn-Erdős sequence.

$b_i = \lg(n-1+i) \mod 1$, i.e.,

$$\lg(n), \lg(n+1), \ldots, \lg(2n-1) \mod 1.$$

To prove this, we show that no two w_k and no two b_i are congruent mod 1, yet every b_i is congruent to exactly one w_k mod 1.

For any two numbers $\lg(x)$ and $\lg(y)$ with $x \geq y$ to be congruent mod 1, it would require

$$\lg(x) - \lg(y) \mod 1 = \lg\left(\frac{x}{y}\right) \mod 1 = 0.$$

This condition holds if and only if $\frac{x}{y}$ is some power of two, i.e., $x = 2^p y$ for some integer p. The sequence $w_1, \ldots, w_n$ consists of logarithms of odd numbers, meaning no two w_k can be congruent. Similarly, the sequence $b_1, \ldots, b_n$, which starts with the logarithm of n and ends with the logarithm of $(2n-1)$, cannot have any congruent members since the ratio between n and $2n-1$ is less than two.

Furthermore, every b_i can be uniquely expressed as $b_i = \lg(2^p c)$, where $p \geq 0$ is a non-negative integer, and c is an odd integer between 1 and $2n-1$. Since $\lg(2^p c)$ is congruent with $\lg(c)$ mod 1 and $\lg(c)$ must be part of $w_1, \ldots, w_n$, it follows that every b_i is congruent with exactly one w_i.

The advantage of the points $b_1, \ldots, b_n$ is that every point b_i is directly next to the point b_{i+1} on the circle. Therefore, the sizes of the intervals, $a_1, \ldots, a_n$, are equal to:

$$\lg\left(\frac{n+1}{n}\right), \lg\left(\frac{n+2}{n+1}\right), \ldots, \lg\left(\frac{2n-1}{2n-2}\right), \lg\left(\frac{2n}{2n-1}\right). \tag{3.8}$$

ordered from largest to smallest. We can conclude

$$nM_n(w) = n\lg\left(1+\frac{1}{n}\right), \quad \text{and} \quad nm_n(w) = n\lg\left(1+\frac{1}{2n-1}\right).$$

Since $nM_n(w)$ is strictly increasing and $nm_n(w)$ is strictly decreasing, it holds that

$$\Lambda(w) = \lim_{n\to\infty} nM_n(w), \qquad \lambda(w) = \lim_{n\to\infty} n \cdot m_n(w), \qquad \mu(w) = \lim_{n\to\infty} \frac{M_n(w)}{m_n(w)} = \frac{\Lambda(w)}{\lambda(w)}.$$

We use the known limit $\lim_{n\to\infty}\left(1+\frac{1}{n}\right)^n = e$ to derive:

$$\Lambda(w) = \lim_{n\to\infty} nM_n(w) = \lim_{n\to\infty} \frac{\ln\left(\left(1+\frac{1}{n}\right)^n\right)}{\ln 2} = \frac{1}{\ln 2}$$

$$\lambda(w) = \lim_{n\to\infty} nm_n(w) = \lim_{n\to\infty} \left(\left(\frac{n}{2n-1}\right) \frac{\ln\left(\left(1+\frac{1}{2n-1}\right)^{2n-1}\right)}{\ln 2}\right) = \left(\frac{1}{2}\right)\frac{1}{\ln 2} = \frac{1}{\ln 4}$$

$$\mu(w) = \frac{\Lambda(w)}{\lambda(w)} = 2$$

which concludes the proof. □

3.2. EXTENSION TO MULTIPLE INTERVALS

In this section, we aim to extend the earlier results for λ, Λ and μ from the minimum and maximum size of a single interval, to the minimum and maximum size of r consecutive intervals. We refer to r consecutive intervals of a sequence as a *r-interval*. Similarly as was done for single intervals, we define $M_n^r(a)$ as the largest r-interval and $m_n^r(a)$ as the smallest r-interval. Using these we can define the generalisations of Λ, λ and μ as:

$$\limsup_{n\to\infty} nM_n^r(a) = \Lambda_r(a)$$

$$\liminf_{n\to\infty} nm_n^r(a) = \lambda_r(a)$$

$$\limsup_{n\to\infty} \frac{M_n^r(a)}{m_n^r(a)} = \mu_r(a)$$

In the following sections, we prove the three following bounds, which originated in the work of De Bruijn and Erdős:

$$\Lambda_r \geq \frac{1}{\ln\left(1+\frac{1}{r}\right)} > r \tag{3.9}$$

$$\lambda_r \leq \frac{\frac{r}{r+1}}{\ln\left(1+\frac{1}{r}\right)} < r \tag{3.10}$$

$$\mu_r \geq 1 + \frac{1}{r} \tag{3.11}$$

It is unknown whether these bounds are tight. De Bruijn and Erdős conjectured the following:

$$(\Lambda_r - r) \to \infty \qquad \text{if } r \to \infty$$

$$(r - \lambda_r) \to \infty \qquad \text{if } r \to \infty$$

$$r(\mu_r - 1) \to \infty \qquad \text{if } r \to \infty$$

3.2.1. LOWER BOUND ON Λ_r

In this subsection, we study the maximum size of r-intervals, and provide a lower bound on Λ_r.

Theorem 3.9 (Lower bound on Λ_r)**.** *Let $w := (w_1, w_2, \ldots)$ be any sequence on the circle. Then for any integer $n > 0$:*

$$\sup_{1 \le k \le n(r+1)} k \cdot M_k^r(w) \ge \frac{1}{H_{n(r+1)-1} - H_{rn-1}},$$

where H_n is the n-th harmonic number. Furthermore, by letting n go to infinity it follows that

$$\Lambda_r \ge \frac{1}{\ln\left(1 + \frac{1}{r}\right)}.$$

Proof of Theorem 3.9. We prove this by contradiction. Assume there exists a sequence w and a positive integer n such that

$$\sup_{1 \le k \le n(r+1)} k \cdot M_k^r(w) < \frac{1}{H_{n(r+1)-1} - H_{rn-1}}. \tag{3.12}$$

Let the intervals be determined by $w_1, \ldots, w_{rn}$. We divide these rn intervals into n disjoint r-intervals $a_1^r, a_2^r, \ldots, a_n^r$, sorted in descending order. It follows that $a_1^r \le M_k^r(w)$. Since any point after w_{rn} can only be placed in one of the r-intervals, the placement of w_{rn+1} leaves either the r-interval of length a_1^r or the r-interval of length a_2^r untouched. Therefore, we know that $M_{rn+1}(w) \ge a_2^r$. We can repeat this for points $w_{rn+2}, \ldots, w_{n(r+1)-1}$ to derive:

$$M_{nr}(w) \ge a_1^r, \quad M_{rn+1}(w) \ge a_2^r, \quad \ldots, \quad M_{rn+k}(w) \ge a_{k+1}^r, \quad \ldots, \quad M_{n(r+1)-1}(w) \ge a_n^r.$$

Since the entirety is a circle with circumference 1, all r-intervals $a_1, \ldots, a_n$ together sum up to one. Therefore, we know that

$$M_{rn}(w) + M_{rn+1}(w) + \cdots + M_{n(r+1)-1}(w) \ge a_1^r + a_2^r + \cdots + a_n^r = 1.$$

Furthermore, from Equation (3.12) we know that $M_k < \frac{1}{k\left(H_{n(r+1)-1} - H_{rn-1}\right)}$ for all $1 \le k \le n(r+1)$. It follows that

$$M_{rn}(w) + \cdots + M_{n(r+1)-1}(w) < \frac{1}{H_{n(r+1)-1} - H_{rn-1}} \left(\frac{1}{rn} + \frac{1}{rn+1} + \cdots + \frac{1}{n(r+1)-1} \right) = 1.$$

Combining these last two equations yields

$$1 \le M_{rn}(w) + M_{rn+1}(w) + \ldots + M_{n(r+1)-1}(w) < 1.$$

This is a clear contradiction, and thus proves the first part of the theorem. Similarly as before, we can show that $H_{n(r+1)-1} - H_{rn-1}$ goes to $\ln\left(1 + \frac{1}{r}\right)$ for $n \to \infty$:

$$\lim_{n \to \infty} \left(H_{n(r+1)-1} - H_{rn-1} \right) = \lim_{n \to \infty} \ln\left(1 + \frac{n}{rn-1}\right) = \ln\left(1 + \frac{1}{r}\right).$$

This concludes the proof. □

3.2.2. UPPER BOUND ON λ_r

In this subsection, we look at the smallest interval and provide an upper bound on λ_r.

Theorem 3.10 (Upper bound on λ)**.** *Let $w := (w_1, w_2, \ldots)$ be any sequence on the circle, then for any integer $n > 0$:*

$$\inf_{nr<k\leq n(r+1)} k \cdot m_k^r(w) \leq \frac{r}{(r+1)\left(H_{n(r+1)} - H_{nr}\right)},$$

where H_n is the n-th harmonic number. Furthermore, by letting n go to infinity it follows that

$$\lambda_r \leq \frac{\frac{r}{r+1}}{\ln\left(1+\frac{1}{r}\right)}.$$

Proof of Theorem 3.10. We prove this by contradiction. Assume there exists a sequence w and a positive integer n such that

$$\inf_{nr<k\leq n(r+1)} k \cdot m_k(w) > \frac{r}{(r+1)\left(H_{n(r+1)} - H_{nr}\right)}. \tag{3.13}$$

Let the length of the r-intervals determined by $w_1, \ldots, w_{n(r+1)}$ be $a_1^r, a_2^r, \ldots, a_{n(r+1)}^r$, sorted in descending order. We have that $m^r_{n(r+1)}(w) = a_{n(r+1)}$. Now we remove the last point placed and look at the sequence when only $n(r+1)-1$ points were placed. Any point is part of exactly $r+1$ r-intervals, thus removing one point can only destroy $r+1$ intervals, and the rest must still exist. Therefore, it must hold that before $w_{n(r+1)}$ was placed, one of the intervals of length $a^r_{n(r+1)}, a^r_{n(r+1)-1}, \ldots, a^r_{(n-1)(r+1)}$ still exists. Thus, we know that $m_{(n)(r+1)-1}(w) \leq a_{(n-1)r+1}$. We can repeat this for points $w_{n(r+1)-2}, \ldots, w_{nr+1}$ to derive:

$$m_{n(r+1)}(w) \leq a^r_{n(r+1)}, \quad \ldots, \quad m_{n(r+1)-k}(w) \leq a^r_{(n-k)(r+1)}, \quad \ldots, \quad m_{nr+1}(w) \leq a^r_{r+1}.$$

Since the entirety is a circle with a circumference of one, the sum of all intervals equals one. If we sum over all possible r-intervals, then every interval is counted exactly r times. Thus, the total of this sum must be r, i.e.,

$$r = \sum_{i=1}^{n(r+1)} a_i^r$$

By leveraging the fact that the intervals are sorted in descending order, we can derive

$$r = \sum_{i=1}^{n(r+1)} a_i^r \geq (r+1) \sum_{i=1}^{n} a^r_{i(r+1)} \geq (r+1) \sum_{i=1}^{n} m_{nr+i}$$

$$\frac{r}{r+1} \geq \sum_{i=1}^{n} m_{nr+i}$$

Furthermore, from Equation (3.13) we know that $m_k > \frac{r}{(r+1)k(H_{n(r+1)}-H_{nr})}$ for all $nr \le k \le n(r+1)$. Thus:

$$\sum_{i=1}^{n} m_{nr+i} > \frac{r}{(r+1)\left(H_{n(r+1)}-H_{nr}\right)}\left(\frac{1}{nr+1}+\cdots+\frac{1}{n(r+1)}\right) = \frac{r}{r+1}\cdot\frac{H_{n(r+1)}-H_{nr}}{\left(H_{n(r+1)}-H_{nr}\right)} = \frac{r}{r+1}$$

Combining these last two equations gives

$$\frac{r}{r+1} \ge \sum_{i=1}^{n} m_{n+i} > \frac{r}{r+1},$$

which is a clear contradiction, and thus proves the theorem. □

3.2.3. MAXIMUM RATIO BETWEEN LARGEST AND SMALLEST INTERVAL μ_r

In this subsection, we prove a lower bound on μ of $1+\frac{1}{r}$. Before we provide this theorem and its proof, we start with a lemma.

Lemma 3.11. *Let $w := (w_1, w_2, \ldots)$ be any sequence on the circle, then for any integer $n > 0$:*

$$\frac{M_n^r}{m_{n+1}^r} \ge 1+\frac{1}{r}.$$

Proof. The proof for $r = 1$ can be found in Section 3.1.4. We now assume $r > 1$.
Let the intervals determined by $w_1, \ldots, w_n$ be $a_1, \ldots, a_n$, ordered in the way they appear on the circle in clockwise order. Let a_i be the interval in which w_{n+1} falls. We want to look at the $r-1$ intervals immediately to the left and to the right of a_i on the circle, i.e., the set of $2r-1$ intervals:

$$a_{i-r+1}, a_{i-r+2}, \ldots, a_i, a_{i+1}, \ldots, a_{i+r-1}. \tag{3.14}$$

which are consecutive on the circle.

Let I_j be the length of interval a_j and let M_a be the maximum length of r consecutive intervals, using only intervals in Equation (3.14). It follows that $M_a \le M_n^r$. Since every r-interval contained in Equation (3.14) must contain the interval a_i, it must also be part of the r-interval with length M_a. Thus, we can say that the sum of the length of the other $r-1$ intervals is $M_a - I_i$. Since at least one of these intervals has to be equal or larger than average, we can say that there must exist an interval a_j for which

$$I_j \ge \frac{M_a - I_i}{r-1}. \tag{3.15}$$

Without loss of generality, assume $j > i$. After w_{n+1} is placed, we can form a r-interval starting with a_{j-r+1} going clockwise, with total length:

$$I_{j-r+1} + \cdots + I_{i-1} + \gamma_1 + \gamma_2 + \cdots + I_{j-1} = M_a - I_j.$$

Combining this with Equation (3.15) allows us to derive

$$m_{n+1}^r \le M_a - I_j \le \frac{r-2}{r-1} M_a + \frac{I_i}{r-1} \le \frac{r-2}{r-1} M_n^r + \frac{I_i}{r-1}$$

This can be rewritten as follows

$$1 + \frac{1}{r-2}\left(1 - \frac{I_i}{m_{n+1}^r}\right) \le \frac{M_n^r}{m_{n+1}^r} \tag{3.16}$$

We can also construct two separate r-intervals from a_{i-r+1} to γ_1 and from γ_2 to a_{i+r-1}. This yields

$$\begin{aligned} m_{n+1}^r &\le I_{i-r+1} + \cdots + \gamma_1 \le M_a - \gamma_1 \le M_n^r - \gamma_1 \\ m_{n+1}^r &\le \gamma_2 + \cdots + I_{i-r+1} \le M_a - \gamma_2 \le M_n^r - \gamma_2 \end{aligned}$$

Combining these two equations gives

$$\begin{aligned} 2m_{n+1}^r &\le 2M_n^r - \gamma_1 - \gamma_2 \\ m_{n+1}^r &\le M_n^r - \frac{1}{2} I_i \\ 1 + \frac{I_i}{2m_{n+1}^r} &\le \frac{M_n^r}{m_{n+1}^r} \end{aligned} \tag{3.17}$$

We want to prove $\frac{M_n^r}{m_{n+1}^r} \ge 1 + \frac{1}{r}$. If $\frac{I_i}{2m} \ge \frac{1}{r}$, this follows directly from Equation (3.17). If $\frac{I_i}{2m_{n+1}^r} < \frac{1}{r}$, we can rewrite Equation (3.16) as follows:

$$\begin{aligned} \frac{M_n^r}{m_{n+1}^r} &\ge 1 + \frac{1}{r-2}\left(1 - \frac{I_i}{m_{n+1}^r}\right) \\ &> 1 + \frac{1}{r-2}\left(1 - \frac{2}{r}\right) = 1 + \frac{1}{r-2}\left(\frac{r-2}{r}\right) \\ &= 1 + \frac{1}{r} \end{aligned}$$

which concludes the proof. □

Now for the main theorem of this section, the bound on μ_r:

Theorem 3.12. *Let $w := (w_1, w_2, \ldots)$ be any sequence on the circle, then for any integer $n > 0$:*

$$\sup_{n \le k \le 2n} \left(1 + \frac{1}{k}\right)^2 \frac{M_k^r(w)}{m_k^r(w)} \ge 1 + \frac{1}{r}.$$

Furthermore, by letting n go to infinity it follows that

$$\mu_r \ge 1 + \frac{1}{r}.$$

Proof. We prove the theorem by contradiction. Assume there exists a sequence w and a positive integer n such that for any k with $n \le k \le 2n$ it holds that

$$\frac{M_k^r(w)}{m_k^r(w)} < \frac{1+\frac{1}{r}}{\left(1+\frac{1}{k}\right)^2}. \tag{3.18}$$

From Lemma 3.11 we know that $M_k^r(w) \ge (1+\frac{1}{r}) m_{k+1}^r(w)$. Inserting this into Equation (3.18) gives:

$$\begin{aligned} \frac{\left(1+\frac{1}{r}\right) m_{k+1}^r(w)}{m_k^r(w)} &< \frac{\left(1+\frac{1}{r}\right)}{\left(1+\frac{1}{k}\right)^2} \\ \frac{m_{k+1}^r(w)}{m_k^r(w)} &< \frac{k^2}{(k+1)^2} \end{aligned} \tag{3.19}$$

Using Equation (3.19) for all values of $n \le k \le 2n$ yields

$$\frac{m_{2n}^r(w)}{m_n^r(w)} = \frac{m_{2n}^r(w)}{m_{n-1}^r(w)} \cdot \frac{m_{2n-1}^r(w)}{m_{2n-2}^r(w)} \cdot \ldots \cdot \frac{m_{n+1}^r(w)}{m_n^r(w)} < \frac{(2n-1)^2}{(2n)^2} \cdot \ldots \cdot \frac{n^2}{(n+1)^2} = \frac{n^2}{(2n)^2} = \frac{1}{4}$$

This can be rewritten in combination with the bound $m_n(w) \le \frac{r}{n}$ as

$$m_{2n}^r(w) < \frac{1}{4} m_n^r(w) \le \frac{r}{4n} \tag{3.20}$$

Using Equation (3.20) and the bound $M_{2n}(w) \ge \frac{r}{2n}$, we can conclude that

$$\frac{M_{2n}^r(w)}{m_{2n}^r(w)} > \frac{\left(\frac{r}{2n}\right)}{\left(\frac{r}{4n}\right)} = 2$$

which contradicts Equation (3.18), and thus the first part of the theorem must hold. Since it is a strictly increasing function, it is maximized by letting n go to infinity:

$$\mu \ge \limsup_{n\to\infty} \frac{M_n^r(w)}{m_n^r(w)} = \lim_{n\to\infty} \frac{M_n^r(w)}{m_n^r(w)} = \lim_{n\to\infty} \frac{\left(1+\frac{1}{r}\right)}{\left(1+\frac{1}{n}\right)^2} = 1 + \frac{1}{r}$$

which concludes the proof. □

3.3. THE DE BRUIJN-ERDŐS CONJECTURES

De Bruijn and Erdős conclude their work with three conjectures that still remain open today. They state that the bounds given on λ_r, Λ_r and μ_r are probably not the best possible for $r \ge 2$ and they conjecture[1] that:

$$(\Lambda_r - r) \to \infty \quad \text{if } r \to \infty \tag{3.21}$$

$$(r - \lambda_r) \to \infty \quad \text{if } r \to \infty \tag{3.22}$$

$$r(\mu_r - 1) \to \infty \quad \text{if } r \to \infty \tag{3.23}$$

[1] In their paper, De Bruijn and Erdős conjecture that the expressions $r(\Lambda_r - 1)$ and $r(1 - \lambda_r)$ tend to infinity if $r \to \infty$, but this is most likely a typing error, and the conjectures were meant as stated here.

Note that since Δ_r and μ_r are greatest lower bounds and λ_r is a lowest upper bound, these conjecture do not need to hold for every sequence. They are already proven if they hold for a single sequence.

The third conjecture can be seen as the most important one, since it combines aspects of the first two. In this section, we investigate this conjecture. We derive three subquestions from this conjecture and use experimental data on van der Corput sequences to gain insights. Finally, De Bruijn and Erdős claim that this conjecture would imply the theorem of van Aardenne-Ehrenfest. We explain why this claim holds in Section 3.3.3.

3.3.1. THREE QUESTIONS FOLLOWING FROM THE CONJECTURE

We break down this conjecture into three subquestions:

Question 1: Does μ_r approach 1?
The first thing to note is that the conjecture implicitly assumes that μ_r approaches 1 for $r \to \infty$. This assumption arises because by definition, μ cannot be smaller than 1, and if it would not approach 1, the conjecture would trivially follow. Thus, it is a necessary condition for the conjecture that μ_r approaches 1 for $r \to \infty$. However, whether this condition holds true is unknown. Therefore, our first question is: Does it hold that $\lim_{r\to\infty} \mu_r = 1$? This question is more difficult than it appears at first glance. For instance, this does not hold for the DBE-sequence.

The DBE-sequence is optimal for $r = 1$ and therefore one might assume that its performance extends to higher values of r. However, as illustrated in Lemma 3.13, this is not the case. Consequently, we use a different sequence for our experimental results.

Lemma 3.13. *The DBE-Sequence has $\mu_r(w) = 2$ for all $r \in \mathbb{N}$*

Proof. From Equation (3.8), we know that the interval lengths of the DBE-Sequence for given n are

$$\lg\left(\frac{n+1}{n}\right), \lg\left(\frac{n+2}{n+1}\right), \ldots, \lg\left(\frac{2n-1}{2n-2}\right), \lg\left(\frac{2n}{2n-1}\right).$$

This means that we can calculate the ratio between the longest and shortest r-intervals after n points have been placed:

$$\frac{\lg\left(\frac{n+1}{n}\right) + \cdots + \lg\left(\frac{n+r}{n+r}\right)}{\lg\left(\frac{2n-r+1}{2n-r}\right) + \cdots + \lg\left(\frac{2n}{2n-1}\right)} = \frac{\lg\left(\frac{n+r}{n}\right)}{\lg\left(\frac{2n}{2n-r}\right)} = \frac{\lg\left(1+\frac{r}{n}\right)}{\lg\left(1+\frac{r}{2n-r}\right)}.$$

Now we can calculate μ_r:

$$\mu_r(w) = \lim_{n\to\infty} \frac{\lg\left(1+\frac{r}{n}\right)}{\lg\left(1+\frac{r}{2n-r}\right)} = \lim_{n\to\infty} \frac{2n-r}{n} \cdot \frac{\lg\left(\left(1+\frac{r}{n}\right)^n\right)}{\lg\left(\left(1+\frac{r}{2n-r}\right)^{2n-r}\right)} = 2 \cdot \frac{\lg(e)}{\lg(e)} = 2.$$

□

Note that this does not disprove the conjecture, as the conjecture only requires there to exist a single sequence w for which $\mu_r(w)$ approaches 1 for $r \to \infty$.

Question 2: Does μ_r approach 1 slower than the provided lower bound?
The important claim the conjecture makes is that the lower bound on μ_r leaves room for improvement, and that μ_r approaches 1 significantly slower than $1+\frac{1}{r}$. To understand what this means, we use the Big Omega notation. Recall that De Bruijn and Erdős provided the lower bound of $\mu_r \geq 1+\frac{1}{r}$. In the hypothetical case some upper bound would exist of the form $(\mu_r - 1) \leq \frac{c}{r}$ for some constant c, we would know that $(\mu_r - 1) = O(\frac{1}{r})$. This would give us a good indication how μ_r behaves for large r and how fast μ_r approaches 1. However, the conjecture claims such an upper bound can not exist, since in that case

$$r(\mu_r - 1) = r\left(1 + \frac{c}{r} - 1\right) = c.$$

Which would contradict the conjecture. Therefore, the conjecture is equivalent to the statement

$$(\mu_r - 1) = \Omega\left(\frac{1}{r}\right).$$

This conjecture was made by de Bruijn and Erdős in 1948 and to the best of our knowledge has remained open ever since.

Question 3: How fast does μ approach 1?
The conjecture claims that μ_r approaches 1 slower than the bound requires, which is an interesting question in its own right, but it also creates an intriguing follow-up question. If the conjecture is correct, then how fast does μ approach 1? Is it perhaps possible to find a lower bound of the type:

$$\mu_r \geq 1 + c\frac{\log(r)}{r}. \tag{3.24}$$

for some constant c? If we require this to be a tight bound, the question becomes:

$$(\mu_r - 1) = \Theta\left(\frac{\log(r)}{r}\right).$$

These are the three questions we investigate. We use an experimental approach and compute μ_r numerically.

3.3.2. EXPERIMENTAL RESULTS

The first question to investigate is whether μ_r approaches 1 for $r \to \infty$. As shown in Lemma 3.13, this does not hold for the DBE-sequence. The DBE-Sequence is designed for $r = 1$, and its μ_1 is optimal. However, it does not perform well for higher r. The r intervals of largest length are always right next to each other, and the same for the intervals of smallest length. Much better results would be possible

for sequences where the r largest and smallest intervals are more spread out, instead of next to each other. Therefore, we have to find another sequence, which does have this property. If we look into equidistribution literature, we find that the van der Corput sequence is a good candidate. Variants of this sequence are often used to create sequences with low discrepancy, which makes it a good candidate for our problem.

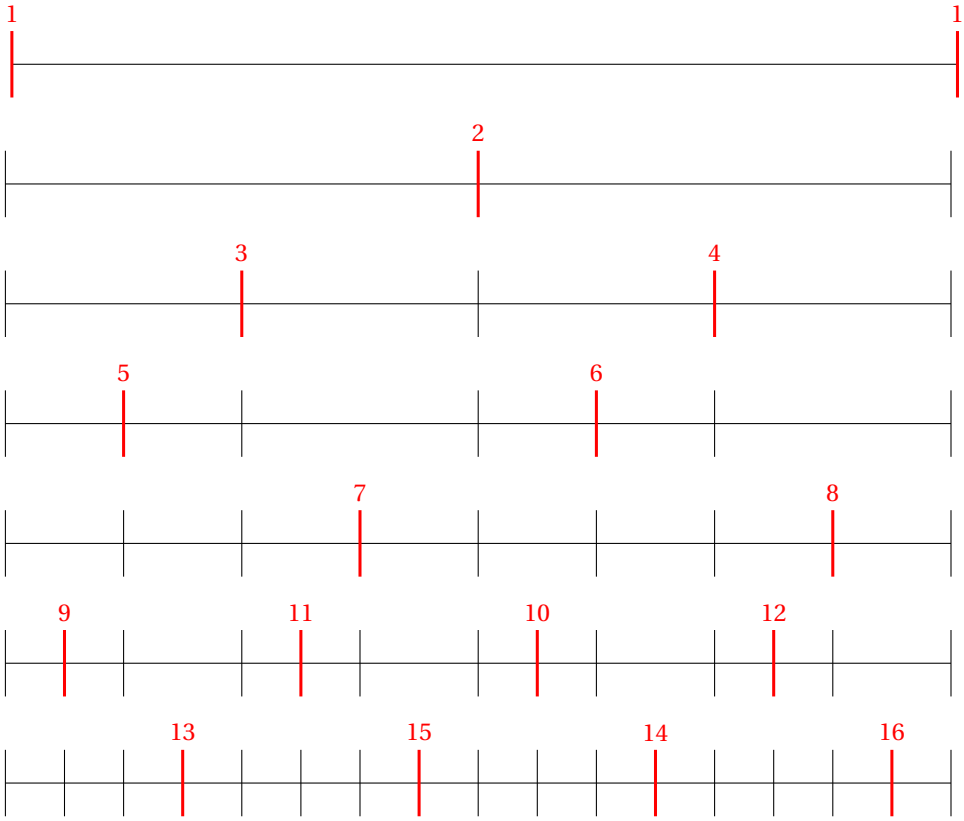

Figure 3.6.: The points of the vdC-sequence.

We test $r = 1, \ldots, 2304$ for vdC-sequence of lengths $n = 4096, \ldots, 8192$. The result can be found in Figure 3.7.

From the figure, we can see that the vdC-sequence does seem to satisfy $\mu_r \to 1$ for $r \to \infty$. It starts out from $\mu_1 = \mu_2 = 2$, and it descends rapidly. This was tested up to $r = 2304$, for which $\mu_{2304} = \frac{2764}{2757} \approx 1.0025$.

Now that we know it is likely that $\mu_r \to 1$, we investigate the vdC-sequence again, this time to determine its order of approximation. In Figure 3.8 we add three

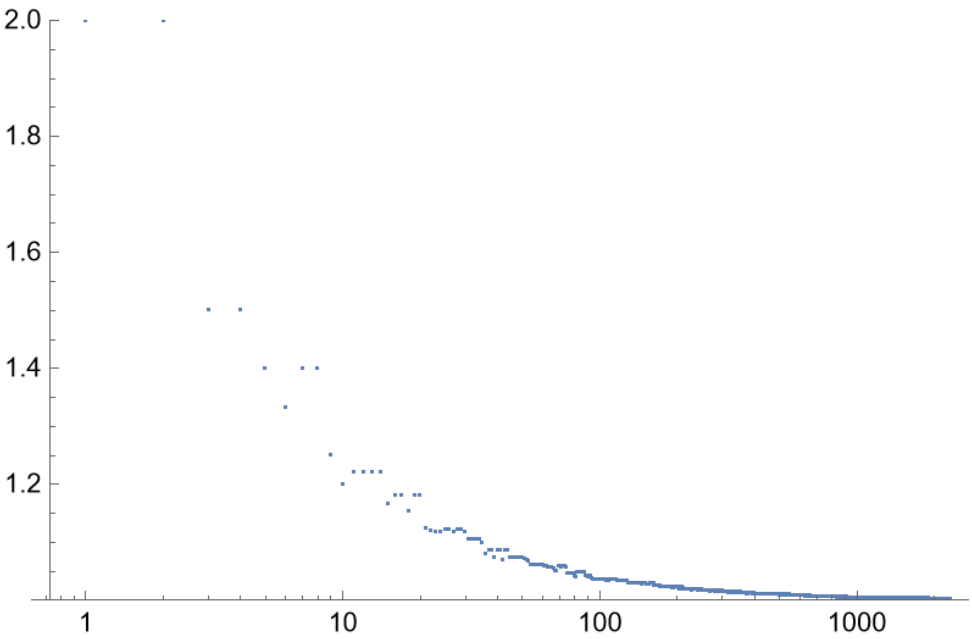

Figure 3.7.: The μ_r of the vdC-sequence, for different r. Tested for the first 1024 numbers of the sequence.

functions to the graph: the red line is the lower bound provided by Erdős and De Bruijn, and the dotted oranges line are the functions:

$$1+\frac{\frac{4}{9}\lg(r)}{r} \qquad \text{and} \qquad 1+\frac{2+\frac{4}{9}\lg(r)}{r} \tag{3.25}$$

In Figure 3.8, there seems to be a significant gap between the lower bound and the data from the vdC-sequence. However, the two functions from (3.25) seem to enclose the data from the vdC-sequence nicely. This implies the data seems to follow a logarithmic trend.

To further investigate if such a function of the form $1+\frac{c\lg(r)}{r}$ would fit as a lower bound on μ_r, we plot $r(\mu_r-1)$ on a logarithmic scale in Figure 3.9.

If a lower bound of this form exists, then the data should be able to be bounded by a straight line in the figure. We also plot the bounds as mentioned in Equation (3.25). The data can be bounded by these equations, and it does appear to follow a straight line in the figure. However, the behaviour is also erratic, so it's hard to say whether these specific bounds would work for all r.

The experimental results suggest there likely exists a lower bound to the vdC-sequence for which $(\mu_r(w)-1)=\Theta\left(\frac{\log(r)}{r}\right)$. The vdC-sequence is the sequence

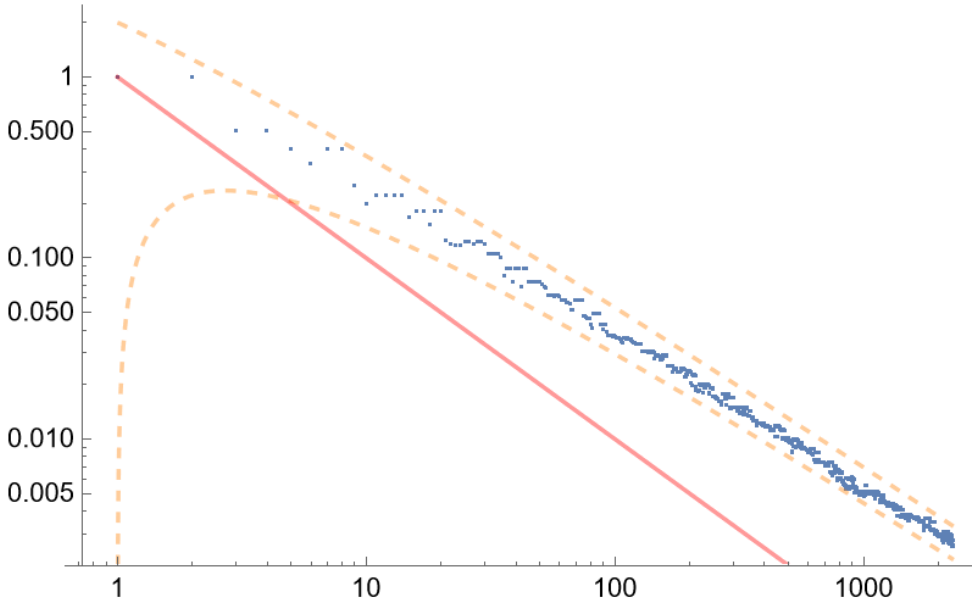

Figure 3.8.: The blue dots are $(\mu_r - 1)$ of the vdC-sequence for different r. The dotted oranges lines are the functions of Equation (3.25). The red line is the known lower bound on μ_r.

with the lowest $\mu_r(w)$ we found, and therefore these results support the original conjecture.

3.3.3. CONNECTION TO VAN AARDENNE-EHRENFEST

De Bruijn-Erdős claim that if their μ conjecture would hold, it would imply the famous theorem by Mrs van Aardenne-Ehrenfest about just "distributions". This claim is not easy to see. Here we show why this claim holds.

Recall that the discrepancy of a sequence is defined as follows:

$$D_N(a) := \sup_{0 \le \alpha < \beta \le 1} \left| \frac{A_N([\alpha, \beta))}{N} - (\beta - \alpha) \right|.$$

The Aardenne-Ehrenfest Theorem stated that $N \cdot D_N(a)$ cannot be bounded by any constant, i.e.,

$$\lim_{N \to \infty} N \cdot D_N(a) = \infty.$$

Now back to the question, how is this implied by the conjecture? We show this in two steps. First, we show that the conjecture of (3.23) implies that at least one of (3.21) or (3.22) has to hold. Afterwards, we show that this implies the Aardenne-Ehrenfest Theorem.

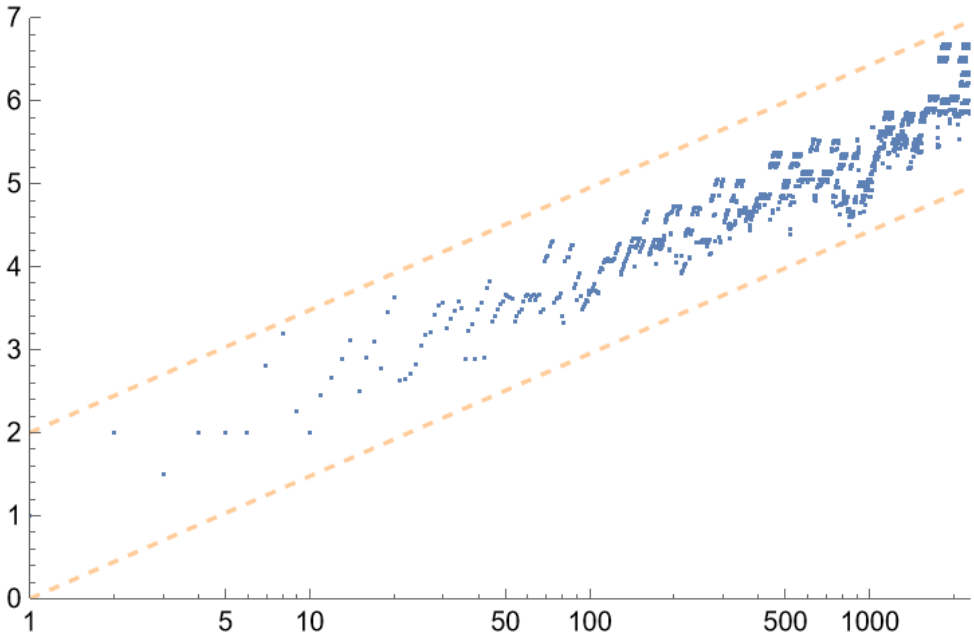

Figure 3.9.: r($\mu_r - 1$) for the vdC-sequence, for different r. Tested for the first 8192 numbers of the sequence.

Lemma 3.14. *If* $r(\mu_r - 1) \to \infty$ *for* $r \to \infty$, *then* $(\Lambda_r - \lambda_r) \to \infty$ *for* $r \to \infty$.

Proof. First, we rewrite the conjecture using the fact that $\mu_r \leq \frac{\Lambda_r}{\lambda_r}$:

$$r(\mu_r - 1) \leq r\left(\frac{\Lambda_r}{\lambda_r} - 1\right) = \frac{r}{\lambda_r}(\Lambda_r - \lambda_r).$$

Now we want to use $\lambda_r \geq \frac{r}{2}$. This is a broad bound we can derive from the vdC-sequence, where all intervals at any given moment only have two different sizes, and one is half the size of the other. Thus:

$$\frac{r}{2n} \leq m_n^r \leq \frac{r}{n} \leq M_n^r, \leq \frac{2r}{n}$$

and therefore

$$\frac{1}{2}r \leq n \cdot m_n^r \leq \lambda_r \leq r \leq \Lambda_r \leq n \cdot M_n^r \leq 2r.$$

We rewrite this bound as $\frac{r}{\lambda_r} \leq 2$, which we can use as follows:

$$r(\mu_r - 1) \leq \frac{r}{\lambda_r}(\Lambda_r - \lambda_r) \leq 2(\Lambda_r - \lambda_r).$$

This means that if $r(\mu_r - 1) \to \infty$ for $r \to \infty$, then it also has to hold that $(\Lambda_r - \lambda_r) \to \infty$ for $r \to \infty$. □

This in turns means that if the μ-conjecture holds, either Equation (3.21) or (3.22) has to hold, because

$$(\Lambda_r - \lambda_r) = (\Lambda_r - r) + (r - \lambda_r)$$

and if the left-hand side goes to infinity for r to infinity, then at least one of the terms on the right-hand side has to as well. We finish the claim by showing that either one of these implies the Aardenne-Ehrenfest Theorem.

Lemma 3.15. *If* $(\Lambda_r - \lambda_r)$ *tends to* ∞*, then* $\lim_{N\to\infty} N \cdot D_N(a) = \infty$.

Proof. We show this by proving the following 2 statements:

$$\Lambda_r - r \leq \sup_{0\leq\alpha<\beta\leq 1} N\left((\beta-\alpha) - \frac{A_N([\alpha,\beta))}{N}\right) \tag{3.26}$$

$$r - \lambda_r \leq \sup_{0\leq\alpha<\beta\leq 1} N\left(\frac{A_N([\alpha,\beta))}{N} - (\beta-\alpha)\right) \tag{3.27}$$

Since $(\Lambda_r - \lambda_r) \to \infty$ implies $\Lambda_r - r$ or $r - \lambda_r$ must tend to ∞, proving these two statements would mean that:

$$\Lambda_r - \lambda_r \text{ tends to } \infty \Rightarrow \sup_{0\leq\alpha<\beta\leq 1} N\left|(\beta-\alpha) - \frac{A_N([\alpha,\beta))}{N}\right| \text{ tends to } \infty,$$

which proves the original statement.

First, we show that Equation (3.26) holds. For any sequence, choose $[\alpha,\beta)$ to be the largest r-interval. Then it must hold that:

$$\sup_{0\leq\alpha<\beta\leq 1} N\left((\beta-\alpha) - \frac{A_N([\alpha,\beta))}{N}\right) \geq N\left(M_N^r(a) - \frac{r}{N}\right) = \left(NM_N^r(a) - r\right) \geq (\Lambda_r - r),$$

which proves Equation (3.26). The proof of Equation (3.27) is similar, but is done with the smallest r-interval:

$$\sup_{0\leq\alpha<\beta\leq 1} N\left(\frac{A_N([\alpha,\beta))}{N} - (\beta-\alpha)\right) \geq N\left(\frac{r}{N} - m_N^r(a)\right) = \left(r - Nm_N^r(a)\right) \geq (r - \lambda_r).$$

This concludes the proof. □

3.4. FINITE DE BRUIJN-ERDŐS SEQUENCES

In this section, we investigate the best possible λ and Λ for finite sequences. We first show that optimal sequences have unique lengths of intervals. Afterwards, we provide a formula for optimal finite De Bruijn-Erdős sequences, and prove their optimality.

Let $m_k(w)$ be the smallest interval after the first k points of the sequence

w have been placed. De Bruijn and Erdős [25] found the upper bound described in Section 3.1.3, which tells us that for any sequence w it holds that:

$$\inf_{1\leq k\leq 2n} k\cdot m_k(w) \leq \frac{1}{2\,(H_{2n}-H_n)}, \tag{3.28}$$

where H_x is the x-th harmonic number. The right side of the equation approaches $\frac{1}{2\ln(2)}$ from above, as n goes to infinity. De Bruijn and Erdős also provided a sequence which matches this upper bound as n goes to infinity, showing that for infinite sequences, no better sequence is possible. However, since the bound is only tight in infinity, it leaves an opportunity for improvement for finite sequences. Especially for small n, there is a decent gap between these. In Figure 3.10 nM_n and nm_n for the first n points of the De Bruijn-Erdős Sequence is plotted versus the best possible values according to the bounds from Sections 3.1.2 and 3.1.3.

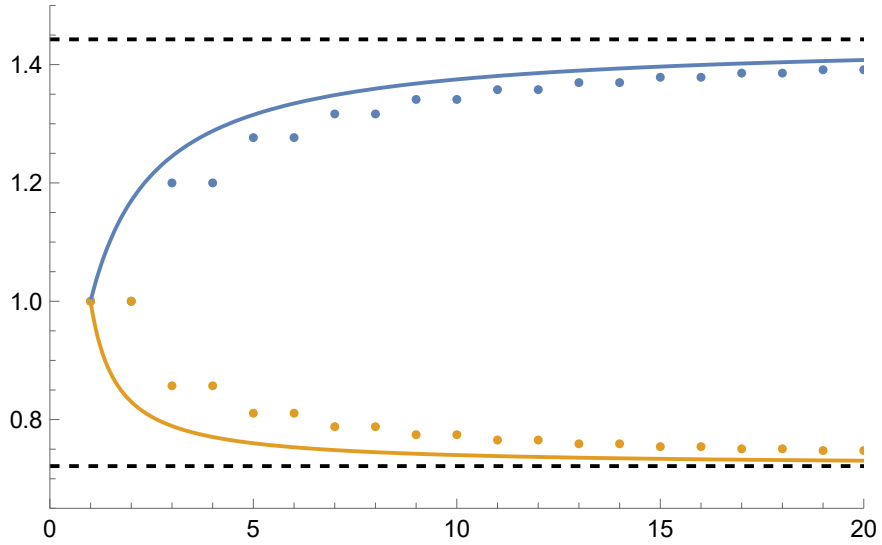

Figure 3.10.: The continuous lines are nM_n and nm_n for the de Bruijn-Erdős sequence, the dots are the best upper and lower bounds possible for a sequence of n length, and the dashed lines are the asymptotes.

We want to close this gap. It turns out that the upper bound of Equation (3.28) is achievable. We first show that any sequence which matches this upper bound has unique lengths of intervals. Afterwards, we give a formula and prove that this does provide an optimal finite DBE-sequence.

3.4.1. UNIQUENESS OF INTERVAL LENGTH

In this section, we show how to construct optimal finite DBE-Sequences and that the lengths of the intervals are uniquely determined. By uniquely determined, we mean that if the interval lengths are sorted on length, the sorted sequence is unique.

If two seating sequences end up with the same sorted interval lengths at every step, we regard those as equivalent. We start with showing that the lengths of the intervals are unique after all the points of the sequence have been placed, and afterwards extend this to show they are unique at every step.

Lemma 3.16. *For any optimal finite DBE-Sequences, the lengths of the intervals are uniquely determined, after all points have been placed*

Proof. Let w be a sequence and let the length of its intervals be $a_1, a_2, \ldots, a_{2n}$, sorted in descending order. Theorem 3.5 provides the following lower bound on all a_j: for any a_j with j even, it holds that:

$$a_{2n} \geq \frac{\lambda(w)}{2n}, \quad \ldots, \quad a_{2n-2k} \geq \frac{\lambda(w)}{2n-k}, \quad \ldots, \quad a_2 \geq \frac{\lambda(w)}{n+1}. \tag{3.29}$$

For any a_j with j odd, $a_j \geq a_{j+1}$ provides a lower bound. Theorem 3.5 establishes an upper bound on λ by summing the lower bounds on the lengths of all intervals present after placing all $2n$ points. Since this DBE-Sequence w is optimal, it is tight on this upper bound on λ. Therefore, it must hold that the lengths of the intervals are tight on these lower bounds. This means that these are the only possible lengths of intervals, and thus unique. □

We now want to extend this to uniqueness at every step. To understand why this is the case, we first look at the example of an optimal DBE-Sequence of length 8, before proving it formally. For an optimal DBE-Sequence w of length 8, the lengths of the 8 intervals after all points have been placed must be: $\frac{\lambda}{8}, \frac{\lambda}{8}, \frac{\lambda}{7}, \frac{\lambda}{7}, \frac{\lambda}{6}, \frac{\lambda}{6}, \frac{\lambda}{5}, \frac{\lambda}{5}$, where the sum of them is exactly 1.

From these interval lengths, we can determine how the sequence was created. Any interval of length $\frac{\lambda}{x}$ can only exist after at least x points have been placed, otherwise the sequence would not have $\lambda(w) = \lambda$. Therefore, the two intervals of length $\frac{\lambda}{8}$ could only be created by the 8th and final point. This means the two intervals of length $\frac{\lambda}{7}$ must have been created by the 7th point, since adding any point can only create two new intervals. In the same way, it follows that the intervals of length $\frac{\lambda}{6}$ and $\frac{\lambda}{5}$ were created by the 6th and 5th point of the sequence respectively.

We have now determined exactly when the eight final intervals were created. They were all created by the placement of points 5, 6, 7 or 8. Since all these intervals exist when all points have been placed, we now know that none of the points 5, 6, 7 or 8 can be adjacent to each other, since this would destroy an earlier created interval. Thus, the sequence would look like this:

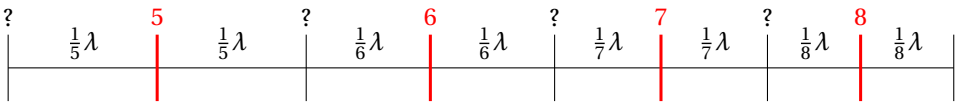

We still don't know the exact locations of the points, and we don't know which points they are adjacent to. We can determine this by looking at the interval after four points have been placed. We now know that the four intervals existing at that moment must have had the specific lengths: $\frac{2\lambda}{5}, \frac{2\lambda}{6}, \frac{2\lambda}{7}$ and $\frac{2\lambda}{8}$. Using the same reasoning as before, it follows that the intervals with length $\frac{2\lambda}{8}$ and $\frac{2\lambda}{7}$ have to be adjacent to the 4th point, and the intervals with length $\frac{2\lambda}{6}$ and $\frac{2\lambda}{5}$ have to be adjacent to the 3rd point.

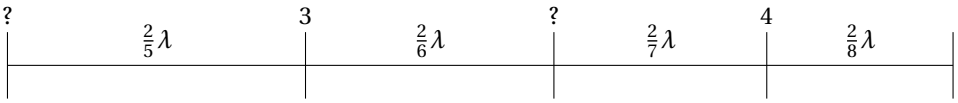

Since the choice of the first and second point are symmetric, this means the interval lengths are fully determined at each step. This process can be repeated for any finite DBE-Sequence, to place all points. In general, it holds that, for any point of any optimal finite DBE-Sequence:

- The length of an interval in which a point is placed is unique.
- The lengths of the two intervals created are unique.
- As a consequence, the lengths of all intervals at every step are unique.

Lemma 3.17. *Let w be an optimal DBE-sequence of length $2n$. After $2j$ points of the sequence have been placed, let the lengths of the intervals be $a_1, a_2, \ldots, a_{2j}$, sorted in descending order. It then holds that:*

$$\frac{\lambda}{j+i-1} > a_{2i-1} \geq a_{2i} \geq \frac{\lambda}{j+i}$$

for $i = 1, \ldots, j$. Furthermore, every time a point is placed, it is placed in the interval with the largest length, and the two newly created intervals are smaller than all pre-existing intervals.

Proof. We prove this by backward induction. From Lemma 3.16, we know that these interval lengths hold after all $2n$ points of the sequence have been placed. We now want to show that if this holds when $2j$ points have been placed, it also holds when $2j-2$ points have been placed. Furthermore, we show that both point $2j$ and $2j-1$ are placed in what was the largest interval at the time, and created the two newly created intervals, which are smaller than all pre-existing intervals.

From the induction hypothesis we can determine that for the smallest two intervals it holds that $\frac{\lambda}{2j-1} > a_{2j-1}, a_{2j}$. However, in an optimal DBE-sequence, any interval smaller than $\frac{\lambda}{x}$ cannot exist after x points have been placed. This must mean that these two intervals were created when the $2j$-th point was added. So, after only $2j-1$ points were placed, a_{2j-1} and a_{2j} still formed one interval together,

of length $a_{2j-1} + a_{2j}$. Let us call this interval y with length I_y. Since $I_y = a_{2j-1} + a_{2j}$, it holds that:

$$\frac{2\lambda}{2j-1} > I_y \geq \frac{2\lambda}{2j}$$
$$\frac{\lambda}{j-1} > \frac{\lambda}{j-\frac{1}{2}} > I_y \geq \frac{\lambda}{j}$$

This means interval y was the interval with the largest length when point $2j$ was placed. Thus, point $2j$ was placed in the interval with the largest length, and the two newly created intervals are smaller than all pre-existing intervals.

Now we look at the intervals with lengths a_{2j-3}, a_{2j-2}. These are the smallest intervals after $2j-1$ points have been placed, since the intervals with lengths a_{2j-1} and a_{2j} no longer exist. From the induction hypothesis we get that $\frac{\lambda}{2j-2} > a_{2j-3}, a_{2j-2}$. Since these intervals are therefore too small to be created by one of the first $2j-2$ points, it must mean that these two intervals were created when the $(2j-1)$-th point was added. So, after only $2j-2$ points were placed, a_{2j-3} and a_{2j-2} formed one interval together. We call this interval z with length I_z. Since $I_z = a_{2j-3} + a_{2j-2}$, it holds that

$$\frac{2\lambda}{2j-2} > I_z \geq \frac{2\lambda}{2j-1}$$
$$\frac{\lambda}{j-1} > I_z \geq \frac{\lambda}{j-\frac{1}{2}} > \frac{\lambda}{j}$$

Since it holds that

$$I_z \geq \frac{\lambda}{j-\frac{1}{2}} > I_y,$$

it follows that z was the interval with the largest length when point $2j-1$ was placed. Hence, point $2j-1$ was also placed in the interval with the largest length, and the two newly created intervals are smaller than all pre-existing intervals.

So, after $2j-2$ points have been placed, there exist $2j-2$ intervals with lengths $I_z \geq I_y \geq a_1 \geq a_2 \geq \cdots \geq a_{2j-4}$. Since we have shown that

$$\frac{\lambda}{j-1} > I_z \geq I_y \geq \frac{\lambda}{j}$$

and it still holds that

$$\frac{\lambda}{j+i-1} > a_{2i-1} \geq a_{2i} \geq \frac{\lambda}{j+i}$$

for $i = 1, \ldots, (j-2)$, we have the bounds on interval lengths required by the induction step. □

Using these two Lemmas, we can prove uniqueness of interval length

Theorem 3.18. *For any optimal finite DBE-Sequences, the lengths of the intervals are unique after any number of points is placed.*

Proof. In Lemma 3.17, we proved that any point of the sequence must always be placed in the largest interval, and splitting it into the two smallest intervals. If the length of these two smaller intervals are unique, then the length of the original largest interval must also be unique. Since we have shown in Lemma 3.16 that the lengths of the intervals are unique when all points are placed, it follows from backwards induction that all lengths of the intervals are unique after any number of points are placed. □

The only difference allowed in optimal finite DBE-Sequences is in symmetries, as there are always two positions that can be chosen to divide an interval into two specific different lengths. For example, to split an interval of length 1 into two intervals of lengths 0.4 and 0.6, you could place a point at either 0.4 or 0.6. In Figure 3.11, there are two optimal finite DBE-Sequences of length 8, in which the location of the second point is chosen differently between them. This causes the fifth and sixth point to differ as well. The lengths of the 8 intervals are still unique, just in a different order.

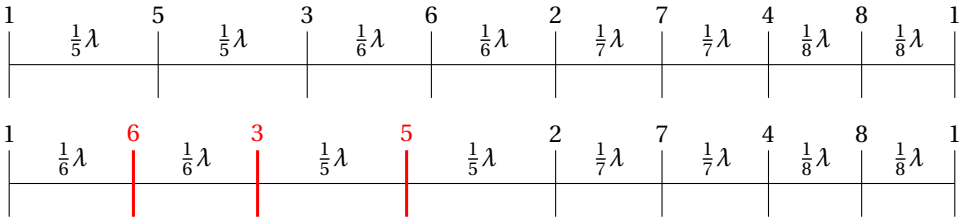

Figure 3.11.: Two optimal DBE-Sequences of length 8

3.4.2. FINITE DBE-SEQUENCE WITH BEST POSSIBLE λ

Now we know what the lengths of the intervals should be, and that they are unique. In this section, we provide a formula for optimal finite DBE-Sequences. We show that the sequence we provide matches the upper bound of Equation (3.28), proving that our sequence is the best possible.

We refer to our sequence as the $2n$-sequence. It is defined as follows:

Definition 3.19 ($2n$-sequence)**.** *Let $2n$ be any even integer. The $2n$-sequence is a finite sequence $w := (w_1, w_2, \ldots, w_{2n})$ where the points are defined as:*

$$w_k = \begin{cases} \dfrac{2H_{b(1)} - 2H_{(2k-1)b(k)}}{2(H_{2n} - H_n)} \mod 1 & \text{For } 1 \le k \le n \\ \dfrac{2H_{b(1)} - H_k - H_{k-1}}{2(H_{2n} - H_n)} \mod 1 & \text{For } n < k \le 2n \end{cases}$$

where

$$b(k) = 2^{\lfloor \lg \frac{2n}{2k-1} \rfloor}$$

We show that this sequence is optimal with the following theorem:

Theorem 3.20. *For the $2n$-sequence, it holds that*

$$\inf_{1 \le k \le 2n} k \cdot m_k(w) = \frac{1}{2(H_{2n} - H_n)}$$

Proof. Let w_k be the k-th point of the $2n$-sequence and let I_l, I_r be the length of the two intervals created by placing w_k. For the theorem to hold, we have to prove that

$$I_l, I_r \ge \frac{1}{2k(H_{2n} - H_n)} \tag{3.30}$$

Since this function is strictly decreasing in k, we only have to prove it for the two new intervals formed. Together with the upper bound of Equation (3.28), the theorem follows. We prove Equation (3.30) in two steps. First we show that this holds in the case of $1 < k \le n$, and afterwards we show this holds for the case $n < k \le 2n$.

Case 1: $1 < k \le n$
In the case of $1 < k \le n$, w_k is placed at

$$\frac{2H_{b(1)} - 2H_{(2k-1)b(k)}}{2(H_{2n} - H_n)} \mod 1$$

To determine I_l and I_r, we need to which of the points $w_1, \ldots, w_{k-1}$ are closest to w_k. Specifically, we are looking for the largest w_l and smallest w_r for which holds that $w_l \le w_k \le w_r$. Since $w_1 = 0$, we know w_l always exists. If no w_i is larger than w_k, take $w_r = 1$, which is equal to $w_0 \mod 1$.

To determine the location of w_l and w_r, we look at the definition of the sequence. The location of a point w_i is completely determined by the value of $(2i-1)b(i)$. If the value of $(2i-1)b(i)$ is close to $(2k-1)b(k)$, then w_i is close to w_k. Specifically, for w_l and w_r, $(2l-1)b(l) > (2k-1)b(k) > (2r-1)b(r)$ are the closest in value for any i. Now we study how close this value can get.

Note that $b(i)$ is a monotone decreasing function, which is always a power of 2. Therefore, for all w_i placed before w_k, $(2i-1)b(i)$ is always divisible by $b(k)$. This means for w_l and w_r that $(2l-1)b(l) \ge (2k)b(k)$ and $(2k-2)b(k) \ge (2r-1)b(r)$.

Therefore, the two closest points possible are:

$$w_l = \frac{2H_{b(1)} - 2H_{(2k)b(k)}}{2(H_{2n} - H_n)} \mod 1$$

and

$$w_r = \frac{2H_{b(1)} - 2H_{(2k-2)b(k)}}{2(H_{2n} - H_n)} \mod 1$$

where the interval I_l is always smaller or equal to I_r. It also follows that the size of this interval is decreasing in k, therefore this is always the smallest interval that exists. The exact size of the interval I_l is:

$$\begin{aligned} I_l = w_l - w_k &= \frac{2H_{(2k)b(k)} - 2H_{(2k-1)b(k)}}{2(H_{2n} - H_n)} \\ &= \frac{1}{2(H_{2n} - H_n)} \sum_{i=(2k-1)b(k)+1}^{(2k)b(k)} \frac{2}{i} \\ &\geq \frac{1}{2(H_{2n} - H_n)} b(k) \frac{2}{2kb(k)} = \frac{1}{2k(H_{2n} - H_n)} \end{aligned}$$

which is the required inequality.

Case 2: $n < k \leq 2n$
In the case of $n < k \leq 2n$, w_k is placed at:

$$\frac{2H_{b(1)} - H_k - H_{k-1}}{2(H_{2n} - H_n)} \mod 1$$

Thus the closest two points possible are:

$$w_l = \frac{2H_{b(1)} - 2H_k}{2(H_{2n} - H_n)} \mod 1$$

and

$$w_r = \frac{2H_{b(1)} - 2H_{(k-1)}}{2(H_{2n} - H_n)} \mod 1$$

The intervals between these points and w_k are both of size:

$$\frac{H_k - H_{k-1}}{2(H_{2n} - H_n)} = \frac{1}{2k(H_{2n} - H_n)}$$

which is exactly the required lower bound. It also follows that the size of this interval is decreasing in k, therefore this is always the smallest interval that exists. This concludes the proof. □

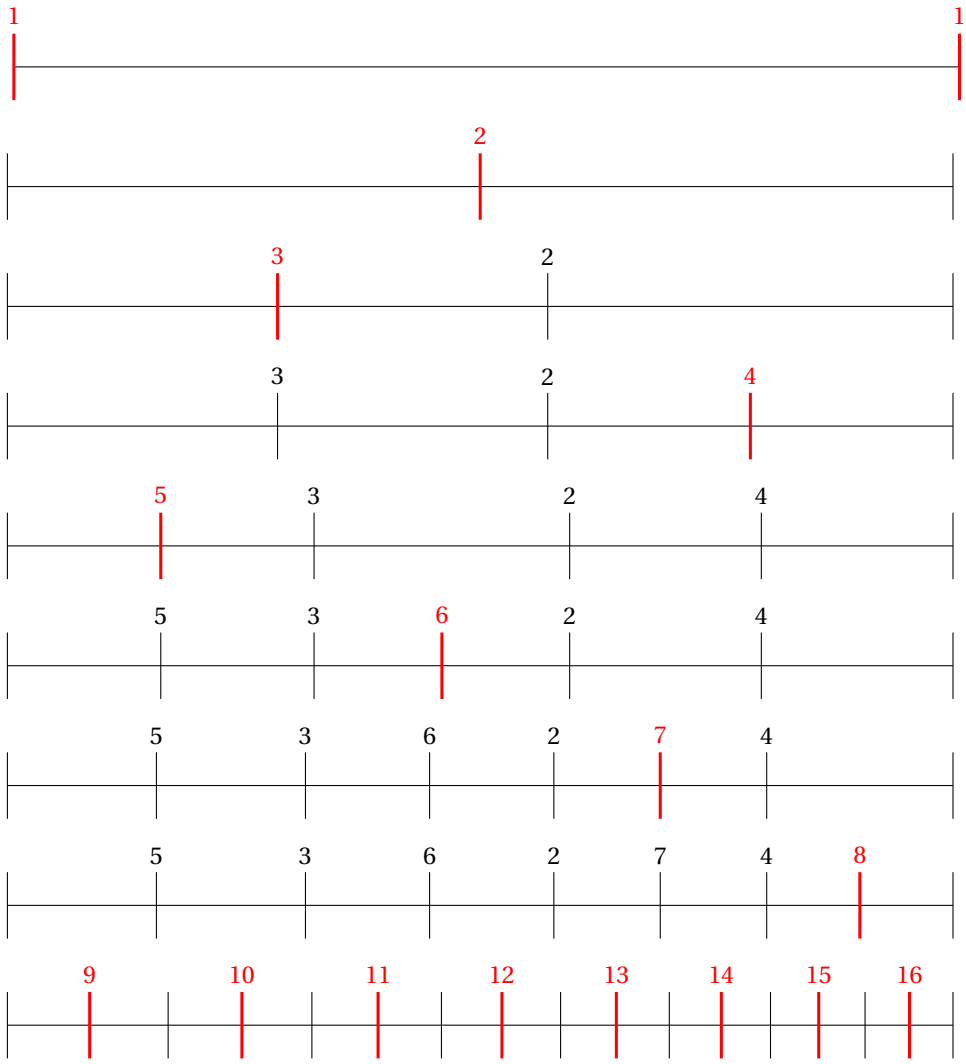
1 1
2
3 2
3 2 4
5 3 2 4
5 3 6 2 4
5 3 6 2 7 4
5 3 6 2 7 4 8
9 10 11 12 13 14 15 16

REFERENCES CHAPTER 3

[1] A. Buijsrogge, R. Lindelauf, A. van de Rijt, and J.-T. Brethouwer. "Self-Organized Social Distancing". In: *Submitted to the Journal of Mathematical Sociology* (2023).

[2] J.-T. Brethouwer, A. Buijsrogge, and R. Fokkink. "On an equidistribution problem of De Bruijn and Erdős". In: *Paper in preparation* (2024).

[25] N. G. de Bruijn and P. Erdös. "Sequences of points on a circle". In: *Proceedings of the Section of Sciences of the Koninklijke Nederlandse Akademie van Wetenschappen te Amsterdam* 52.1 (1949), pp. 14–17.

[26] A. Ostrowski. "Eine Verschärfung des Schubfächerprinzips in einem linearen Intervall". In: *Archiv der Mathematik* 8.1 (1957), pp. 1–10.

[27] G. Toulmin. "Subdivision of an interval by a sequence of points". In: *Archiv der Mathematik* 8.3 (1957), pp. 158–161.

[28] L. Ramshaw. "On the gap structure of sequences of points on a circle". In: *Indagationes Mathematicae (Proceedings)*. Vol. 81. 1. Elsevier. 1978, pp. 527–541.

[29] F. Chung and R. Graham. "On the discrepancy of circular sequences of reals". In: *Journal of Number Theory* 164 (2016), pp. 52–65.

4

"STAY NEARBY OR GET CHECKED": A COVID-19 CONTROL STRATEGY

In this chapter, we study the spread of COVID-19, using social network models. This research was done at the height of the outbreak in 2020. These were times filled with a sense of uncertainty, as this epidemic was unprecedented in the modern world. The epidemic presented novel challenges, prompting widespread measures like lockdowns and a swift transition to remote work. The abrupt reduction in social contacts had negative effects on most people. This chapter contains our ideas on how to control the spread of the epidemic, while allowing for more social contacts. This work is written with the data available at that time, as we wanted to offer our solutions as soon as possible. This means we mostly use data up until June 2020, and focus our ideas on reducing the second wave, as these were important issues at the time.

Our model is based on the classical insight from network theory that long-distance connections drive disease propagation. We repurpose this insight into a strategy for controlling COVID-19. We simulate a scenario in which long-range transmission in a population is kept at a minimum. Simulated spreading patterns resemble recent distributions of COVID-19 across EU member states, German and Italian regions, and New York City zip codes, providing some model validation. Results suggest that our proposed strategy may significantly reduce peak infection. We also find that flare-ups remain local longer, providing more time for geographical containment. These results suggest a tailored policy in which individuals who frequently travel to places where they interact with many people are offered greater protection, tracked more closely, and are regularly tested. This policy can be communicated to the general public as a simple and reasonable principle: Stay nearby or get checked.

This work eventually led us to compete in the COVID-19 prediction challenge, a challenge in which researchers could use a prediction model to predict the number of COVID-19 deaths. We participated in the USA category, in which our

Parts of this chapter have been published in Infectious Disease Modelling **6**, 36–45 (2021) [3].

model outperformed all other participants. The challenge organisers have written a paper about the challenge and its results, of which we are coauthor [4].

4.1. INTRODUCTION

Many countries are currently experiencing a second wave of COVID-19 after having exited a lockdown regime in which person-to-person contact was severely restricted. The constraints placed on social and economic interaction have had high costs. Public support for nation-wide restraints on freedom of movement has waned. This raises the question what alternative control strategies may be possible that are less taxing?

Here we explore the leverage gained from differentiating between short-distance and long-distance ties in post-lockdown policy. The idea is that the blockage of transmission through long-distance ties increases the effective *diameter* of a network, which is inversely related to the speed of propagation [30, 31]. In practice, such geographic differentiation may be achieved through prioritization of non-local travel and transport in policy restrictions, enforcement and medical testing as well as location tracking technologies. The relative sparsity of long-range ties may make tight control feasible through a focus of resources on a small number of key individuals or interactions.

Results show that reductions in transmission through long-range ties slow down COVID-19 to a much greater extent than reductions in short-range ties. Selective scrutiny of long-distance ties has two added benefits: Flare-ups of COVID-19 are local, allowing geographically focused interventions that are of limited economic damage and logistically more feasible. And social toll is diminished, as the intimacy of human relations and need for face-to-face contact are known to decrease sharply with geographical distance [32–38].

Our work is organized as follows. In Section 4.2 we describe our proposed strategy. In Section 4.3 we describe our mathematical model and validate it against the data. In Section 4.4 we present the results of model simulations. Section 4.5 summarizes our findings and recommendations.

4.2. RELATED WORK

Social network models of disease spreading have been around for decades. What sets our work apart is an analysis of the epidemiological leverage of government policies that differentiate long-distance from short-distance ties in social networks.

4.2.1. SOCIAL NETWORK MODELS OF INFECTIOUS DISEASE SPREAD

Many epidemiological studies assume random mixing of individuals within demographic subgroups (e.g. by age) [39, 40]. However, most contact occurs between people who live very close to one another [41, 42]. We draw on the well-known

small-world model of Watts and Strogatz [17] to capture the fundamental difference in viral risk between close-range and long-range ties: Close-range ties connect infected individuals with others who are already infected or will probably be soon anyway. Long-range ties connect infected areas with uninfected areas, acting as highways of transmission.

The small-world approach to the study of epidemiological dynamics is not new. Network analysis was introduced into mainstream epidemiology at the turn of the century to explicitly incorporate the contact structure among individuals. It is well known that diffusion processes on networks depend on the corresponding connectivity patterns [43]. Research has shown that subtle features of the network structure have a major impact on the transmission of an epidemic [44, 45] and that social networks can be modelled through random modifications of regular networks, such as lattice networks [17, 46]. This subtle difference consists of a small portion of random ties to distant localities on the lattice, producing a dramatic reduction in a network's diameter. The epidemiological dynamics on such networks has been examined for a range of models in [47–49], which all show that the speed of the spread is inversely proportional to the diameter. As social networks have a small diameter (the well known six degrees of freedom), epidemics are hard to contain in time within confined regions of a population.

Since all social networks show similar epidemiological dynamics,[1] we choose to model the COVID-19 epidemic on a small-world graph, which is a very well understood model. A small-world SEIR model was used in [50] to model an influenza outbreak in the city of Oran (Algeria). In a study closest to ours, Small and Tse investigate disease spread in a small-world network with separate infection probabilities for short-distance and long-distance ties [51]. Using a SEIR model of the SARS epidemic dynamics they find that exponential growth in infection occurs upon onset of several non-local infections. They conclude that key to capturing the empirically observed transmission dynamics is differentiating local from non-local transmission probabilities. We build on this observation to explore the leverage that the targeting of Covid-19 policy at reductions of non-local transmission may provide to global, national, or regional policy makers.

4.2.2. INTERVENTIONS

In epidemiological models, effects of both general and targeted interventions on disease spread have been studied [52]. General interventions such as social distancing and school closures aim to bring down overall infection probabilities or those within and between demographic subgroups [40]. Targeted interventions seek to identify high-risk individuals [39]: Antiviral treatment and household isolation of identified cases, prophylaxis and quarantine of household members. We propose a kind of targeting that is aimed at *nodes* that connect dangerous *edges* in a network.

[1] This applies to diseases such as influenza or COVID-19, which affect the entire society. Sexually transmitted diseases such as HIV require more special network models [47]

A challenge faced by contemporary policy makers is when and how to ease interventions. It is well known that when a lockdown is lifted, a virus tends to re-appear [53] and this has indeed happened in many countries. How can a second wave be contained while at the same time preventing enormous economic costs? Therefore, it is of paramount importance to find ways to regain some form of normal life (alleviating lockdown) while at the same time maintaining control over the virus. The main idea proposed here is that restricting certain high-risk interactions within the social network may be an effective alternative strategy to restricting movement of an entire population. 'Long-distance' ties represent interaction between individuals that are distant to each other in a network. Typically, this means they are also physically distant, i.e., think of a truck driver that delivers goods to a company on the other side of the country or individuals traveling by plane that encounter each other at airports and in airplanes where social distancing is difficult or next to impossible. Small-world models suggest that long-distance ties greatly accelerate the speed of transmission. Long-range ties stemming from infected individuals allow disease to start spreading in not-yet-infected individuals and regions. At a global level, long ties predominantly involve international highways and airline transportation. Topological properties of airline transportation networks can explain patterns in viral disease spread worldwide [42, 54]. At a national level, long ties pertain to mobility through major roads and trains between cities. At a regional level, they involve commuting and local delivery services.

4.3. MODEL

4.3.1. SMALL WORLD SEIR MODEL

We model the spread of the disease by a small world network, in which each node of the network is either Susceptible, Exposed, Infectious, or Recovered (an SEIR model [50, 55]). In this model, nodes are individuals and we extrapolate our results to large communities (countries, continents). Initially, a node is in state S. If it is infected, it moves through states E, I, and R. While in state I, a node may infect each of its neighbors with a probability r per time step (fixed at one day in our simulations). The duration of state E is the incubation period, and the duration of state I is the infection period, both of which are lognormally distributed [56]. The probability r is our single calibration parameter, and all other parameters are fixed according to values that have been reported in the literature. In our simulations, the incubation period has a mean of 5 days and the infection time has a mean of 6.5 days, both periods have a standard deviation of 3 days. This is comparable to values reported in [40, 57–59]. Each simulation is started by infecting a single random node (patient zero).

The network in our model is the familiar Watts-Strogatz small world network, which distinguishes between short and long ties. An illustration of a small example network with $N = 100$, $k = 20$, and $p = 0.05$ is shown in Figure 4.1. It allows us to focus on a policy in which individuals that travel and interact with many

people need to be regularly tested (checked). We call this policy: stay nearby or get checked.

The network is described by two parameters k, p, where k is the number of ties per node, which is equal for all nodes, and p is the fraction of randomly selected long ties. In the simulations we fix $N = 10000$, $k = 20$, and $p = 0.1$, which is in the standard range [60] and has been used to model an influenza outbreak in the Oran region of Algeria [50]. Results are robust to reasonable changes in these parameters.

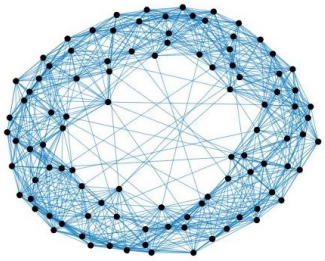

Figure 4.1.: An example of a Watts-Strogatz small-world graph with $N = 100$, $k = 20$ and $p = 0.05$.

4.3.2. MODEL CALIBRATION

We calibrated our model against the number of infections in Wuhan (source: Johns Hopkins), which went into an initial lockdown from January 23, followed by a heavy lockdown from February 10 [59]. A substantial number of infections remained undetected and our simulations are based on the estimate that only ten percent of the infected cases were officially confirmed [61]. After an exposed individual becomes infectious, it may take several days to develop symptoms, and from development of symptoms it takes an average of around 5 days to diagnosis [59], after which the patient quarantines and no longer spreads the disease. We therefore set the duration of the infectious state to 10 days in our model. We calibrated our model parameter r with values 0.055 in the period before lockdown, 0.0065 for the initial lockdown and 0.0012 for the severe lockdown. By using these values, we were able to reproduce the total number of officially confirmed cases, as demonstrated in Figure 4.2.

The reproduction number R_0 at the onset of the epidemic is equal to $r \cdot k \cdot t$ in our model. This value is high at the onset, but reduces already before the initial lockdown due to the clustered structure of the network. We find an average $R_0 = 3.9$ pre-lockdown, $R_0 = 0.54$ during the initial lockdown and 0.12 during the severe lockdown. These numbers agree with the statistical analysis in [59].

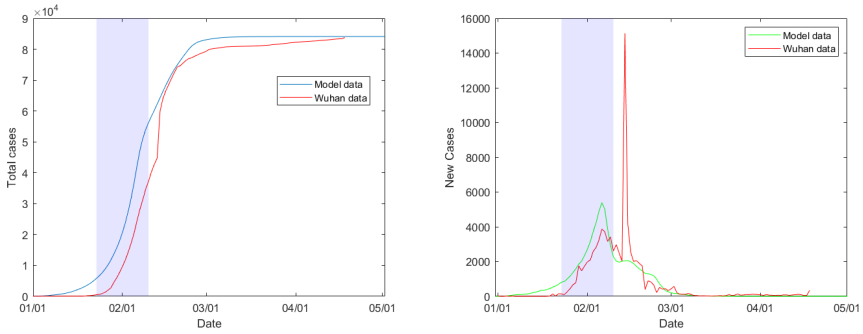

Figure 4.2.: Total number of officially confirmed cases (left) and daily number of new cases in the Hubei area. The shaded part represents the initial lockdown, between Jan 23 and Feb 10. The spike in new cases on Feb 12 was due to an inclusion of previously uncounted clinically diagnosed patients. The model data are an average of 200 Monte Carlo simulations.

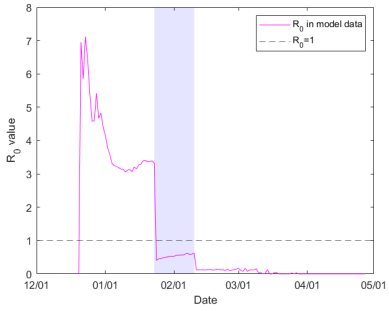

Figure 4.3.: The computed reproduction number R_0 during the simulation reduces from an initial 7.15 (from $r = 0.055, k = 20, t = 6.5$) but drops even before the lockdown of January 23. Its average is 0.54 during the initial lockdown (shaded area) and reduces even further during the severe lockdown.

We fixed $r = 0.055$ for all simulations of the spread of the disease before lockdown. We calibrated r after lockdown against the data of several European countries: Italy, Austria, Sweden, Germany. Italy announced its lockdown relatively late. We used $r = 0.01$ after lockdown. We find $R_0 = 4.0$ pre-lockdown, which is marginally higher than the 3.8 found in [59], and $R_0 = 0.84$ post-lockdown.

Austria implemented a relatively severe lockdown. We found that a parameter value of $r = 0.0055$ post-lockdown reproduces the number of confirmed cases.

To verify if the spread of the virus in our network model matches the observed spread of the disease, we compare our model to data on different scales: countries (American states, European countries), regions (in Italy and Germany), and cities

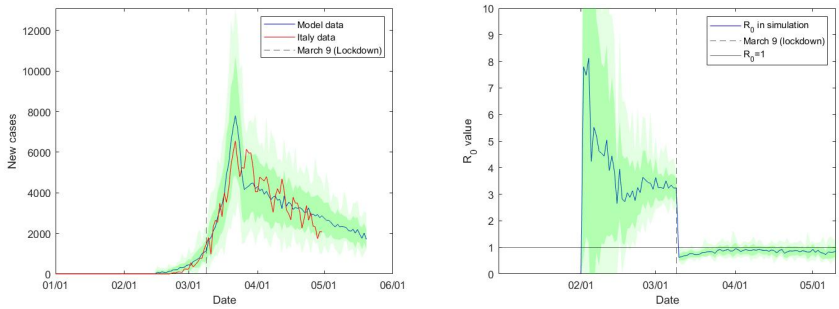

Figure 4.4.: Daily number of officially confirmed new cases in Italy (left) with $r = 0.01$ after lockdown. Our simulation starts with a single infected node on January 31 and we set the initial date of the lockdown on March 9, when the government announced nationwide regulations. We plotted one standard deviation difference in dark green, and a 98 percent confidence interval in light green around the model data to illustrate the accuracy of our model. We find an average reproduction number $R_0 = 4.0$ (right) before lockdown and $R_0 = 0.84$ after lockdown.

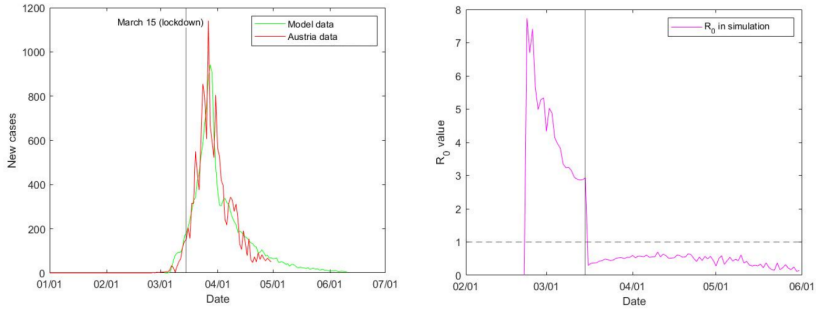

Figure 4.5.: Daily number of officially confirmed new cases in Austria (left) with $r = 0.0055$ after lockdown. Our simulation starts with a single infected node on February 22 and a lockdown at March 15. We find an average reproduction number $R_0 = 4.2$ (right) before lockdown and $R_0 = 0.55$ after lockdown.

(New York City zip codes). We order the data from largest to smallest and normalize by dividing by the largest number of cases. We find that the spread of the disease in our network model is comparable to the data, as illustrated in Figure 4.7. We summarize our calibration of the model in a table:

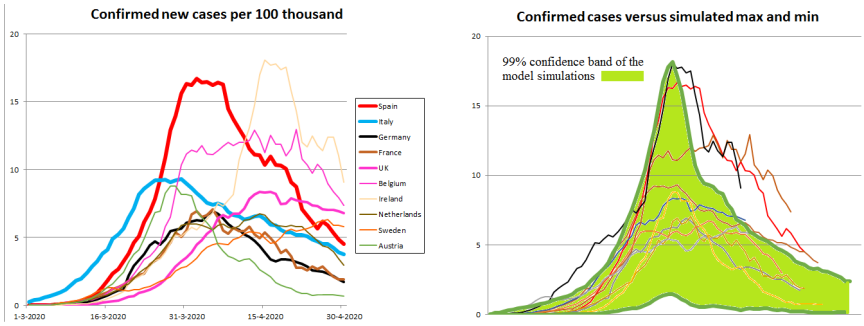

Figure 4.6.: A comparison of the daily number of officially confirmed new cases in ten EU countries during March and April 2020. The numbers are averaged over six days. In the right-hand figure, this data is adjusted so that the peak of the number of cases occurs after 50 days. This is compared to the 99% confidence band of a model computation with $r = 0.055$ pre-lockdown and $r = 0.0075$ during lockdown. Not all countries fit in the confidence band because their waves plateaued, while our model shows a sharp peak. The increase and decrease of the wave in our model does match the data.

r	Interpretation
0.001	Complete lockdown as in Wuhan after February 10th. Fully controlled society.
0.005	Severe lockdown as in Austria. Strong restrictions on travel, shopping, gatherings.
0.01	Moderate regulations and social distancing. As in many EU countries after March 15.
0.02	Requested social distancing, but no regulations.
0.055	Pre-lockdown situation. No social distancing.

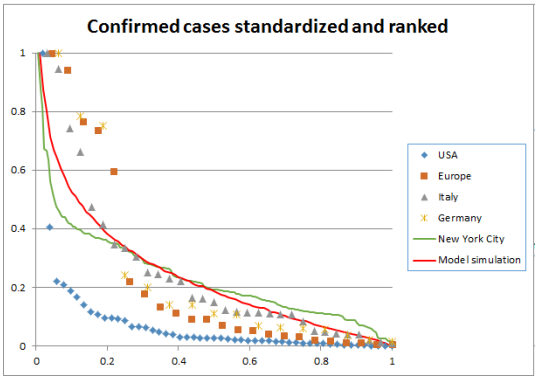

Figure 4.7.: Number of confirmed cases on three different scales: USA and Europe – Regione and Bundesländer – NYC zip codes. The data is ranked from largest to smallest and normalized. On each scale, the spread of the disease displays a similar exponential decay. The figure also shows the spatial distribution of Covid-19 spread in our model after 60 days, 25 days into lockdown. To this end, we arbitrarily divided the ring lattice of N = 10,000 nodes into 100 regions of 100 nodes each. The spatial distribution in our network is comparable to the data of Europe, Germany, Italy, and New York City. The spread of the disease in the USA is more concentrated, with an exceptional number of cases in New York and New Jersey.

4.3.3. MODEL VALIDATION

We calibrated our model against the initial outbreaks in China and the subsequent outbreaks in Europe at the beginning of 2020. In the European Union, the outbreak was followed by a lockdown which was more or less imposed simultaneously and uniformly by all member states in March, and was eased cautiously about three months later by first opening internal borders mid-June, followed by some external borders on 1 July, and a further relaxation of the rules in August. The response of the USA to the disease was more checkered. After an initial lockdown, which as in the EU began in March, some states eased their regulations at the end of April, and others did this one month later. This was followed by more tightened regulations, again varying from state to state, at the end of July.

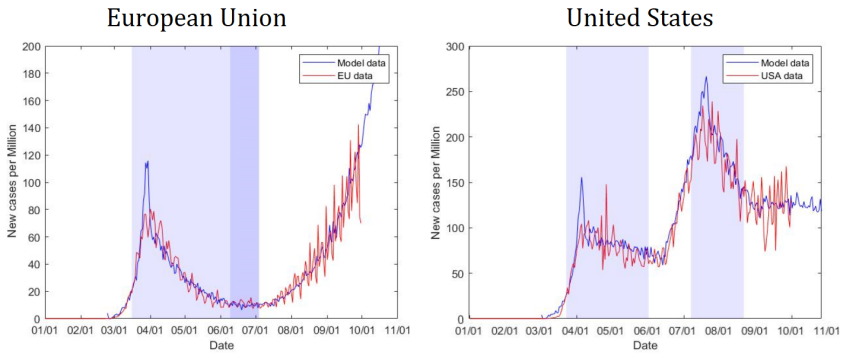

Figure 4.8.: Number of infections per 1 million of the population (source:Johns Hopkins). Europe versus USA. Our model parameters were $r = 0.008$ during a lockdown of eighty-five days in the EU and $r = 0.01$ for seventy days in the USA. We split the post-lockdown period of EU into 2 parts. The first is thirty-five days where we used $r = 0.011$, followed by $r = 0.015$ for the remaining days. For the USA we used $r = 0.016$ for the post-lockdown. The post-lockdown in the USA lasted for thirty-six days in our model computations, after which we reduced to $r = 0.01$ again for forty-five days, followed by $r = 0.012$ for the remaining days. To match the number of infections in our model with the real world data, we assumed that currently only 10 percent of positive cases are detected.

We validated our model against the number of infections in the EU and the USA using the calibrated parameters. For our simulation of the number of infections, we varied r uniformly. For EU, it was set at 0.008 during lockdown, 0.011 after lockdown when the internal borders opened up, and 0.015 post-lockdown. For the USA, we used a more varied approach. The lockdown was shorter and was followed by a post-lockdown parameter of 0.016. This was followed by a reduction to 0.01 thirty-six days later. After another forty-five days, it was set to 0.012 for the remaining days. The results in Figure 4.8 show that our small word SEIR model is able to reproduce the transmission of the disease quite well.

4.4. IMPACT OF A STAY-NEARBY-OR-GET-CHECKED POLICY

4.4.1. PEAK REDUCTION

As countries get out of lockdown, restrictions are lifted, and the basic reproduction number increases, inducing a second wave. Our proposed policy is to control the long ties to flatten the second wave. To simulate this policy, we use the parameters of the calibrated model. During an initial lockdown of 75 days, spreading risk is reduced to $r = 0.0075$. After lockdown, the parameter is increased to $r = 0.02$ (requested social distancing, but no regulations), a value (slightly) above the current values for the EU and US but sufficient to evaluate the effect of our policies. Some fraction of edges is checked, preventing propagation along those edges. Figure 4.9 contrasts a scenario in which random edges are checked (panel A) with one in which only long edges are checked (panel B). Results show that targeting long edges is efficient. Without intervention, a second wave occurs with a peak several times higher than the first. By targeting long ties, checking 7.5% of ties is sufficient to bring the second peak below the first peak, thereby also delaying its occurrence. If instead random ties are chosen, the second wave peak remains well above the first.

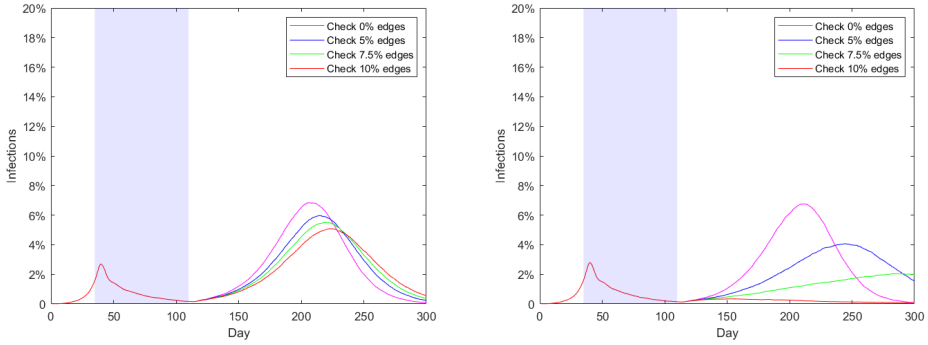

(a) Check random edges

(b) Check long edges

Figure 4.9.: Peak reduction with baseline $r = 0.02$ and some edges checked

In Figure 4.10 we contrast three post-lockdown strategies for controlling a second wave. Here we use r_{short} to denote transmission probabilities on all short ties and r_{long} transmission probabilities on long ties. The first strategy is to not differentiate long ties from short ties (panel A). Results show that at $r_{long} = r_{short} = 0.02$ (requested social distancing without further regulations) the second wave peaks much higher than the first, and that further regulation is needed to control it.

The second strategy is to open up society back to what it was before the pandemic ($r_{short} = 0.055$), with no social distancing, and then target the 10% of long ties for checking. Panel B shows various levels of effectiveness in intervening on long ties, varying r_{long}. Panel B shows that this strategy only works if disease propagation

in long ties can be fully prevented. In panel C, society is opened back up but social distancing is requested at an r = 0.02. Now, imperfect checking of long ties r_{long} = 0.005 can also accomplish a reduction of the second peak below the first.

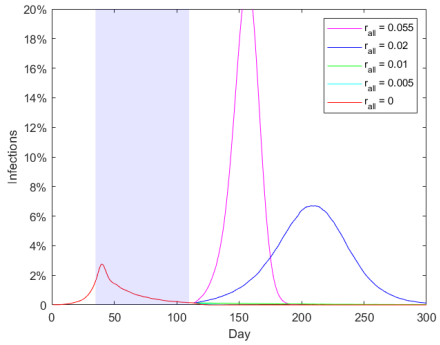

(a) Vary r_{short} and r_{long} together

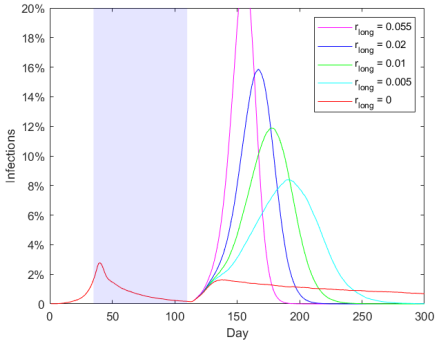

(b) Vary r_{long}, keep $r_{short} = 0.055$

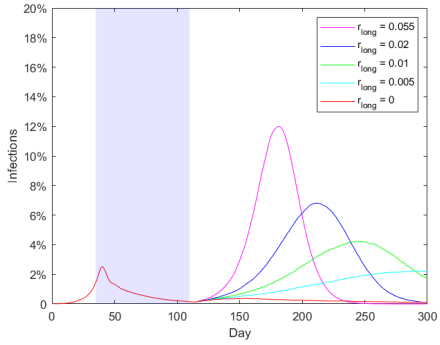

(c) Vary r_{long}, keep $r_{short} = 0.02$

Figure 4.10.: Three policy approaches to opening up a lockdown of 75 days, with varying post-lockdown levels of r: (a) policy does not differentiate long and short ties, (b) policy targets long ties while all other restrictions are lifted, and (c) policy targets long ties while social distancing is encouraged.

4.4.2. SPATIAL CONCENTRATION

Post-lockdown flare-ups are more easily controlled with geographically focused efforts when they remain local longer. Economic and social costs of control measures are then also lower. We study the spatial concentration of COVID-19 outbreaks by measuring the number of components of the subgraph of infected nodes and short edges. Figure 4.9 compares the spread of the virus for the scenario where $r_{long} = r_{short}$ = 0.055 with the alternative scenario where long-range transmission is maximally repressed, $r_{long} = 0$. The latter scenario is characterized by a smaller

number of components during the second wave. The spread of the virus with $r_{long} = 0$ is contained in one region.

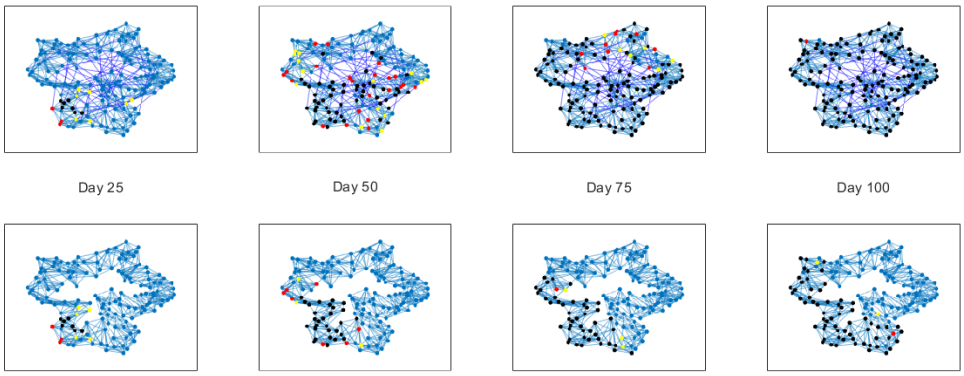

Figure 4.11.: Effect of shutting down long-range transmission. From left to right graphs show disease propagation at 25-day intervals in a small-world network with $N = 150$, $k = 10$ and $p = 0.1$. All graphs have $r_{short} = 0.055$. The top graphs have $r_{long} = 0.055$, while the bottom graphs have $r_{long} = 0$. Node color indicates SEIR states, blue = susceptible, yellow = exposed, red = infectious, black = resistant.

4.5. DISCUSSION AND POLICY

In this work, we have through model simulation explored spatially differentiating policies in which interventions target nonlocal spread of COVID-19. Our results show that reductions of long-distance transmission are highly efficient for curbing the spread of COVID-19. The close monitoring and checking of long-distance ties allows overall policy to be more permissible and still control a second wave. Because flare-ups remain local longer, interventions can be of limited geographical scope and thus less costly and invasive.

What policies could constrain long-range transmission? Medical testing and mobility-tracking apps may be targeted specifically at transport, travel, and delivery. Perhaps medical testing and / or mobility tracking should be encouraged or required for flight, use of highways, trains, regional bus lines and for individuals with jobs in the transport and delivery sector. Self-isolation after exposure of such individuals may perhaps be more stringently enforced. What helps is that long-range ties are relatively sparse, so resources may be focused on a limited number of individuals or activities. That said, our results show that effects are particularly strong when transmission through long-range ties is not just reduced, but largely eliminated. This concords with studies showing that international traffic constraints are particularly effective when severe [42]. The logistical, technological and ethical challenges of

geographic targeting in location tracking, testing, and police enforcement require further interdisciplinary study.

Finally, we point out that we studied the effect of our proposed policy by a mathematical model, which necessarily leaves out potentially relevant real world details. In the real world, the pandemic will cease if a sufficient percentage of the population reaches immunity (either through contracting the disease or through immunization). In our model, immunity is only reached if everybody has contracted the disease. The size of our network is in the order of 10 thousand nodes, while the actual scale of the societies that we model is 10 to 100 million people. Our model is too coarse to capture the passing of the epidemic, which is a known weakness of SEIR models, see [62]. However, the model does reproduce the early and middle stage, when government policy can be most effective. The small-world network that we use in our computations is a simple approximation of actual societal networks. It only has two scales (short and long) while real social networks have more scales, and can even be scale-free. There is reason to expect that our proposed policy of 'getting checked' will be even more effective in the real world than in our model. The small world network lacks highly connected nodes (superspreaders) that contact surveys reveal exist[39]. Such hubs could be efficiently targeted, neutralizing a large fraction of dangerous edges through restrictions on a small number of individuals.

REFERENCES CHAPTER 4

[3] J.-T. Brethouwer, A. van de Rijt, R. Lindelauf, and R. Fokkink. ""Stay nearby or get checked": A Covid-19 control strategy". In: *Infectious Disease Modelling* 6 (2021), pp. 36–45.

[4] M. A. Golden, T. Slough, H. Zhai, A. Scacco, M. Humphreys, E. Vivalt, A. Diaz-Cayeros, K. Y. Dionne, S. KC, E. Nazrullaeva, P. M. Aronow, J.-T. Brethouwer, A. Buijsrogge, J. Burnett, S. DeMora, J. R. Enríquez, R. Fokkink, C. Fu, N. Haas, S. V. Hayes, H. Hilbig, W. R. Hobbs, D. Honig, M. Kavanagh, R. H. A. Lindelauf, N. McMurry, J. L. Merolla, A. Robinson, J. S. Solís Arce, M. ten Thij, F. F. Türkmen, and S. Utych. "Gathering, Evaluating, and Aggregating Social Scientific Models". In: *Available at SSRN 4570855, submitted to Political Analysis* (2023).

[17] D. J. Watts and S. H. Strogatz. "Collective dynamics of 'small-world' networks". In: *Nature* 393.6684 (1998), p. 440.

[30] M. Kretzschmar and J. Wallinga. "Mathematical models in infectious disease epidemiology". In: *Modern Infectious Disease Epidemiology*. Springer, 2009, pp. 209–221.

[31] J. Wallinga, W. J. Edmunds, and M. Kretzschmar. "Perspective: human contact patterns and the spread of airborne infectious diseases". In: *TRENDS in Microbiology* 7.9 (1999), pp. 372–377.

[32] R. E. Park. "The concept of social distance: As applied to the study of racial relations". In: *Journal of applied sociology* 8 (1924), pp. 339–334.

[33] G. K. Zipf. "Human behavior and the principle of least effort." In: (1949).

[34] M. Granovetter. "The strength of weak ties: A network theory revisited". In: *Sociological theory* (1983), pp. 201–233.

[35] P. V. Marsden and K. E. Campbell. "Measuring tie strength". In: *Social forces* 63.2 (1984), pp. 482–501.

[36] B. Latané, J. H. Liu, A. Nowak, M. Bonevento, and L. Zheng. "Distance matters: Physical space and social impact". In: *Personality and Social Psychology Bulletin* 21.8 (1995), pp. 795–805.

[37] G. Groh, F. Straub, J. Eicher, and D. Grob. "Geographic aspects of tie strength and value of information in social networking". In: *Proceedings of the 6th ACM SIGSPATIAL International Workshop on Location-Based Social Networks*. 2013, pp. 1–10.

[38] A. Kaltenbrunner, S. Scellato, Y. Volkovich, D. Laniado, D. Currie, E. J. Jutemar, and C. Mascolo. “Far from the eyes, close on the web: impact of geographic distance on online social interactions”. In: *Proceedings of the 2012 ACM workshop on Workshop on online social networks*. 2012, pp. 19–24.

[39] G. Manzo and A. van der Rijt. “Halting sars-cov-2 by targeting high-contact individuals”. In: *arXiv* 2005.08907 (2020).

[40] K. Prem, Y. Liu, T. W. Russell, A. J. Kucharski, R. M. Eggo, and N. Davies. “The effect of control strategies to reduce social mixing on outcomes of the COVID-19 epidemic in Wuhan, China: a modelling study”. In: *The Lancet* (2020).

[41] C. T. Butts and K. Carley. “Spatial models of large-scale interpersonal networks”. In: *Doctoral Disser* (2002).

[42] N. M. Ferguson, D. A. Cummings, C. Fraser, J. C. Cajka, P. C. Cooley, and D. S. Burke. “Strategies for mitigating an influenza pandemic”. In: *Nature* 442.7101 (2006), pp. 448–452.

[43] J. Kleinberg. “Cascading behavior in Networks: Algorithmic and Economic Issues”. In: *In: Algorithmic Game Theory* Chapter 24 (2007), pp. 613–632.

[44] H. Sun and Z. Gao. “Dynamical behaviors of epidemics on scale-free networks with community structure”. In: *Physica A: Statistical Mechanics and its Applications* 381 (2007), pp. 491–496.

[45] H. Sun and Z. Gao. “Effects of contact network structure on epidemic transmission trees: implications for data required to estimate network structure”. In: *Stat. Med.* 37.2 (2018), pp. 236–248.

[46] J. M. Kleinberg. “Navigation in a small world”. In: *Nature* 406.6798 (2000), pp. 845–845.

[47] M. Keeling and K. Eames. “Networks and epidemic models”. In: *J.R. Soc. Interface* 2 (2005), pp. 295–307.

[48] M. Newman. “Spread of epidemic disease on networks”. In: *Phys. Rev. E* 66 (2002).

[49] C. Moore and M. Newman. “Epidemics and percolation in small-world networks”. In: *Phys. Rev. E* 61 (2000).

[50] F.-Z. Younsi, A. Bounekkar, D. Hamdadou, and O. Boussaid. “SEIR-SW, Simulation Model of Influenza Spread Based on the Small World Network”. In: *Tsinghua Science Technology* (2015).

[51] M. Small and C. Tse. “Small world and Scale free Model of Transmission of SARS”. In: *International Journal of Bifurcation and Chaos* 15.05 (2005), pp. 1745–1755.

[52] M. E. Halloran, N. M. Ferguson, and S. Eubank et al. “Modeling targeted layered containment of an influenza pandemic in the United States”. In: *PNAS* 105.12 (2008).

[53] N. M. Ferguson, D. Laydon, and G. Nedjati-Gilani et al. “Impact of non-pharmaceutical interventions (NPIs) to reduce COVID-19 mortality and healthcare demand”. In: *Imperial College Covid-19 Response Team* (2020).

[54] V. Colizza, A. Barrat, M. Barthelemy, and A. Vespignani. “The role of the airline transporation network in the prediction and predicitability of global epidemics”. In: *PNAS* 103.7 (2007).

[55] M. Martcheva. *An introduction to mathematical epidimiology.* Springer Texts in Applied Mathematics, 2015.

[56] B. Ottino-Loffler, J. G. Scott, and S. H. Strogatz. “Evolutionary dynamics of incubation periods”. In: *eLife* 6 (2017), e30212.

[57] Q. Li, X. Guan, and W. Peng et al. “Early Transmission Dynamics in Wuhan, China, of Novel Coronavirus-Infected Pneumonia”. In: *The New England Journal of Medicine* 382.13 (2020), pp. 1199–1207.

[58] A. J. Kucharski, T. W. Russell, H. Diamond, and Y. Liu et al. “Early dynamics of transmission and control of COVID-19: a mathematical modelling study”. In: *The Lancet Infectious Diseases* (2020).

[59] L. Li, Z. Yang, Z. Dang, C. Meng, and J. Huang. “Propagation analysis and prediction of the COVID-19”. In: *Infectious Disease Modelling* 5 (2020), pp. 282–292.

[60] E. J. Neuman and M. S. Mizruchi. “Structure and bias in the network autocorrelation model”. In: *Social Networks* 32 (2010), pp. 290–300.

[61] R. Li, S. Pei, B. Chen, Y. Song, T. Zhang, W. Yang, and J. Shaman. “Substantial undocumented infection facilitates the rapid dissemination of novel coronavirus (SARS-CoV-2)”. In: *Science* 368.6490 (2020), pp. 489–493.

[62] M. Castro, S. Ares, J. A. Cuesta, and S. Manrubia. “The turning point and end of an expanding epidemic cannot be precisely forecast”. In: vol. 117. 42. National Acad Sciences, 2020, pp. 26190–26196.

II

Game Theory in Contemporary Conflicts

5

GENERAL LOTTO GAMES WITH SCOUTS: INFORMATION VERSUS STRENGTH

In this chapter, we describe the work we did with the Robotic autonomous systems (RAS) unit, the unit of Royal Netherlands Army dedicated to autonomous drones and vehicles. They asked us to analyse the scenario of retaking a river area with several bridges from the opposing forces. There are two main questions. First, how should the troops be divided over the different bridges for the best results? Secondly, if they could send out some scouting drones to gain some information about the distribution of the opposing troops, how would that change the scenario? To model this scenario, we introduce General Lotto games with Scouts. Solving this game then provides the strategies for optimal troop distributions. Furthermore, we quantify the value of information gathered by the scouts. This allows us to describe the best combinations of scouting information versus firepower, for given budgets. Finally, we discuss what these results mean for the original scenario provided by RAS.

5.1. INTRODUCTION

The Colonel Blotto game in its most basic form was introduced by Borel in 1921 [18]. The main idea is that two opposing Colonels simultaneously allocate a fixed amount of resources over a finite number of fields. Each field is won by whichever player sends the most resources there, and the goal is to win as many fields as possible. The Colonel Blotto game and its variations and generalisations have been used to model various strategic situations, ranging from division of troops and the placement of missiles [63] to budget allocation during elections [64, 65].

Borel introduced two versions of the Colonel Blotto game in his original

Parts of this chapter have been submitted to Dynamic Games and Applications [5].

paper: the discrete Colonel Blotto game, where the number of resources sent to a field has to be an integer, and the continuous Colonel Blotto game, where the number of resources can be any non-negative number. The first solutions to the continuous Colonel Blotto game were found by Gross and Wagner in 1950 [23]. They solved the game completely for two fields. They also provided solutions for three or more fields, under the condition that both sides have an equal number of resources. The continuous Blotto game was eventually completely solved by Roberson in 2006 [24], allowing for any number of fields and asymmetric resource numbers between players. The discrete version turned out to be quite difficult to solve, as even now it is considered very computationally intensive to find solutions. There is a substantial literature on the computational complexity of the discrete Blotto game, see the work of Behnezhad [66] and the references therein. Even so, Liang [67] showed that the equilibrium payoff for two-battlefield games is generally the same in the continuous version as in the discrete version.

Hart [68] introduced a more computable variant of Colonel Blotto games, which he called General Lotto games. These games relax the budget constraint on the number of resources allocated to a field, only requiring it to hold in expectation. Hart showed how these games could be used to find optimal strategies for symmetric discrete Colonel Blotto games. While General Lotto games were introduced as a tool to study Colonel Blotto games, they have shown to be interesting games in their own right.

In standard General Lotto games, the resources allocated to each of the fields are revealed simultaneously. In practice, however, this need not always be the case. Intelligence, surveillance and reconnaissance efforts might unveil adversary troop allocations beforehand. A reconnaissance drone or satellite image could identify troops en route to the field, a spy might uncover the number of missiles in a specific location, or a leaked document could detail the budget allocated to a certain state during elections. Knowledge of such events significantly influences the strategies of both players.

In this chapter, we present a new variation of the General Lotto game that accommodates such information. We consider the following variation of a General Lotto game. Consider two players, Blue and Red. First, Red allocates a number of resources to the field, as done in a standard General Lotto game. Next, Blue may obtain knowledge of Red's resource allocation, i.e., with some probability Blue learns the exact number of resources Red has allocated. Blue can now choose to match this number and win the corresponding field, or allocate no resources to the field. Since it is a General Lotto game, the number of resources allocated by the players has to match their budget in expectation.

Our research is inspired by the real-world scenario of a scouting drone spotting enemy troops on their way to a field, which is a problem that was provided to us by the Dutch ministry of Defence. This setting has since then only grown

in relevance, with the war in Ukraine using surveillance drones on a large scale, making troop movements more transparent than ever [69]. We abstracted this to a problem of information versus strength with fixed budgets.

The goal of this chapter is to study the effect of information asymmetry on resource allocation. Furthermore, we want to gain insights into optimal configurations of different types of resources: resources that yield strength (troops) or information (drones). We focus on two main research questions. First, we assume that the amount of information and strength is predetermined. With the information that is provided, what are the optimal strategies? Specifically, how does Blue use his information efficiently, and how does Red change her strategy to deal with Blue possibly gaining information? We provide several insights and guidelines to answer these questions.

The second research question is a generalisation of the first: What if you are allowed to choose your own configuration of information and strength under a given budget? This is the so-called weapons mix problem [70]. You are about to face a series of battles, and you have to assemble your troops. Given is a fixed budget to divide between scouting drones which provide information, and weaponized unmanned vehicles which provide firepower. What is the mix of information and strength that maximises expected wins?

RELEVANT LITERATURE

General Lotto games are a valuable framework for exploring information and asymmetry in resource allocation. There are many aspects of the game where there can exist asymmetry: players may have different field valuations, resources could vary in strength between players, or a player might have a strategic advantage, such as in our game.

Several extensions of General Lotto Games have been developed to investigate the effects of these asymmetries. An example is work by Kovenock and Roberson [71], where the players have asymmetric valuations for the fields, which are known to both players. Another approach is in the work of Paarporn [72], where the valuation of fields is the same for both players, but only one player knows the exact value, and the other player only knows its distribution.

Vu and Loiseau [73] provided solutions for General Lotto games with favouritism, where some of the resources are pre-allocated beforehand, and remaining resources have differing strengths per field and player. The number of resources pre-allocated for each field is fixed. Chandan et al. [74] build upon this idea, by including pre-allocation in the strategy. They extend General Lotto games to two-stage games, where in the first phase a fixed budget of resources must be pre-allocated over fields, but the player now has freedom to choose how to divide these resources. In the second stage, these resources are revealed, and the General Lotto game with favouritism is played.

An alternate extension of General Lotto games are Winner-Take-All games, as studied by Alpern and Howard [75]. Where General Lotto games have two players competing, Winner-Take-All games allow for any number of players. Each player is tasked with selecting a distribution following predefined constraints. Subsequently, scores are sampled from these distributions, and the player achieving the highest score wins. Notably, two player Winner-Take-All games with constraints on the expectation of the distribution are equivalent to General Lotto games.

Main contributions and results

We first study General Lotto games with Scouts on a single field. We show that based on the amount of resources and the probability that the field is revealed, the analysis of this game can be split into three different cases. We provide optimal strategies for all three. We also study a multi-stage version of the game with multiple fields, which all have their own value and own probability to be revealed. For this version, we provide upper and lower bounds on the value of the game. These bounds are tight in some settings. We devise several ways to compare the value of information and resources. We conclude with several qualitative insights.

Overview of the chapter

We first introduce the game model and its notation in Section 5.2. We focus on single field General Lotto games with Scouts in Section 5.3, where we provide optimal strategies for both players. In Section 5.4 we move on to a multi-stage version with multiple fields and provide upper and lower bounds on the value of this game. In Section 5.5, we introduce methods to measure information versus strength. We discuss the insights gained about the value of information in Section 5.6. We conclude and discuss future work in Section 5.7.

5.2. Model, notation and assumptions

As described in the introduction, General Lotto games as introduced by Hart [68] are a relaxed version of Colonel Blotto games, in the sense that the resource constraint should only hold in expectation, rather than with probability 1. We want to study a version of the General Lotto game where one player receives information on the resource configuration chosen by the other player. This act of receiving information is symbolised by the idea of sending a scout. The game is therefore denoted as *GL-S*, meaning General Lotto with Scouts. In this section we first formally introduce the General Lotto game and its optimal strategies. Afterwards we generalise it to General Lotto with Scouts on a single field, which exhibits insightful properties. In later sections we analyse a multi-stage version with multiple fields, which will be introduced in the relevant section.

5.2.1. GENERAL LOTTO

Before introducing General Lotto with Scouts, we first define the General Lotto game. This game involves two players, Red and Blue, competing on a single field. Blue is endowed with resource budget $B > 0$, and Red possesses a resource budget $R > 0$. Red chooses as her strategy a (distribution of a) nonnegative random variable X with $\mathbb{E}(X) = R$, Blue chooses as his strategy a (distribution of a) nonnegative random variable Y with $E(Y) = B$.

To determine the winner, two numbers, r and b, representing the amount of resources allocated to the field by Red and Blue respectively, are sampled from their strategies. The player with the highest amount of allocated resources wins the game, with ties being resolved in favor of Blue. I.e., the game is constant-sum with the following pay-off for Blue:

$$P(b,r) = \mathbb{1}(b \geq r).$$

The way in which ties are broken is chosen to avoid technical complications and does not influence the value of the game. We define the value of the game as the probability Blue wins:

$$V = P(X \leq Y)$$

This game was solved by [68]. He proved the value of the game and the optimal strategies were as in Theorem 5.1.

Theorem 5.1 (Hart)**.** *Let $R \geq B > 0$. The value V of the General Lotto game is*

$$V = \frac{B}{2R}$$

and the unique optimal strategies are X^* for Red and Y^* for Blue, where

$$X^* \sim \mathbb{U}[0, 2R]$$
$$Y^* \sim \mathbb{U}[0, 2R] \text{ with prob. } \frac{B}{R}, \text{ else } 0$$

5.2.2. GENERAL LOTTO WITH SCOUTS

We now consider General Lotto games with Scouts, denoted as $GL\text{-}S(B, R, u)$. Similar to the standard General Lotto game, $GL-S$ involves the two players Blue and Red, with resource budgets $B, R > 0$, competing on a single field. However, in this variant, Blue obtains information insight into Red's resource allocation with a probability $u \in [0, 1]$. This influences how both players approach the game.

To describe the feasible strategies, we begin with an assumption and an observation.

- First, we assume that both players choose their strategies before knowing whether the number of Red resources will be revealed. This means that the strategy of Blue consists of two parts: actions in case the field is revealed, and actions for when it is not. The expectation over these two together has to match Blue's total resources B.
- Second, note that if the number of resources allocated by Red is revealed, Blue either allocates the exact same amount of resources (Call) or allocates no resources at all (Fold). It is clear that any other course of action is less beneficial for Blue, i.e., is dominated by this strategy.

A strategy for Red, denoted by $\sigma_R = (X)$, is a random variable X on $[0,\infty)$ that satisfies:

$$\mathbb{E}(X) \leq R.$$

The space of all Reds strategies is denoted by Σ_R. We denote the number of resources allocated by Red by $T_R(X)$.

A strategy for Blue, denoted by $\sigma_B = (t, Z)$, consists of a function $t : [0,\infty) \to [0,1]$ and a random variable Z on $[0,\infty)$. Here $t(x)$ is defined as the probability that Blue calls if it is revealed that Red has allocated x resources, and Z determines the number of resources that Blue allocates if the field is not revealed. We denote the number of resources allocated by Blue by $T_B(t, Z, X)$. Now we see that

$$T_B(t,Z,X) = \begin{cases} X \text{ with prob. } t(X), \text{ else } 0 & \text{if the field is revealed} \\ Z, & \text{if the field is not revealed} \end{cases}$$

Given that Red plays strategy $\sigma_R = (X)$ and Blue plays strategy $\sigma_B = (t, Z)$, we see that

$$\mathbb{E}T_B(t,Z,X) = u\mathbb{E}(t(X)X) + (1-u)\mathbb{E}(Z).$$

Since the Blue resource constraint must hold for any strategy of Red, we require that

$$u\mathbb{E}(t(X)X) + (1-u)\mathbb{E}(Z) = \mathbb{E}T_B(t,Z,X) \leq B$$

for all random variables X on $[0,\infty)$ that satisfy $\mathbb{E}(X) \leq R$. The space of all such strategies of B is denoted by Σ_B.

The value of the game is the expected payoff to Blue. Given that Blue plays strategy $\sigma_B = (t, Z)$ and Red plays strategy $\sigma_R = (X)$, the value of the game V is given by

$$V = P(\sigma_B, \sigma_R) = u\mathbb{E}(t(X)) + (1-u)\mathbb{P}(Z \geq X).$$

Blue want to find a strategy which maximises the value, and Red want to find a strategy which minimises the value.

5.3. GENERAL LOTTO WITH SCOUTS: SINGLE FIELD

In the last section, we introduced the *GL-S* game. In this section, we find its value and optimal strategies. The main result is given in Theorem 5.5 at the end of the section.

Based on the resource ratio B/R, we split the analysis into the following three cases:

- Case 1: *GL-S* with $1 \le B/R$
- Case 2: *GL-S* with $u \le B/R \le 1$
- Case 3: *GL-S* with $B/R \le u$

The cases have different optimal strategies and are therefore treated separately. At the end of the section, the results are combined into Theorem 5.5. Every time we propose two strategies and show that they both guarantee the same payoff V. Thus, these strategies must be optimal and the value of the game is V.

5.3.1. CASE 1: *GL-S* WITH $1 \le B/R$

We introduce two new parameters $q(u)$ and $C(u)$:

$$q(u) = \frac{1-u}{\left(\frac{B}{R}\right)-u}$$
$$C(u) = \frac{R}{q(u)} = R\left(\frac{\frac{B}{R}-u}{1-u}\right) = B + u\frac{B-R}{1-u}$$

Since $B \ge R$, it follows that $0 \le q(u) \le 1$ and $C(u) \ge B \ge R$.

We show that $\sigma_R^* = (X^*)$ and $\sigma_R^* = (t^*, Z^*)$ are optimal strategies, where:

$$X^* \sim \mathbb{U}[0, 2C(u)] \text{ with prob. } q(u), \text{ else } 0$$
$$t^* = 1 \quad \forall x$$
$$Z^* \sim \mathbb{U}[0, 2C(u)]$$

$\mathbb{U}[a,b]$ denotes the uniform distribution with support $[a,b]$. This strategy consists of Blue always replicating Red's allocation if the field is revealed, or Blue plays a uniform distribution if the field is not revealed. Red plays the same uniform distribution with probability $q(u)$, and 0 with probability $1-q(u)$.

Lemma 5.2. *These strategies are optimal strategies in the case* $\frac{B}{R} \ge 1$*, and the value of the game equals* $V = 1 - \frac{(1-u)^2}{2(\frac{B}{R}-u)}$.

Proof. First we show that the resource constraints are satisfied:

$$\begin{aligned}\mathbb{E}T_R(X^*) &= \mathbb{E}(X^*) = q(u)\cdot C(u) + (1-q(u))\cdot 0 = q(u)\cdot\frac{R}{q(u)} = R\\ \mathbb{E}T_B(t^*,Z^*,X) &= u\mathbb{E}\left(t^*(X)X\right) + (1-u)\mathbb{E}(Z^*) = u\cdot R + (1-u)\cdot C(u) = B,\end{aligned}$$

where X is an arbitrary non-negative random variable such that $\mathbb{E}X = R$.
Now it suffices to prove the following two claims.

Claim 1: given that Red plays σ_R^*, the payoff is at most V.
If Red plays σ_R^*, the payoff for any σ_B is:

$$P(\sigma_B,\sigma_R^*) = u\mathbb{E}(t(X^*)) + (1-u)\mathbb{E}\left(\mathbb{1}[Z\geq X^*]\right)$$

We can rewrite $\mathbb{E}(\mathbb{1}[Z\geq X^*])$ by conditioning on Z:

$$\mathbb{E}\left(\mathbb{1}[Z\geq X^*]\right) = \mathbb{E}\left(\mathbb{E}\left(\mathbb{1}[Z\geq X^*]|Z\right)\right) = 1-q(u)+q(u)\mathbb{E}(\mathbb{E}(\mathbb{1}[Z\geq U]|Z))$$

Where $U\sim\mathbb{U}[0,2C(u)]$. We can use this to rewrite as follows:

$$\begin{aligned}\mathbb{E}(\mathbb{1}[Z\geq U]|Z) &= \left(\frac{Z}{2C(u)}\right)\mathbb{1}[2C(u)\geq Z] + 1\cdot\mathbb{1}[2C(u)<Z]\\ &= \left(\frac{Z}{2C(u)}\right)(1-\mathbb{1}[2C(u)<Z]) + 1\cdot\mathbb{1}[2C(u)<Z]\\ &= \left(\frac{Z}{2C(u)}\right) - \left(\frac{Z}{2C(u)}-1\right)\cdot\mathbb{1}[2C(u)<Z]\end{aligned}$$

Plugging this back in gives:

$$\begin{aligned}\mathbb{E}\left(\mathbb{1}[Z\geq X^*]\right) &= 1-q(u)+q(u)\left(\mathbb{E}\left(\frac{Z}{2C(u)}\right) - \mathbb{E}\left(\left(\frac{Z}{2C(u)}-1\right)\cdot\mathbb{1}[2C(u)<Z]\right)\right)\\ &= 1-q(u)+q(u)\left(\frac{\mathbb{E}(Z)}{2C(u)} - \mathbb{E}\left(\left(\frac{Z}{2C(u)}-1\right)\cdot\mathbb{1}[2C(u)<Z]\right)\right)\\ &= 1-q(u)\left(1-\frac{\mathbb{E}(Z)}{2C(u)}\right) - q(u)\mathbb{E}\left(\left(\frac{Z}{2C(u)}-1\right)\cdot\mathbb{1}[2C(u)<Z]\right)\\ &\leq 1-q(u)\left(1-\frac{\mathbb{E}(Z)}{2C(u)}\right)\end{aligned}$$

Using this equation, we can rewrite the payoff as:

$$\begin{aligned}P(\sigma_B,\sigma_R^*) &\leq u\mathbb{E}(t(X^*)) + (1-u)\left(1-q(u)\left(1-\frac{\mathbb{E}(Z)}{2C(u)}\right)\right)\\ &= u\mathbb{E}(t(X^*)) + (1-u)(1-q(u)) + \frac{q(u)}{2C(u)}\left(B - u\mathbb{E}\left(t(X^*)X^*\right)\right)\\ &= u\mathbb{E}\left(t(X^*)\left(1-\frac{q(u)X^*}{2C(u)}\right)\right) + (1-u)(1-q(u)) + \frac{q(u)B}{2C(u)}\end{aligned}$$

Since $0 \leq \left(1 - \frac{q(u)X^*}{2C(u)}\right)$, this expression is maximised by taking $t(x) = 1 \forall x$. This yields

$$\begin{aligned} P(\sigma_B, \sigma_R^*) &\leq u\mathbb{E}\left(1 - \frac{q(u)X^*}{2C(u)}\right) + (1-u)(1-q(u)) + \frac{q(u)B}{2C(u)} \\ &= 1 + u - u - q(u)(1-u) + \frac{q(u)}{2C(u)}(B - uR) \\ &= 1 - q(u)(1-u) + \frac{q(u)}{2}\frac{B-uR}{C(u)} \\ &= 1 - \frac{1}{2}q(u)(1-u) = 1 - \frac{(1-u)^2}{2(\frac{B}{R} - u)} = V \end{aligned}$$

This proves Claim 1.

Claim 2: given Blue plays σ_B^*, the payoff is at least V.
If Blue uses the strategy σ_B^*, the payoff for any σ_R is:

$$\begin{aligned} P(\sigma_B^*, \sigma_R) &= u\mathbb{E}(t^*(X)) + (1-u)\mathbb{E}\left(\mathbb{1}[Z^* \geq X]\right) \\ &= u\mathbb{E}(1) + (1-u)\mathbb{E}\left(\mathbb{1}[Z^* \geq X]\right) \\ &= u + (1-u)\mathbb{E}\left(\mathbb{1}[Z^* \geq X]\right) \end{aligned}$$

We can rewrite $\mathbb{E}(\mathbb{1}[Z^* \geq X])$ by conditioning on X:

$$\mathbb{E}\left(\mathbb{1}[Z^* \geq X]\right) = \mathbb{E}\left(\mathbb{E}\left(\mathbb{1}[Z^* \geq X]|X\right)\right)$$

Where $Z^* \sim \mathbb{U}[0, 2C(u)]$. We can use this to rewrite as follows:

$$\begin{aligned} \mathbb{E}\left(\mathbb{E}\left(\mathbb{1}[Z^* \geq X]|X\right)\right) &= \mathbb{E}\left(\left(1 - \frac{X}{2C(u)}\right)\mathbb{1}[2C(u) \geq X] + 0 \cdot \mathbb{1}[2C(u) < X]\right) \\ &= \mathbb{E}\left(\left(1 - \frac{X}{2C(u)}\right)(1 - \mathbb{1}[2C(u) < X])\right) \\ &= \mathbb{E}\left(1 - \frac{X}{2C(u)}\right) + \mathbb{E}\left(\mathbb{1}[2C(u) < X]\left(\frac{X}{2C(u)} - 1\right)\right) \\ &= 1 - \frac{R}{2C(u)} + \mathbb{E}\left(\mathbb{1}[2C(u) < X]\left(\frac{X}{2C(u)} - 1\right)\right) \\ &\geq 1 - \frac{R}{2C(u)} = 1 - \frac{q(u)}{2} \end{aligned}$$

The last step follows from the fact that the expectation on the RHS is non-negative. Plugging this into the original equation for payoff gives:

$$\begin{aligned} P(\sigma_B^*, \sigma_R) &\geq u + (1-u)\left(1 - \frac{q(u)}{2}\right) = 1 - (1-u)\frac{q(u)}{2} \\ &= 1 - \frac{(1-u)^2}{2(\frac{B}{R} - u)} = V \end{aligned}$$

This proves Claim 2 and therefore completes the proof. □

5.3.2. CASE 2: *GL-S* WITH $u \le B/R \le 1$

This is the most interesting of the three scenarios. Blue is outnumbered, but can use information to be competitive. We introduce the following parameter:

$$p(u) = \frac{\frac{B}{R} - u}{1-u} = \frac{1}{q(u)}$$

Since $u \le \frac{B}{R} \le 1$, it follows that $0 \le p(u) \le 1$.

We show that $\sigma_R^* = (X^*)$ and $\sigma_R^* = (t^*, Z^*)$ are optimal strategies, where:

$$\begin{aligned} X^* &\sim \mathbb{U}[0, 2R] \\ t^* &= 1 \quad \forall x \\ Z^* &\sim \mathbb{U}[0, 2R] \text{ with prob. } p(u), \text{ else } 0 \end{aligned}$$

This strategy consists of Blue always replicating Red's allocation if the field is revealed, or Blue plays a uniform distribution with probability $p(u)$ if the field is not revealed, and 0 with probability $1 - p(u)$. Red always plays the same uniform distribution, which is equivalent to her strategy in General Lotto games without scouts.

Lemma 5.3. *These strategies are optimal in the case $u \le \frac{B}{R} \le 1$, and the value of the game equals $V = \frac{1}{2}\left(u + \frac{B}{R}\right)$.*

Proof. First, we show that the resource constraints are satisfied:

$$\begin{aligned} \mathbb{E}T_R(X^*) &= \mathbb{E}(X^*) = R \\ \mathbb{E}T_B(t^*, Z^*, X) &= u\mathbb{E}\left(t^*(X)X\right) + (1-u)\mathbb{E}(Z^*) = uR + (1-u)p(u)R = B, \end{aligned}$$

where X is an arbitrary non-negative random variable such that $\mathbb{E}X = R$.
Now it suffices to prove the following two claims.

Claim 1: given that Red plays σ_R^*, the payoff is at most V.
If Red plays σ_R^*, the payoff for any σ_B is:

$$P(\sigma_B, \sigma_R^*) = u\mathbb{E}(t(X^*)) + (1-u)\mathbb{E}\left(\mathbb{1}[Z \ge X^*]\right)$$

We can rewrite $\mathbb{E}(\mathbb{1}[Z \ge X^*])$ by conditioning on Z:

$$\mathbb{E}\left(\mathbb{1}[Z \ge X^*]\right) = \mathbb{E}\left(\mathbb{E}\left(\mathbb{1}[Z \ge X^*] | Z\right)\right)$$

Where $X^* \sim \mathbb{U}[0,2R]$. We can use this to rewrite as follows:

$$\begin{aligned}
\mathbb{E}\left(\mathbb{E}\left(\mathbb{1}[Z \geq X^*]|Z\right)\right) &= \mathbb{E}\left(\left(\frac{Z}{2R}\right)\mathbb{1}[2R \geq Z] + 1 \cdot \mathbb{1}[2R < Z]\right) \\
&= \mathbb{E}\left(\left(\frac{Z}{2R}\right)(1 - \mathbb{1}[2R < Z]) + 1 \cdot \mathbb{1}[2R < Z]\right) \\
&= \mathbb{E}\left(\frac{Z}{2R}\right) - \mathbb{E}\left(\left(\frac{Z}{2R} - 1\right) \cdot \mathbb{1}[2R < Z]\right) \\
&= \frac{\mathbb{E}(Z)}{2R} - \mathbb{E}\left(\left(\frac{Z}{2R} - 1\right) \cdot \mathbb{1}[2R < Z]\right) \\
&\leq \frac{\mathbb{E}(Z)}{2R}
\end{aligned}$$

Using this equation, we can rewrite the payoff as:

$$P(\sigma_B, \sigma_R^*) \leq u\mathbb{E}(t(X^*)) + (1-u)\left(\frac{\mathbb{E}(Z)}{2R}\right)$$

If we rewrite the expectation requirement, we get:

$$(1-u)\mathbb{E}(Z) = B - u\mathbb{E}\left(t(X)X\right)$$

Plugging this in gives:

$$\begin{aligned}
P(\sigma_B, \sigma_R^*) &\leq u\mathbb{E}(t(X^*)) + \frac{1}{2R}\left(B - u\mathbb{E}\left(t(X^*)X^*\right)\right) \\
&= \frac{B}{2R} + u\mathbb{E}\left(t(X^*)\left(1 - \frac{X^*}{2R}\right)\right)
\end{aligned}$$

Since $0 \leq \left(1 - \frac{X^*}{2R}\right)$, the payoff is optimised by taking $t(\cdot)$ as large as possible. It is therefore maximised by taking $t(x) = 1 \forall x$, which gives:

$$\begin{aligned}
P(\sigma_B, \sigma_R^*) &\leq \frac{B}{2R} + u\mathbb{E}\left(1\left(1 - \frac{X^*}{2R}\right)\right) = \frac{B}{2R} + u\left(1 - \frac{R}{2R}\right) \\
&= \frac{1}{2}\left(\frac{B}{R} + u\right) = V
\end{aligned}$$

This proves Claim 1.

Claim 2: given that Blue plays σ_B^*, the payoff is at least V.
If Blue uses the strategy σ_B^*, the payoff for any σ_R is:

$$\begin{aligned}
P(\sigma_B^*, \sigma_R) &= u\mathbb{E}(t^*(X)) + (1-u)\mathbb{E}\left(\mathbb{1}[Z^* \geq X]\right) \\
&= u\mathbb{E}(1) + (1-u)\mathbb{E}\left(\mathbb{1}[Z^* \geq X]\right) \\
&= u + (1-u)\mathbb{E}\left(\mathbb{1}[Z^* \geq X]\right)
\end{aligned}$$

We can rewrite $\mathbb{E}(\mathbb{1}[Z^* \geq X])$ by conditioning on X:

$$\begin{aligned}\mathbb{E}\left(\mathbb{1}[Z^* \geq X]\right) &= \mathbb{E}\left(\mathbb{E}\left(\mathbb{1}[Z^* \geq X]|X\right)\right)\\ &= \mathbb{E}\left(\mathbb{E}\left((1-p(u))\cdot 0 + p(u)\mathbb{1}[U \geq X]|X\right)\right)\\ &= p(u)\mathbb{E}\left(\mathbb{E}\left(\mathbb{1}[U \geq X]|X\right)\right)\end{aligned}$$

Where $U \sim \mathbb{U}[0,2R]$. We can use this to rewrite as follows:

$$\begin{aligned}\mathbb{E}\left(\mathbb{E}\left(\mathbb{1}[U \geq X]|X\right)\right) &= \mathbb{E}\left(\left(1-\frac{X}{2R}\right)\mathbb{1}[2R \geq X] + 0\cdot\mathbb{1}[2R < X]\right)\\ &= \mathbb{E}\left(\left(1-\frac{X}{2R}\right)(1-\mathbb{1}[2R < X])\right)\\ &= \mathbb{E}\left(1-\frac{X}{2R}\right) + \mathbb{E}\left(\mathbb{1}[2R < X]\left(\frac{X}{2R}-1\right)\right)\\ &= \left(1-\frac{R}{2R}\right) + \mathbb{E}\left(\mathbb{1}[2R < X]\left(\frac{X}{2R}-1\right)\right)\\ &= \frac{1}{2} + \mathbb{E}\left(\mathbb{1}[2R < X]\left(\frac{X}{2R}-1\right)\right)\\ &\geq \frac{1}{2}\end{aligned}$$

Here, the last step follows from the fact that the expectation on the RHS is non-negative. Plugging this into the original equation for the game payoff yields

$$\begin{aligned}P(\sigma_B^*, \sigma_R) &\geq u + (1-u)\left(\frac{p(u)}{2}\right) = u + \frac{\frac{B}{R}-u}{2}\\ &= \frac{1}{2}\left(u + \frac{B}{R}\right) = V\end{aligned}$$

This proves Claim 2 and therefore completes the proof. □

5.3.3. Case 3: *GL-S* with $B/R \leq u$

In this case Blue is outnumbered, but has a significant amount of information. The optimal strategies of this case are surprising, as Red will do away with any randomness in her strategy.

We show that $\sigma_R^* = (X^*)$ and $\sigma_R^* = (t^*, Z^*)$ are optimal strategies, where:

$$\begin{aligned}X^* &= R\\ t^* &= \frac{B}{uR} \quad \forall x\\ Z^* &= 0\end{aligned}$$

This strategy consists of Blue replicating Reds allocation with probability $\frac{B}{uR}$ whenever the field is revealed, independently of the number of resources spotted.

If the field is not revealed, Blue allocates no resources. Red always allocates R resources, effectively removing any random element from her strategy, and thus removing the advantage Blue has with his scouts.

Lemma 5.4. *These strategies are optimal strategies in the case $u \geq \frac{B}{R}$, and the value of the game is $V = \frac{B}{R}$:*

Proof. First we show that the resource constraints are satisfied:

$$\begin{aligned} \mathbb{E}T_R(X^*) &= \mathbb{E}(X^*) = R \\ \mathbb{E}T_B(t^*, Z^*, X) &= u\mathbb{E}\left(t^*(X)X\right) + (1-u)\mathbb{E}(Z^*)u\left(\frac{B}{uR}\right)\mathbb{E}(X) + (1-u)\cdot 0 = B, \end{aligned}$$

where X is an arbitrary non-negative random variable such that $\mathbb{E}X = R$.
Now it suffices to prove the following two claims.

Claim 1: given that Red plays σ_R^*, the payoff is at most V.
If Red uses the strategy σ_R^*, the payoff for any σ_B is:

$$\begin{aligned} P(\sigma_B, \sigma_R^*) &= u\mathbb{E}(t(X^*)) + (1-u)\mathbb{E}\left(\mathbb{1}[Z \geq X^*]\right) \\ &= u\mathbb{E}(t(X^*)) + (1-u)\mathbb{E}\left(\mathbb{1}[Z \geq R]\right) \\ &= \frac{1}{R}\left(u\mathbb{E}(R \cdot t(X^*)) + (1-u)\mathbb{E}\left(R \cdot \mathbb{1}[Z \geq R]\right)\right) \end{aligned}$$

Note that:

$$\mathbb{E}(R \cdot t(X^*)) = \mathbb{E}(t(X^*)X^*)$$

and

$$\mathbb{E}\left(R \cdot \mathbb{1}[Z \geq R]\right) \leq \mathbb{E}\left(Z \cdot \mathbb{1}[Z \geq R]\right) \leq \mathbb{E}(Z)$$

Plugging these into the equation for the payoff gives:

$$\begin{aligned} P(\sigma_B, \sigma_R^*) &\leq \frac{1}{R}\left(u\mathbb{E}\left(t(X^*)X^*\right) + (1-u)\mathbb{E}(Z)\right) \\ &= \frac{1}{R}(B) = \frac{B}{R} = V, \end{aligned}$$

where the last step follows from the expectation requirement for Blue.
This proves Claim 1.

Claim 2: given that Blue plays σ_B^*, the payoff is at least V.
If Blue uses the strategy σ_B^*, the payoff for any σ_R is:

$$\begin{aligned} P(\sigma_B^*, \sigma_R) &= u\mathbb{E}(t^*(X)) + (1-u)\mathbb{E}\left(\mathbb{1}[Z^* \geq X]\right) \\ &= u\left(\frac{B}{uR}\right) + (1-u)\cdot P[X=0] \\ &\geq \frac{B}{R} = V. \end{aligned}$$

This proves Claim 2 and therefore completes the proof. □

As the payoff in this case no longer depends on the u, it follows that increasing the u past $\frac{B}{R}$ no longer increases the payoff.

5.3.4. Solution of *GL-S*

We combine the results of Lemma 5.2, 5.3 and 5.4 to form our main result:

Theorem 5.5. *In GL-S, it is optimal for Blue to play $\sigma_B^* = (t^*, Z^*)$ and optimal for Red to play $\sigma_R^* = (X^*)$, where X^*, t^* and Z^* are chosen according to Table 5.1.*

	X^*	$t^*(\cdot)$	Z^*
$\frac{B}{R} \leq u$	R	$\frac{B}{uR}$	0
$u \leq \frac{B}{R} \leq 1$	$\mathbb{U}[0,2R]$	1	$\mathbb{U}[0,2R]$ w.p. $p(u)$, else 0
$1 \leq \frac{B}{R}$	$\mathbb{U}[0,2C(u)]$ w.p. $q(u)$, else 0	1	$\mathbb{U}[0,2C(u)]$

Table 5.1.: Optimal strategy of *GL-S*.

The value V of GL-S is therefore:

$$V = P(\sigma_B^*, \sigma_R^*) = \begin{cases} \frac{B}{R}, & \text{if } \frac{B}{R} \leq u, \\ \frac{u+\frac{B}{R}}{2}, & \text{if } u \leq \frac{B}{R} \leq 1 \\ 1 - \frac{(1-u)^2}{2(\frac{B}{R}-u)}, & \text{if } 1 \leq \frac{B}{R}, \end{cases}$$

The value of *GL-S* depends on both u and the ratio B/R. We illustrate this function in three different figures. The detection chance u is fixed in Figure 5.1, the ratio B/R is fixed in Figure 5.2 and the value of the game is portrayed as a heatmap in Figure 5.3.

Some interesting insights follow from this optimal solution to the *GL-S* game. The first is that $t(\cdot)$ is always maximised, meaning that Blue calls as many fields as he can, given his budget. Calling a field is always a more efficient way of using resources, than using resources on a field that was not revealed.

The second insight follows from the question whether Red should distribute her resources more or less evenly compared to a standard Lotto game. The answer is both, but in different cases. If Red heavily outnumbers Blue, i.e., $\frac{B}{R} < u$, she plays as evenly as possible, sending exactly R resources every time. However, if Blue outnumbers Red, Red plays riskier than in the standard General Lotto game, allowing a higher number of resources per round, but also sending 0 resources more often. This also means that, as long as $u < 1$, Red always has a chance to win, even if heavily outnumbered.

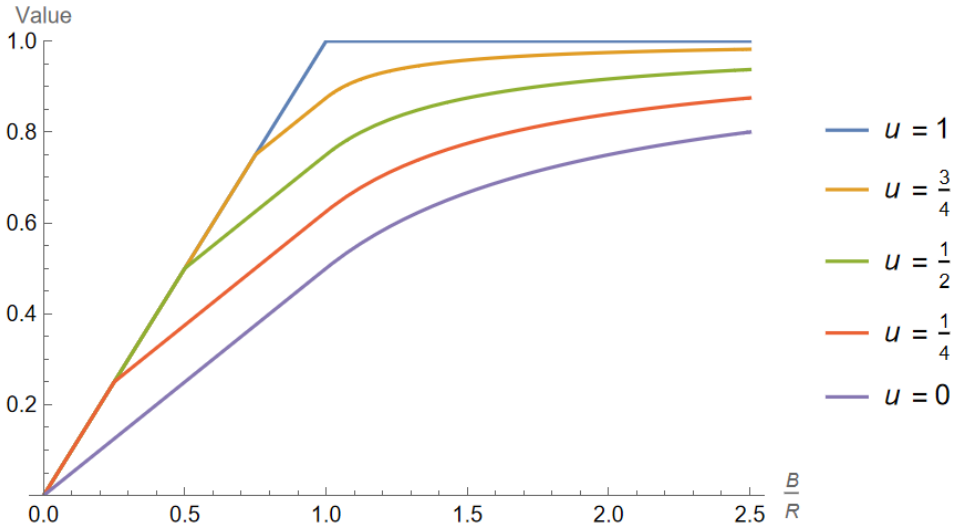

Figure 5.1.: The value of *GL-S* for fixed detection probability u as a function of B/R.

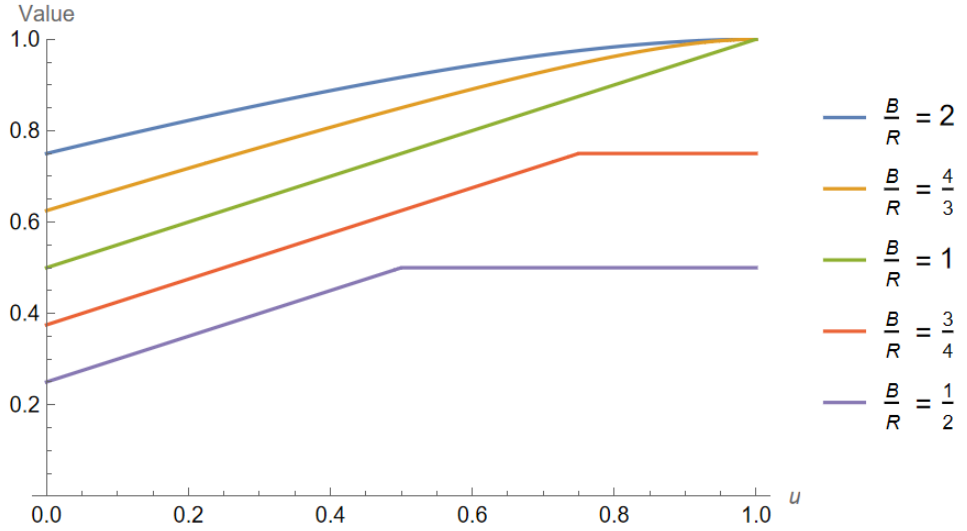

Figure 5.2.: The value of *GL-S* for fixed B/R ratios as a function of the detection probability u.

Remark 5.6 (Comparison with known results when $u = 0$)**.** *By setting the detection probability u in GL-S to 0, we retrieve a General Lotto game of which the value should be consistent with earlier work. The value of this game is $\frac{B}{2R}$ whenever $B \leq R$ and $1 - \frac{R}{2B}$ otherwise. This is consistent with Corollary 1 of Kovenock and Roberson*

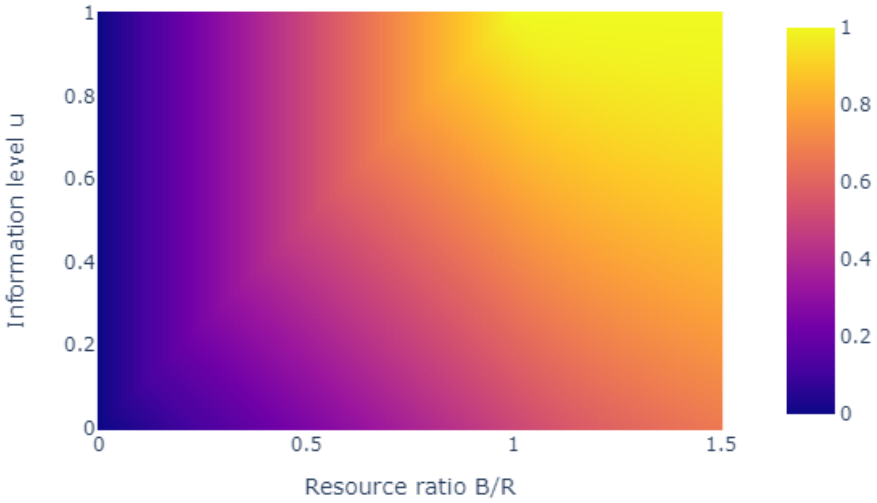

Figure 5.3.: A heatmap of the value of *GL-S*, with the resource ratio B/R on the x-axis and the detection probability u on the y-axis.

[71]. Furthermore, the optimal strategies found there coincide with the optimal strategies that we use. It is also consistent with Hart [68] and Sahuguet and Persico [76] who showed this result earlier.

Remark 5.7 (Comparison with known results when $u = 1$)**.** *By setting $u = 1$ we obtain a game that is in some respects similar to the pre-allocation game in Chandan et al. [74]. Namely, when $u = 1$ Blue always sees what Red does and in that sense Red 'pre-allocates'. There are two major differences. The first is that in our case, Red does not get the opportunity to allocate any additional resources and in that sense forcibly pre-allocates all her resources. The second difference is that the pre-allocation in their work is performed 'Blotto-style', i.e., such that the sum of the pre-allocated resources equals a fixed constant. In our case, it should only in expectation equal the total resources.*

5.4. General Lotto with Scouts: Multistage

In this section, we consider a multistage version *GL-MS* of *GL-S* where Blue and Red first divide their total resources over the battlefield and then play *GL-S* on each battlefield. The latter step was solved in Section 5.3, so we know the value of the games on the individual fields. Therefore, this multistage version of the game can be considered a Colonel Blotto game with a complicated payoff function given by those

game values. First, we introduce the game and discuss under which conditions the game value exists. Subsequently, we provide strategies for Blue and Red, which provide upper and lower bounds on the value of the multistage game. Lastly, we specify under which conditions these bounds coincide, in which case these strategies must be optimal.

5.4.1. THE MULTISTAGE GAME

We start out with the same two players with total resources $B, R > 0$, respectively. Next, let there be n fields, where n is an integer larger than one. Each field is endowed with a worth $w_i > 0$ and a detection probability $u_i \in [0,1]$. We assume that $\sum_i w_i = 1$. We denote the Multistage General Lotto game with Scouts with these parameters by $GL\text{-}MS(B, R, \{u_i\}, \{w_i\})$.

The game is played in two stages.

i) Red chooses a distribution $\underline{R} = (R_1, .., R_n)$ of her total resources over the fields such that $\sum_i R_i = R$. Simultaneously, Blue chooses a distribution $\underline{B} = (B_1, .., B_n)$ of his total resources over the fields such that $\sum_i B_i = B$.

ii) On each field, a $GL\text{-}S(B_i, R_i, u_i)$ game is played with worth w_i.

The total payoff for Blue is the sum of the individual payoffs.

Recall from Section 5.3 that given the resources B_i, R_i at field i and given its worth w_i and the detection probability u_i, the payoff at field i equals $\phi_i(B_i/R_i)$ where

$$\phi_i(x) = w_i \begin{cases} x & x \le u_i \\ \frac{1}{2}(x + u_i) & u_i \le x \le 1 \\ 1 - \frac{(1-u)^2}{2(x-u)} & x \ge 1 \end{cases}$$

Note that the field worth w_i was not present before, but is included in ϕ_i here. Since for $n = 1$ there is just one field with worth 1, this is consistent with before.

Therefore, the first stage of the game has payoff function

$$H(\underline{B}, \underline{R}) = \sum_{i=1}^{n} \phi_i \left(\frac{B_i}{R_i} \right).$$

Our goal is to solve this game with the constraints

$$\sum_{i=1}^{n} B_i = B, \qquad \sum_{i=1}^{n} R_i = R.$$

5.4.2. EXISTENCE OF GAME VALUE

There are three things that make it difficult to derive the game value. First, even though H is concave in $B_1, .., B_n$, it is not convex in $R_1, .., R_n$. Second, H is not

everywhere differentiable, because of the sharp turn in the ϕ_i's at $x = u_i$. Third, H is ill-defined at $B_i = R_i = 0$ for any i and cannot be continuously extended there.

Without the singularity at (0,0), the payoff function is continuous and we can guarantee the existence of the game value. Allocating zero resources to a field is both theoretically and in practice unlikely to be an optimal strategy. It is possible to remove this singularity from the game in the following way: we fix $\epsilon > 0$ and require that $B_i, R_i \geq \epsilon$ for all i. This creates a new, slightly more restricted game. As a result of this restriction H is continuous on the domain of strategies while the domain is still compact. By a classical result of Glicksberg [77], there must exist a Nash equilibrium for the corresponding game.

Now that we have discussed existence, we want to study the exact value of the game. To bound the value of the game, we provide strategies for Red And Blue and prove that these strategies guarantee certain upper and lower bounds. Whenever those bounds coincide, we know the exact value of the game.

5

To find a good guess for optimal strategies for Red and blue, we explore the case where H is continuously differentiable, even though it is not. If the ϕ's were C^1, then any Nash equilibrium would have to satisfy the equations in Lemma 5.8, with the provided optimal strategies. We use these strategies to provide bounds on the original game.

Lemma 5.8. *Let $\phi_i : [0,\infty) \to \mathbb{R}$, $i = 1,..,n$, be C^1 and increasing and let $B, R > 0$. Suppose that $B_1,..,B_n$, $R_1,..,R_n$ satisfy*

$$\sum_{i=1}^{n} \phi_i\left(\frac{B_i}{R_i}\right) = \inf_{R'_1,..,R'_n} \max_{B'_1,..,B'_n} \sum_{i=1}^{n} \phi_i\left(\frac{B'_i}{R'_i}\right) = \sup_{B'_1,..,B'_n} \min_{R'_1,..,R'_n} \sum_{i=1}^{n} \phi_i\left(\frac{B'_i}{R'_i}\right) \tag{5.1}$$

given

$$\sum_{i=1}^{n} B_i = B, \qquad \sum_{i=1}^{n} R_i = R, \qquad B_i, R_i \geq 0.$$

Then $B_i = c_i B$ and $R_i = c_i R$, where

$$c_i = \frac{\phi'_i(B/R)}{\sum_{j=1}^{n} \phi'_j(B/R)}.$$

Proof. Suppose that $B_1,..,B_n$, $R_1,..,R_n$, form a solution. Then in particular $B_1,..,B_n$ maximise

$$f : (x_1,..,x_n) \longmapsto \sum_{i=1}^{n} \phi_i\left(\frac{x_i}{R_i}\right)$$

given $0 = g(x_1,..,x_n) := x_1 + .. + x_n - B$. Using the theory of Lagrange multipliers, we see that then for all i:

$$\lambda = \frac{\partial}{\partial x_i} f(x_1,..,x_n)\Big|_{B_1,..,B_n} = \frac{1}{R_i}\phi'_i\left(\frac{B_i}{R_i}\right), \tag{5.2}$$

where $\lambda \in \mathbb{R}$ is a fixed constant. Reasoning similarly starting from the RHS of (5.1), we see that there is a Lagrange multiplier μ such that

$$\mu = \frac{-B_i}{R_i^2}\phi_i'\left(\frac{B_i}{R_i}\right). \tag{5.3}$$

Plugging (5.2) into (5.3), we see that

$$\mu = \frac{-B_i}{R_i^2}\phi_i'\left(\frac{B_i}{R_i}\right) = \frac{-B_i}{R_i}\frac{1}{R_i}\phi_i'\left(\frac{B_i}{R_i}\right) = \frac{-B_i}{R_i}\lambda,$$

so

$$\frac{B_i}{R_i} = \frac{-\mu}{\lambda} := c$$

is constant. Using the boundary conditions, we obtain

$$B = \sum_{i=1}^{n} B_i = \sum_{i=1}^{n} cR_i = c\sum_{i=1}^{n} R_i = cR,$$

so $c = \frac{B}{R}$, so in particular $B_i = \frac{B}{R}R_i$. Plugging this back into (5.2) and rearranging yields

$$R_i = \frac{1}{\lambda}\phi_i'\left(\frac{B}{R}\right).$$

Since $R_1, .., R_n$ must sum to R, this implies that

$$\lambda = \frac{1}{R}\sum_{j=1}^{n}\phi_j'\left(\frac{B}{R}\right),$$

so $R_i = c_i R$ with c_i defined as in the lemma statement. Using now that $B_i = \frac{B}{R}R_i$, this gives what we wanted. □

5.4.3. UPPER BOUND ON THE GAME VALUE

To obtain an upper bound on the game value, we let Red use the strategy that is suggested by Lemma 5.8.

Lemma 5.9 (Upper bound)**.** *The game value is bounded from above by*

$$\sum_{i=1}^{n}\phi_i\left(\frac{B}{R}\right).$$

Proof. First, we assume that $\frac{B}{R} \neq u_i$ for all i. This implies that each ϕ_i is differentiable at B/R, so we can set R_i according to Lemma 5.8:

$$R_i = R\frac{\phi_i'(B/R)}{\sum_{j=1}^{n}\phi_j'(B/R)}.$$

Now let $B_1,..,B_n$ be an arbitrary strategy of Lotto. Then, using a Taylor expansion for each i of ϕ_i around B/R and the concavity of the ϕ_i's, we obtain the following bound for the payoff:

$$P(R_1,..,R_n,B_1,..,B_n)=\sum_{i=1}^{n}\phi_i\left(\frac{B_i}{R_i}\right)\leq\sum_{i=1}^{n}\left[\phi_i\left(\frac{B}{R}\right)+\phi_i'\left(\frac{B}{R}\right)\left(\frac{B_i}{R_i}-\frac{B}{R}\right)\right].$$

Now substituting the expression for R_i we see that

$$\begin{aligned}\sum_{i=1}^{n}\phi_i'\left(\frac{B}{R}\right)\left(\frac{B_i}{R_i}-\frac{B}{R}\right) &= \sum_{i=1}^{n}\phi_i'\left(\frac{B}{R}\right)\frac{B_i\sum_j\phi_j'\left(\frac{B}{R}\right)}{R\phi_i'\left(\frac{B}{R}\right)}-\frac{B}{R}\sum_{i=1}^{n}\phi_i'\left(\frac{B}{R}\right)\\ &= \frac{1}{R}\sum_{i=1}^{n}B_i\sum_{j=1}^{n}\phi_j'\left(\frac{B}{R}\right)-\frac{B}{R}\sum_{i=1}^{n}\phi_i'\left(\frac{B}{R}\right)=0,\end{aligned}$$

where in the last equation we used that the B_i's sum to B. This implies that

$$H(B_1,..,B_n,R_1,..,R_n)\leq\sum_{i=1}^{n}\phi_i\left(\frac{B}{R}\right),$$

which is what we wanted.

To deal with the case where $u_i=B/R$ for some (or possibly multiple u_i), change all such u_i by at most ϵ to u_i^*. Now note that there is a constant L such that each ϕ_i only changes by at most $L\epsilon$ (with respect to the uniform norm). This implies that the game value can change by at most $nL\epsilon$. Similarly, the bound in this lemma only changes by at most a constant times ϵ. Since this holds for all ϵ, the bound of this lemma must also hold for $\epsilon=0$. □

Now we work out what this means in the case $\frac{B}{R}<1$. We assume WLOG that $u_1\leq u_2..\leq u_n$. Suppose there is $0\leq k\leq n$ such that $u_k<\frac{B}{R}<u_{k+1}$ (where we set $u_0=0$ and $u_{n+1}=1$). In this case, we obtain that

$$\phi_i'\left(\frac{B}{R}\right)=\begin{cases}\frac{w_i}{2} & i\leq k\\ w_i & i>k\end{cases}$$

Denoting $w_{(k)}=\sum_{i\leq k}w_i$, this implies that

$$\sum_{i=1}^{n}\phi_i'\left(\frac{B}{R}\right)=1-\frac{w_{(k)}}{2}.$$

The strategy for Red from Lemma 5.8 is therefore given by

$$R_i=\begin{cases}R\frac{w_i}{2-w_{(k)}} & i\leq k\\ R\frac{2w_i}{2-w_{(k)}} & i>k\end{cases}$$

The upper bound from Lemma 5.9 now equals

$$\begin{aligned}\sum_{i=1}^{n}\phi_i\left(\frac{B}{R}\right) &= \sum_{i=1}^{k}\frac{w_i}{2}\left(u_i+\frac{B}{R}\right)+\sum_{i=k+1}^{n}w_i\frac{B}{R}\\ &= \frac{1}{2}\sum_{i=1}^{k}w_iu_i+\frac{B}{R}\left(1-\frac{w_{(k)}}{2}\right).\end{aligned}$$

5.4.4. LOWER BOUND ON THE GAME VALUE

As noted before, *GL-MS* does not generally have a Nash equilibrium because of the non-convexity of H. This non-convexity is in turn caused by the non-convexity of $\phi_i(1/\cdot)$ for each i. To obtain a lower bound on the game value, we devise a different version of the game where this convexity does hold and find the optimal solution for that game.

NEW PAYOFF FUNCTION

To devise the new game, we take the following steps:

i) We take the functions ϕ_i and consider $\psi_i : x \mapsto \phi_i(1/x)$.

ii) We then define $\psi_i^\dagger$ as the lower convex envelope of ψ_i (i.e., the largest convex function that is dominated by ψ_i).

iii) We transform $\psi_i^\dagger$ back in the same way to define $\phi_i^\dagger : x \mapsto \psi_i^\dagger(1/x)$. This function is dominated by ϕ_i and is still concave. However, by construction $\phi_i^\dagger(1/\cdot)$ is now convex.

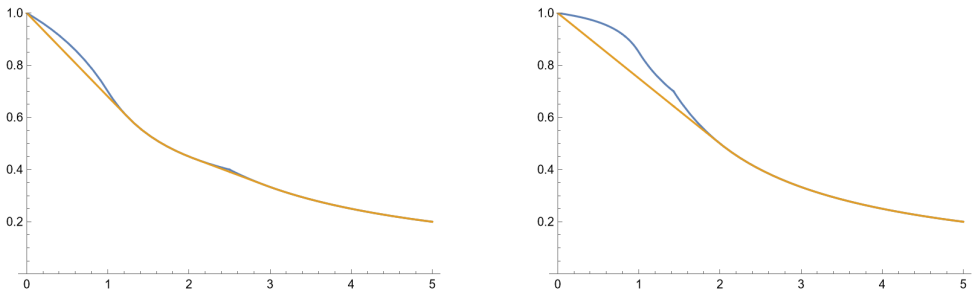

(a) ψ_i and $\psi_i^\dagger$ for $u_i = \frac{2}{5}$

(b) ψ_i and $\psi_i^\dagger$ for $u_i = \frac{7}{10}$

Figure 5.4.: The function ψ_i and its convex envelope $\psi_i^\dagger$ for two different u_i, both with $w_i = 1$.

We first follow this recipe for $u_i > 0$. In that case we get

$$\frac{1}{w_i}\psi_i(x) = \begin{cases} 1-\frac{x(1-u_i)^2}{2(1-u_ix)} & x \le 1 \\ \frac{u_i}{2}-\frac{1}{2x} & 1 \le x \le \frac{1}{u_i} \\ \frac{1}{x} & x \ge \frac{1}{u_i} \end{cases}.$$

To understand how to obtain the convex envelope $\psi_i^\dagger$, the graph of ψ_i is shown in Figure 5.4 for two different u_i, along with their convex envelopes. As can be observed from the graph, depending on u_i, there are two different versions of the convex envelope. The formulas are straightforward to derive.

i) For $u_i \le 2-\sqrt{2}$ there is a linear part, then $u/2+1/(2x)$, another linear part and finally $1/x$. The equations are straightforward to derive and are given by

$$\frac{1}{w_i}\psi_i^\dagger(x) = \begin{cases} 1-\frac{x}{2\alpha_i^2} & x \le \alpha_i \\ \frac{u}{2}+\frac{1}{2x} & \alpha_i \le x \le \beta_i \\ \frac{2\gamma_i - x}{\gamma_i^2} & \beta_i \le x \le \gamma_i \\ \frac{1}{x} & x \ge \gamma_i, \end{cases}$$

where

$$\alpha_i = \frac{2}{2-u_i}, \qquad \beta_i = \frac{2(\sqrt{2}-1)}{u_i}, \qquad \gamma_i = \frac{2(2-\sqrt{2})}{u_i}.$$

Note that for all i

$$1 \le \alpha_i \le \beta_i \le \frac{1}{u_i} \le \gamma_i.$$

ii) For $u_i \ge 2-\sqrt{2}$ we get a linear part, followed by $1/x$:

$$\frac{1}{w_i}\psi_i^\dagger(x) = \begin{cases} 1-\frac{x}{4} & x \le 2 \\ \frac{1}{x} & x \ge 2 \end{cases}.$$

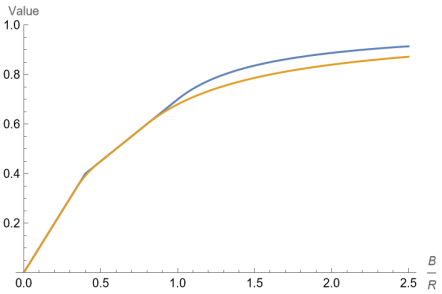

(a) ϕ_i and $\phi_i^\dagger$ for $u_i = \frac{2}{5}$

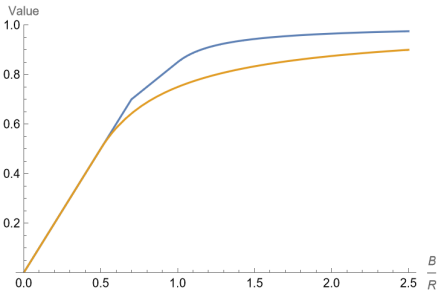

(b) ϕ_i and $\phi_i^\dagger$ for $u_i = \frac{7}{10}$

Figure 5.5.: The function ϕ_i and the transformed convex envelope $\phi_i^\dagger$ for two different u_i, both with $w_i = 1$.

Now we transform this to $\phi_i^\dagger$ by again considering $\psi_i^\dagger(1/x)$. The two different versions are shown in Figure 5.5. The formulas are as follows.

i) For $u_i \le 2-\sqrt{2}$

$$\frac{1}{w_i}\phi_i^\dagger(x) = \begin{cases} x & x \le \frac{1}{\gamma_i} \\ \frac{2\gamma_i x - 1}{\gamma_i^2 x} & \frac{1}{\gamma_i} \le x \le \frac{1}{\beta_i} \\ \frac{u}{2} + \frac{x}{2} & \frac{1}{\beta_i} \le x \le \frac{1}{\alpha_i} \\ 1 - \frac{1}{2\alpha_i^2 x} & x \ge \frac{1}{\alpha_i} \end{cases}$$

ii) For $u_i \ge 2-\sqrt{2}$

$$\frac{1}{w_i}\phi_i^\dagger(x) = \begin{cases} x & x \le \frac{1}{2} \\ 1 - \frac{1}{4x} & x \ge \frac{1}{2} \end{cases}.$$

This was all in case $u_i > 0$. For $u_i = 0$, we see analogously that

$$\frac{1}{w_i}\phi_i(x) = \begin{cases} \frac{x}{2} & x \le 1 \\ 1 - \frac{1}{2x} & x \ge 1 \end{cases}$$

so

$$\frac{1}{w_i}\psi_i(x) = \begin{cases} 1 - \frac{x}{2} & x \le 1 \\ \frac{1}{2x} & x \ge 1. \end{cases}$$

Note that this function is already convex. Therefore $\psi_i^\dagger = \psi_i$ and $\phi_i^\dagger = \phi_i$.

By construction, the $\phi_i^\dagger$ are now reciprocally concave, i.e., $\phi_i^\dagger$ is concave and $\phi_i^\dagger(1/\cdot)$ is convex. We use these to define a new payoff function

$$H^\dagger(B_1,..,B_n,R_1,..,R_n) = \sum_{i=1}^n \phi_i^\dagger\left(\frac{B_i}{R_i}\right).$$

Note that $H^\dagger$ is concave in $B_1,..,B_n$ and convex in $R_1,..,R_n$. Also note that setting $\phi_i(B_i/0) = 1$ and $B_i \ge \epsilon > 0$ ensures continuity of $H^\dagger$ everywhere.

VALUE OF THE DOMINATED GAME

We now define a new game with payoff $H^\dagger$, which has the required convex-concavity. First fix $B, R > 0$ and set

$$c_i = \frac{(\phi_i^\dagger)'(B/R)}{\sum_{j=1}^n (\phi_j^\dagger)'(B/R)}.$$

We fix ϵ so that $0 < \epsilon < B \min_i c_i$ and require that $B_i \ge \epsilon$ for all i. Note that this extra restriction can only lower the value for Blue, so the value of the resulting game is still a lower bound for the original game.

All the $\phi_i^\dagger$'s are C^1, so we can apply Lemma 5.8 to conclude that the unique Nash equilibrium is obtained by setting $B_i = c_i B$ and $R_i = c_i R$. Moreover, the game value is $\sum_i \phi_i^\dagger(B/R)$. Note that by construction of ϵ, the B_i all satisfy the restriction $B_i \ge \epsilon$.

To compute the c_i's more explicitly, one needs the derivative of $\phi_i^\dagger$, which is given below.

i) For $u_i = 0$

$$\frac{1}{w_i}(\phi_i^\dagger)'(x) = \begin{cases} \frac{1}{2} & x \le 1 \\ \frac{1}{2x^2} & x \ge 1 \end{cases}$$

ii) For $0 \le u_i \le 2-\sqrt{2}$

$$\frac{1}{w_i}(\phi_i^\dagger)'(x) = \begin{cases} 1 & x \le \frac{1}{\gamma_i} \\ \frac{1}{\gamma_i^2 x^2} & \frac{1}{\gamma_i} \le x \le \frac{1}{\beta_i} \\ \frac{1}{2} & \frac{1}{\beta_i} \le x \le \frac{1}{\alpha_i} \\ \frac{1}{2\alpha_i^2 x^2} & x \ge \frac{1}{\alpha_i} \end{cases}$$

iii) For $u_i \ge 2-\sqrt{2}$

$$\frac{1}{w_i}(\phi_i^\dagger)' = \begin{cases} 1 & x \le \frac{1}{2} \\ \frac{1}{4x^2} & x \ge \frac{1}{2} \end{cases}$$

5.4.5. VALUE OF THE ORIGINAL GAME

So far we have obtained an upper bound and a lower bound for the game. Now note that in some cases, the c_i's as computed in Section 5.4.4 coincide with the ones that were used in Section 5.4.3. Namely, when for each i one of the following conditions holds:

i) $u_i = 0$

ii) $0 \le u_i \le 2-\sqrt{2}$ and either

$$\frac{B}{R} \le 1/\gamma_i = \frac{u_i}{2(2-\sqrt{2})}$$

or

$$\frac{u_i}{2(\sqrt{2}-1)} = 1/\beta_i \le \frac{B}{R} \le 1/\alpha_i = 1 - u_i/2$$

iii) $u_i \ge 2-\sqrt{2}$ and $\frac{B}{R} \le 1/2$

Therefore, in these cases the upper and lower bound coincide. This implies that the value of the game equals

$$\sum_{i=1}^{n} \phi_i\left(\frac{B}{R}\right),$$

since this is the upper bound we found. In particular, when all u_i's are 0, the value is

$$\frac{1}{2}\frac{B}{R}.$$

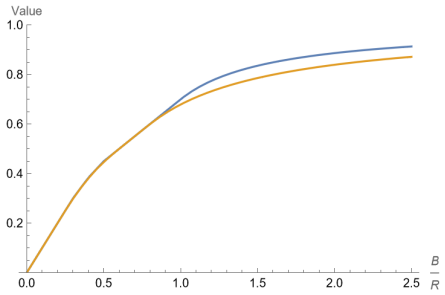

(a) $u_1 = \frac{3}{10}, u_2 = \frac{4}{10}, u_3 = \frac{5}{10}$

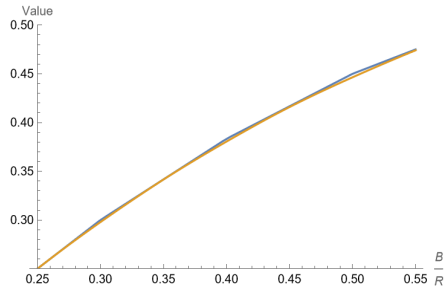

(b) $u_1 = \frac{3}{10}, u_2 = \frac{4}{10}, u_3 = \frac{5}{10}$

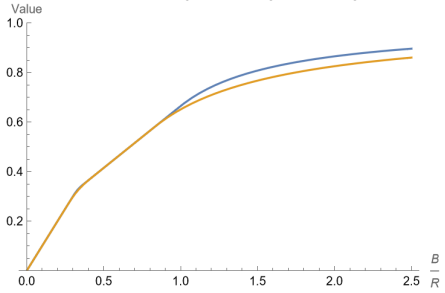

(c) $u_1 = 0.31, u_2 = 0.33, u_3 = 0.35$

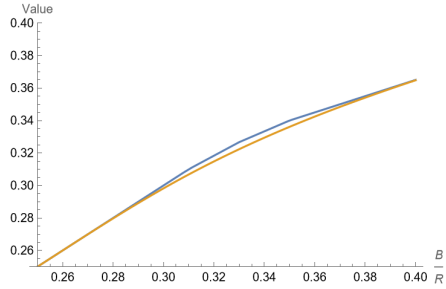

(d) $u_1 = 0.31, u_2 = 0.33, u_3 = 0.35$

Figure 5.6.: The value of the GL-MS with 3 fields, for different values of u_i. All three fields have value 1/3. The right figures are zoomed-in versions of the left figures.

We get back to this in Section 5.6. In the other cases, the bounds do not coincide, so we only obtain a range of possible game values. Figure 5.6 shows the lower and upper bounds for a fixed choice of w_i, u_i as a function of B/R.

Remark 5.10 (Comparison with known results)**.** *When all u_i's are set to 0, we obtain the following unique second-stage strategy: $B_i = w_i B$ and $R_i = w_i R$. Then on each field a single field General Lotto game is played with the same resource ratio $B_i/R_i = B/R$. The total expected payoff still equals $\frac{B}{2R}$ whenever $B \leq R$ and $1 - \frac{R}{2B}$ otherwise. This is (like in Remark 5.6) consistent with Corollary 1 of Kovenock and Roberson [71]. The difference between our case and theirs is that they treat the game as a one-shot game. Apparently, changing the game to a multistage variant did not affect the value.*

5.5. Measuring information versus strength

In the preceding sections, we have determined the optimal strategies and value for games with fixed amounts of resources and information, effectively addressing our first main research question. For this section, we transition to our second main research question: The influence of information versus strength and the weapons mix problem. The weapons mix problem consists of choosing the optimal combination of information (scouting drones) and resources which provide strength (troops). In this section, we present three different ways to compare the influence of information against the influence of resources for *GL-S*, ending with the weapons mix problem. Two of these ways are similar to methods that were independently used in Chandan et al. [74].

5.5.1. Influence ratio

One way to measure the influence of information versus strength is to compare the increase in game value under the addition of information against the increase of the game value under the addition of resources. To this end we fix $R > 0$ and compute for each pair of B, u, the ratio of derivatives of the game value with respect to B and u, respectively. This yields the following:

$$V_u := \frac{\partial V}{\partial u} = \begin{cases} 0 & \frac{B}{R} < u \\ \frac{1}{2} & u < \frac{B}{R} < 1 \\ \frac{(1-u)(2B/R-1-u)}{2\left(\frac{B}{R}-u\right)^2} & 1 < \frac{B}{R} \end{cases}$$

$$V_B := \frac{\partial V}{\partial B} = \begin{cases} \frac{1}{R} & \frac{B}{R} < u \\ \frac{1}{2R} & u < \frac{B}{R} < 1 \\ \frac{(1-u)^2}{2R(B/R-u)^2} & 1 < \frac{B}{R} \end{cases}$$

This allows us to define the influence ratio IR:

$$IR := \frac{1}{R}\frac{V_u}{V_B} = \begin{cases} 0 & \frac{B}{R} < u \\ 1 & u < \frac{B}{R} < 1 \\ 1 + \frac{2}{1-u}\left(\frac{B}{R} - 1\right) & 1 < \frac{B}{R} \end{cases}$$

The graph of the influence ratio is shown for $R = 1$ in Figure 5.7. The diagonal line $u = B$ between blue and purple marks the 'Exploitation Line', i.e., under this line additional information is valuable because it can be used, but above this line there are simply not enough resources. Using this, the graph can be divided into 3 parts. Directly above the exploitation line we have the upper triangular region, where the influence ratio is 0, which means adding information does not increase the value of the game. Directly below the exploitation line is the lower triangular region, where the influence ratio is exactly 1, which means everywhere in the lower triangle, increasing either u or B by the same amount, leads to the same increase in value. And on the right side we have the right rectangle, where the influence ratio is larger than 1, which means the value increases more for an increase in u than

for the same increase in B. Note the interesting behaviour around the point $(1,1)$. The reason is that for $B<1$, going from information $u=1-\epsilon$ to $u=1$ is not valuable at all, because there are not enough resources to use the information. However, for $B>1$ the increase of information from $1-\epsilon$ to 1 is extremely valuable. The reason for this is that when $u=1-\epsilon$ adding resources will never yield a value of 1, where adding just the final ϵ bit of information does yield game value 1.

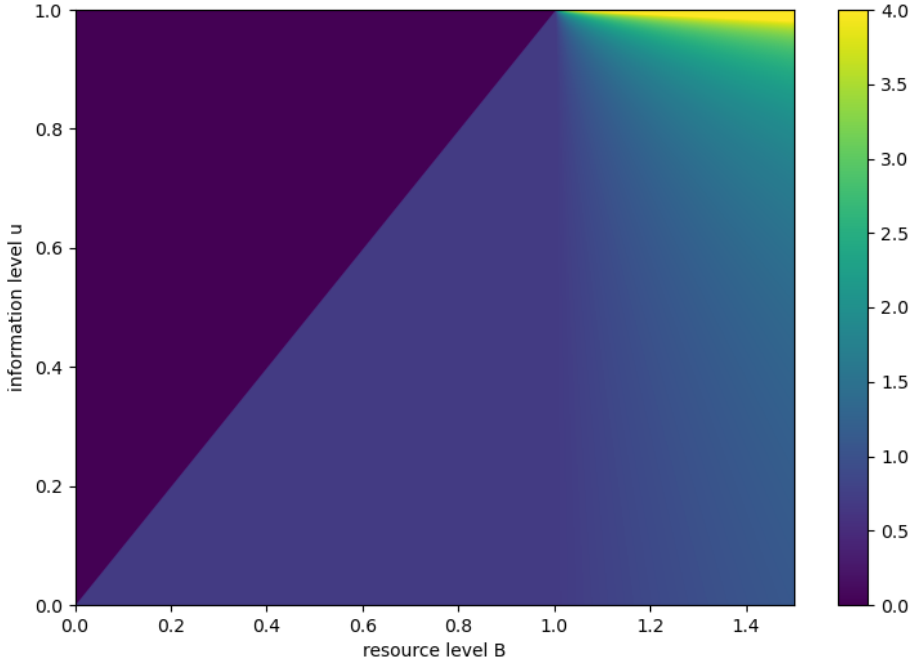

Figure 5.7.: Heatmap of the Influence Ratio, as a function of resources B and information u. A higher influence ratio indicates that information is more valuable.

5.5.2. RESOURCES NEEDED TO ATTAIN A GIVEN GAME VALUE

Another way to quantify the influence of information is by studying how many resources are needed to obtain a certain game value given a level of information. The resource ratio B/R that is needed to attain game value v given information u equals

$$\frac{B}{R}=\begin{cases} u+\frac{(1-u)^2}{2(1-v)} & u\leq 2v-1 \\ 2v-u & 2v-1\leq u\leq v \\ v & u\geq v \end{cases}$$

Note that for any given fixed value v, the equation above exactly represents the contour line of the value function for this particular value v. In Figure 5.8, we display several of these contour lines. This visualization also provides insight into how to maximize the game value with minimal additional information or resource allocation. Specifically, this can be achieved by moving perpendicular to the contour lines. Notably, in the top-left region, we observe once again that adding information does not enhance the game value; instead, only the addition of resources can lead to an increase.

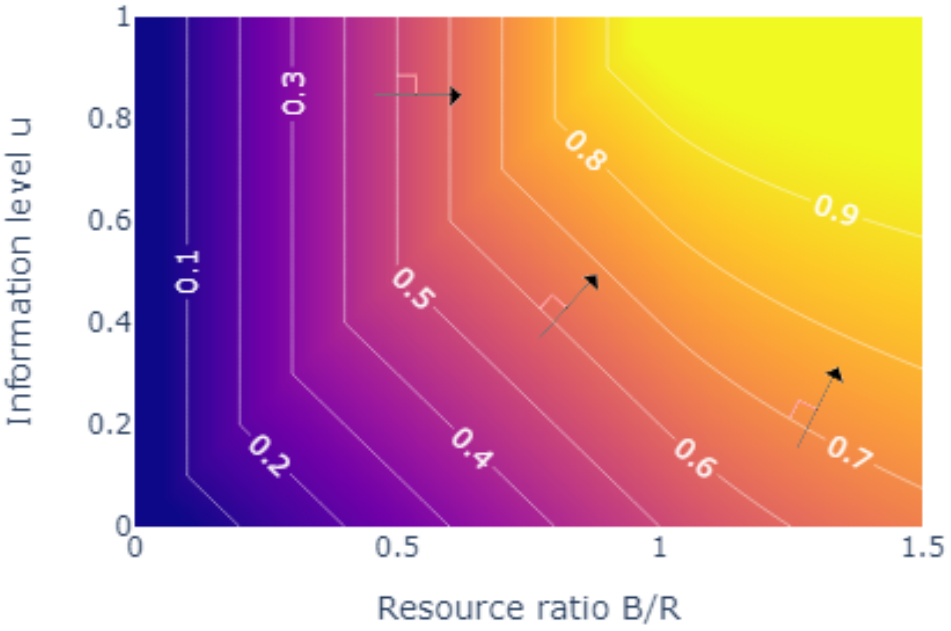

Figure 5.8.: Contour plot of the value of *GL-S* as a function of B/R and u. The arrows indicate the direction in which the value increases most steeply.

5.5.3. Optimising information vs strength

In this section, we delve into the weapons mix problem, which revolves around a fixed budget D to be divided between resources and information. We assume $R = 1$ and set the cost of resources B to 1 per unit and the cost of information at c per unit. This yields the restriction that $B + cu \leq D$. Using the solution found to *GL-S* in Section 5.3, we can determine the B and u that maximise the game value under this constraint, thereby identifying the optimal allocation of the budget between resources and information.

Varying the total budget D produces the graphs in Figure 5.9. The line

corresponding to $c = 100$ was included to illustrate the case in which information is so expensive that it is not used at all, resembling the 'no-information case'.

The top-left graph of Figure 5.9 shows the maximum attainable value for a budget D. It's evident that a higher cost c of information always leads to a lower game value.

Moving to the top-right graph, we see that for $c < 1$ it is optimal for any budget D to invest in both resources and information, with both steadily increasing for higher budgets until a game value of 1 is reached. For $c > 1$ it is better to only invest in resources for when the budget is small. However, if we increase the budget, there is a certain point after which it also becomes worthwhile to invest in information as well. Interestingly, from that point onwards Blue will actually start decreasing the amount spent on resources, as his investment in information increases faster than the increase in budget. The decrease in resources bought can be seen in the bottom-left graph.

Finally, note from the top-left graph that a budget $D \geq 1 + c$ ensures that the game value is 1. This outcome is understandable since c can be spent on buying information, thereby acquiring perfect information $u = 1$. With perfect information, Blue only needs to spend $R = 1$ on resources to always match Red and thus always win. Since a budget of $1 + c$ guarantees Blue always wins, the surplus budget need not be used. The unused budget is shown in the bottom-right graph.

5.6. INTERPRETATION

In the previous sections, we have tackled the two main research questions outlined at the start of this chapter: the weapons mix problem and efficient strategies when using scouts. Now, our focus shifts towards interpreting these questions and their respective solutions within a military context, particularly concerning the scenario of troops providing firepower and scouting drones providing information. In this section we outline general guidelines for optimal strategies, the most effective combination of troops and scouting drones, and whether to prioritise additional troops or additional scouting drones. Underlying these guidelines are the insights obtained in various parts of the chapter. We use the strategies and values calculated for the *GL-S* model and employ the three distinct ways to compare information and strength within these models.

5.6.1. EFFICIENT STRATEGIES WITH SCOUTS

We start with guidelines for efficient strategies when the number of resources and the amount of information are predetermined. The situation we analyse is as follows: Red and Blue will face each other in a number of battles. Both have a given amount of resources and additionally Blue has a given number of scouts, which roughly translates to a probability to gain information about Red's allocation of resources.

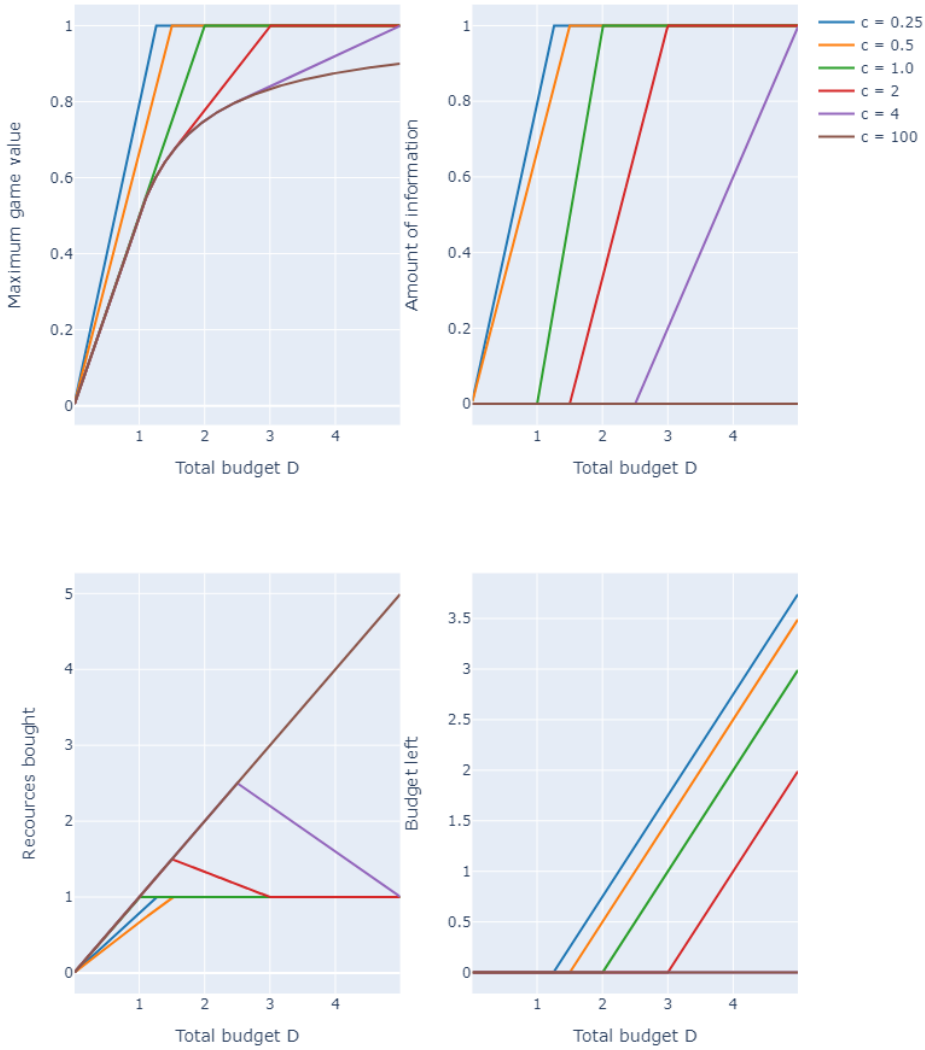

Figure 5.9.: Let D be the fixed budget to be spent between information and resources. Here we plot the characteristics as function of the total budget D, for several different costs of information c.

Blue and Red have different challenges in formulating their strategies. For Blue, the strategy can be split into two sub-strategies: what to do if Blue gains

information, and what to do if Blue doesn't gain information. How does Blue best convert his scouting advantage into the battle? Red aims to provide a strategy that is as scout-resistant as possible, recognising the possibility of her allocation to be scouted to Blue. Is this achieved by playing more stable and always sending the same number of resources, which causes Blue to learn nothing extra when he gains information? Or is this done by playing more risky and pooling a large part of resources together for a large attack, hoping that this one is not revealed?

The answer to all of these questions depends on the probability of Blue gaining information and the resource ratio B/R. There are three distinct cases, each with its own set of strategies for Blue and Red. We discuss these cases separately and provide insights based on Theorem 5.5, which describes an optimal solution to *GL-S*.

RED HEAVILY OUTNUMBERS BLUE, WHO HAS MANY SCOUTS ($B/R < u$)

In this case, Blue's optimal strategy involves only allocating resources when information about Red's allocation is obtained, conserving resources otherwise. Blue does not have enough resources to match Red every time the field is revealed, but should try to match as often as possible. Red's best response is to always allocate the exact same number of resources, thus neutralising the advantage Blue has when he gets information about Red's allocation.

RED OUTNUMBERS BLUE, WHO HAS FEW SCOUTS ($u < B/R < 1$)

Here Red uses the same strategy as she would in a standard General Lotto Game, always allocating resources but randomising the exact amount slightly. Blue can match Red's allocation whenever it is revealed and still have resources left in his resource budget. Therefore, Blue should also allocate resources occasionally when he has no information about Red's allocation. If Blue decides to allocate resources, he should follow Red's strategy for determining the exact number.

BLUE OUTNUMBERS RED ($1 < B/R$)

Now Blue can match Red's allocation whenever it is revealed and additionally allocate resources every time it is not revealed. The exact amount should be randomised slightly. For Red, it is best to allocate resources even less often than in a standard General Lotto game. This means that Red should often not allocate any resources, and occasionally allocate a large number, while still randomising the exact amount. The level of risk taken by Red increases with both the ratio with which she is outnumbered and how often Blue gains information on her resource allocation. If Red decides to allocate resources, she should follow Blue's strategy for determining the exact number.

5.6.2. WEAPONS MIX PROBLEM

Now that we have provided guidelines for efficient strategies given fixed amounts of resources and information, we discuss guidelines for when the amounts of resources

and information are not fixed, and can instead be chosen under a fixed budget. First, we discuss the influence of information and resources, respectively, and how they relate to military practice and experience. Then we consider the budget constraints, thereby addressing the weapons mix problem.

THE VALUE OF INFORMATION

To analyse the value of information, recall Figure 5.2. Two modes of behaviour exist, depending on whether Blue has more ($B/R > 1$) or less ($B/R < 1$) resources than Red. In the first case, an increase in information always leads to an increase of value. However, in the second case, there is a cut-off point: initially, extra information is beneficial, but beyond the cut-off point, there is no additional gain. The main takeaway from these considerations is that information only provides value as long as there are enough resources in strength available to take advantage of this information.

We see something similar in military practice, for instance in the war following the Russian invasion of Ukraine. Ukraine has a great intelligence position due to help from many allies. However, beyond a certain point, more intelligence does not yield any better results. Knowing exactly what the opponent does is not helpful when there are no resources to counter them.

THE VALUE OF RESOURCES

For a deeper analysis of the value of resources, we turn to Figure 5.1. Again, there is a clear breakpoint. When B/R is smaller than u, all of the Blue forces are used to counter Red forces when they are observed, hence they are always employed effectively. However, when B/R is larger than u, some of the Blue resources are used in situations where Red is not observed. These Blue resources are used less effectively. This results in a smaller increase in game value after the break point.

Similarly, in military practice, deploying troops is much more effective when the strength of the opponent in the area is known. As soon as all available information on the opponent has been exploited, any new troops are used in more uncertain situations and are therefore less effective. We find this reflected in the Russian-Ukrainian war, where Russia has many more troops and weaponry to deploy but has an inferior intelligence position. This makes the deployment of Russian troops less effective.

BUDGET CONSTRAINTS

Finally, we arrive at our second research question: how to optimally distribute a military budget over resources and information. We studied this question most directly in Section 5.5.3, of which the main results are shown in Figure 5.9. From this figure, we can extract three regimes, which we show in Table 5.2.

(I) In this case, information is cheap compared to resources. This corresponds to $c < 1$ in Figure 5.9. In this case it is directly worthwhile to buy information, so as budget increases resources and information are bought equally.

(II) Here information is expensive (so $c > 1$) and there is a low budget. In this case it is not worthwhile to invest in information, and it is best to spend the entire budget on resources.

(III) As in case (II) information is expensive (so $c > 1$), but there is also a high budget. Now it is again worthwhile to buy information. In fact, with a higher budget, some resources are exchanged for more information (as one can tell from the decreasing lines in the bottom-left graph of Figure 5.9).

The main takeaway here is that if information is cheap, you should always buy it, along with resources. If information is expensive, you should focus on resources first and only buy information if your budget is high enough.

		Information	
		Cheap	**Expensive**
Budget	**Low**	(I) Combine	(II) Only resources
	High		(III) Focus on information

Table 5.2.: Preferred strategy in cases of high and low budget and with cheap and expensive information. Derived from Figure 5.9.

5.7. DISCUSSION

In this chapter, we introduced the General Lotto Game with Scouts, a resource allocation game enhanced with the possibility of gaining information on the opposing player through scouting. We provided a complete solution for the game concerning a single field. Subsequently, we extended our analysis to a multistage version, establishing upper and lower bounds for its value and determining conditions on when they coincide. Additionally, we introduced several metrics to quantify the trade-off between information and resources. Finally, we interpreted these findings and drew qualitative conclusions, summarised as follows:

- Information is only useful when there are enough resources to exploit it.
- Resources are employed more efficiently in the presence of information.
- When information is cheap, one should always buy it alongside resources. When it is expensive, one should first focus on buying resources and only invest in information if the budget is high enough.
- When Blue receives information, it is always best to call as often as possible.
- Red should play very stable if she heavily outnumbers Blue, and very risky if Blue heavily outnumbers her.

In this section, we discuss the model and results. We conclude with some suggestions for future work.

5.7.1. Discussion of the model and results

Lotto constraint before or after observing Red's resource allocation

The characterising feature of a General Lotto model is the constraint that the total allocated budget should equal a fixed constant in expectation. Since our studied situation involves potential information revelation, one faces a decision when this constraint should be applied: one can require the expected total resources to equal a constant before or after potentially revealing Red's resource allocation.

The second option might seem more natural, but has certain curiosities in the General Lotto framework. For instance: whenever Red allocates less resources than Blue's total budget, she always loses. Therefore, Red will likely alternate between allocating nothing and allocating significantly more than Blue's budget. Additionally, Blue has only one sensible response when Red's allocation is revealed, namely matching Red with the highest possible probability.

In this chapter, we chose for the former definition: requiring the budget constraint before the allocation is revealed. This allows Blue to decide how much of the budget he wants to allocate in the information and no-information case, which in turn allows us to study where he can use his budget most effectively. The only drawback is that since Blue's allocation depends on Red's, his allocation distribution depends on Red's allocation distribution.

Constant price of information

In Section 5.5.3, we examined a fixed budget D to be divided between resources and information. We assigned information a fixed cost of c per unit. However, this straightforward approach implies that the cost of increasing information from 0 to 0.1 is identical to the cost of increasing from 0.9 to 1. In practical scenarios, obtaining basic information about a situation is often much cheaper than acquiring the final details.

This choice for a fixed cost model significantly impacts the perceived value of information in comparison to resources. In particular, in the top-right part of Figure 5.7, the value of information is much larger than the value of resources. This large difference stems from the fact that even a marginal increase in information can elevate the game value to 1, a feat unachievable solely through an increase in resources.

To better reflect real-world conditions, one could consider assigning information a non-linear cost. For instance, introducing a cost function such as $F(u) = 1/(1-u) - 1$ would result in the cost of acquiring information increasing with each unit purchased. Consequently, perfect information becomes impossibly expensive to attain, thereby imposing a practical limit on information acquisition.

5.7.2. FUTURE WORK

We conclude this work with potential avenues for extending our research beyond its current scope. While we have already mentioned adjusting the Lotto constraint and the introduction of a non-linear price of information, there are several additional options for future research.

First, one could consider more complicated scenarios for the single field case. For instance, one could investigate scenarios where the information obtained by Blue is partial, perhaps by revealing each of Red's units independently with certain probabilities. Another intriguing possibility is to introduce false signals, complicating the accuracy of the information gained by Blue and adding an element of uncertainty.

Second, it could be interesting to study extensions to the multistage version of the game. For example, one could explore allowing Blue to optimise the detection probabilities $u_1,..,u_n$ under a fixed budget constraint. Additionally, each field could have a 'visibility' parameter, which influences how hard it is for Blue to obtain information, resulting in varying information costs per field. Another option is to give Blue a fixed amount of scouts, which he must then distribute strategically among the fields. I.e., if blue has only two scouts, only the two fields he sends these to could be revealed. These extensions might give a 'search game dynamic' where a trade-off will be sought between allocating resources and search capacity to more and less visible fields.

REFERENCES CHAPTER 5

[5] J.-T. Brethouwer, B. Van Ginkel, and R. Lindelauf. "General Lotto Games with Scouts: Information versus Strength". In: *preprint, arXiv:2404.05841, submitted to Dynamic Games and Applications* (2024).

[18] E. Borel. "La théorie du jeu et les équations intégralesa noyau symétrique". In: *Comptes rendus de l'Académie des Sciences* 173.1304-1308 (1921), p. 58.

[23] O. Gross and R. Wagner. *A continuous Colonel Blotto game*. Rand Corporation, 1950.

[24] B. Roberson. "The Colonel Blotto game". In: *Economic Theory* 29.1 (2006), pp. 1–24.

[63] A. R. Eckler and S. A. Burr. *Mathematical models of target coverage and missile allocation*. -: Military Operations Research Society Alexandria, VA, 1972.

[64] A. Washburn. "OR forum—Blotto politics". In: *Operations Research* 61.3 (2013), pp. 532–543.

[65] J.-F. Laslier and N. Picard. "Distributive politics and electoral competition". In: *Journal of Economic Theory* 103.1 (2002), pp. 106–130.

[66] S. Behnezhad, S. Dehghani, M. Derakhshan, M. HajiAghayi, and S. Seddighin. "Faster and simpler algorithm for optimal strategies of Blotto game". In: *Proceedings of the AAAI Conference on Artificial Intelligence*. Vol. 31. 1. 2017.

[67] D. Liang, Y. Wang, Z. Cao, and X. Yang. "Discrete Colonel Blotto games with two battlefields". In: *International Journal of Game Theory* (2023), pp. 1–41.

[68] S. Hart. "Discrete Colonel Blotto and General Lotto games". In: *International Journal of Game Theory* 36.3 (2008), pp. 441–460.

[69] F.-S. Gady. "How an Army of Drones Changed the Battlefield in Ukraine". In: *Foreign Policy* (2023).

[70] N. K. Jaiswal. *Military operations research: quantitative decision making*. Vol. 5. Springer Science & Business Media, 2012.

[71] D. Kovenock and B. Roberson. "Generalizations of the General Lotto and Colonel Blotto games". In: *Economic Theory* 71 (2021), pp. 997–1032.

[72] K. Paarporn, R. Chandan, M. Alizadeh, and J. R. Marden. "Asymmetric battlefield uncertainty in General Lotto games". In: *IEEE Control Systems Letters* 6 (2022), pp. 2822–2827.

[73] D. Q. Vu and P. Loiseau. "Colonel Blotto games with favoritism: Competitions with pre-allocations and asymmetric effectiveness". In: *Proceedings of the 22nd ACM Conference on Economics and Computation*. 2021, pp. 862–863.

[74] R. Chandan, K. Paarporn, M. Alizadeh, and J. R. Marden. “Strategic investments in multi-stage General Lotto games”. In: *2022 IEEE 61st Conference on Decision and Control (CDC)*. IEEE. 2022, pp. 4444–4448.

[75] S. Alpern and J. Howard. “Winner-take-all games: The strategic optimisation of rank”. In: *Operations Research* 65.5 (2017), pp. 1165–1176.

[76] N. Sahuguet and N. Persico. “Campaign spending regulation in a model of redistributive politics”. In: *Economic Theory* 28 (2006), pp. 95–124.

[77] I. L. Glicksberg. “A further generalization of the Kakutani fixed theorem, with application to Nash equilibrium points”. In: *Proceedings of the American Mathematical Society* 3.1 (1952), pp. 170–174.

6

RISING TENSION IN THE HIMALAYAS: A GEOSPATIAL ANALYSIS

The China-India border is the longest disputed border in the world. The countries went to war in 1962 and there have been recurring border skirmishes ever since. Reports of Chinese incursions into Indian territory are now a frequent occurrence. This rising tension between the world's most populous countries not only poses risks for global security and the world economy, but also has a negative impact on the unique ecology of the Himalayas, because of the expanding military infrastructure. We have assembled a unique data set of the dates and locations of the major incursions over the past 15 years. We find that the conflict can be separated into two independent conflicts, the western and eastern sectors. The incursions in these sectors are statistically independent. However, major incidents do lead to an increased tension that persists for years all along the entire Line of Actual Control (LAC). This leads us to conclude that an agreement on the exact location of a limited number of contested regions, such as the Doklam plateau on the China-Bhutan border, has the potential to significantly defuse the conflict, and could potentially settle the dispute at a further date. Building on insights from game theory, we find that the Chinese incursions in the west are strategically planned and may aim for a more permanent control over specific contested areas. This finding is in agreement with other studies into the expansionist strategy of the current Chinese government.

6.1. INTRODUCTION

On 15 June 2020, an Indian patrol and a Chinese patrol clashed in the Galwan river valley, a disputed area along the China-India border. The patrols were unarmed in accordance with bilateral agreements, but the soldiers used rocks and sticks. This

Parts of this chapter have been published in PloS one [6].

resulted in the deaths of 20 Indian soldiers and an unknown number of Chinese soldiers [78] (the Chinese government reported 4 deaths, while Time magazine [79] estimated 35). This was by far the most violent border incident in years, but the number of Chinese incursions along the China-India border had been steadily increasing, and it seemed like an accident waiting to happen [80]. Immediately after the clash, both sides sought to reduce the tension through rounds of talks [81], meanwhile increasing their military presence [82]. In 2021, they agreed to withdraw their troops from a number of red-zones and the number of incursions now seems to be dropping [83].

The Line of Actual Control (LAC) between China and India remains the longest disputed land border on earth. After a brief war in 1962, the two countries signed several bilateral agreements. In 2005, this culminated in a protocol [84] to develop a long-term constructive partnership, pending an ultimate resolution of the conflict. The countries agreed to not use force, nor threaten to use force, against each other. However, since then, the relationship has deteriorated for several reasons. The trade surplus that India enjoyed up until 2005 has turned into a multi-billion dollar deficit, which has created strong undercurrents of mistrust [85]. Moreover, China significantly increased both its military spending and its military support for Pakistan, which raised a high degree of concern in India [86].

China and India possess nuclear weapons, but both countries subscribe to a no-first-use policy, and the risk of nuclear escalation seems minimal. However, the border conflict could escalate into the use of conventional missiles. Experts have pointed out that these are co-located with nuclear missiles, and that it is challenging to distinguish between the two [87]. The risk of nuclear escalation therefore is minimal, but not negligible. Meanwhile, the conventional escalation of the conflict is ongoing. Tens of thousands of troops are now stationed across the mountains [88]. To support their military presence, both countries keep extending their infrastructure, which leads to ecological degradation of the borderlands [89].

This paper seeks to build an understanding of what drives the conflict. We have assembled an original data set on Chinese incursions into India over the period 2006-2020, starting at a time of détente and ending with a year of heightened tension, when the pandemic had not yet disrupted the world.[1] We apply statistical and game-theoretic methods to study the dynamic of rising and falling tensions along the LAC. Our findings provide a glimmer of hope for a possible way out of the conflict through a step-by-step de-escalation. A resolution of the conflict would be of great benefit for international security, the world economy as well as the economies of the two countries (which are strongly linked), and the ecological preservation of the Himalayas.

STATUS QUO OF THE LAC

The LAC separates the territories controlled by China and India and is perceived by both sides as a kind of working border. It was first suggested by Chinese

[1] We do not consider border incursions by India into China because there are relatively few reports of such incursions during the 15-year period of our study.

prime minister Zhou Enlai in a letter to Indian prime minister Jawaharlal Nehru in 1959 [90]. It is a legacy of agreements between foreign powers. Indeed, a part of it is still named after a British administrator. Historically, the LAC is divided into three sectors [90–92], as illustrated in Fig 6.1:

1. The western sector from the Karakoram pass to Mount Gya, along Chinese controlled Aksai Chin. The Galwan river valley is located here.
2. The middle sector from Mount Gya to the border with Nepal, which is the least contested part of the border.
3. The eastern sector, also known as the McMahon line, along the state of Arunachal Pradesh on the Indian side. This sector also includes the border between Sikkim and Tibet.

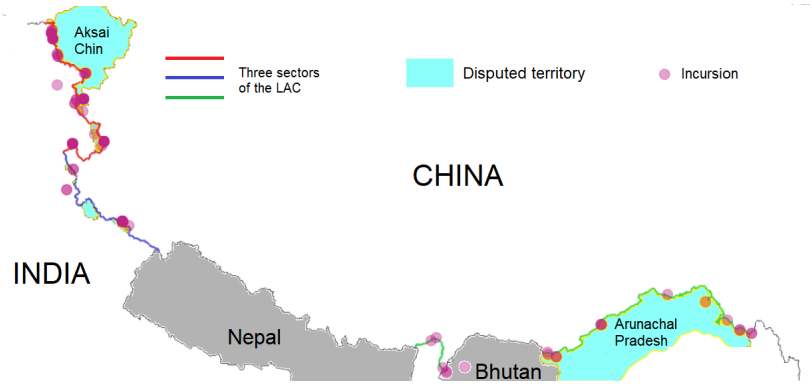

Figure 6.1.: **A map of the LAC and its three sectors.** The locations of incursions along the LAC. The shade represents the number of incursions. The largest contested territories are Aksai Chin in the west and Arunachal Pradesh in the east. (Topographic base maps in our article are accessed from the USGS National Map Viewer).

Formally, both countries claim large areas that are controlled by the other side. The Indian claim of Chinese controlled Aksai Chin, a highland of 40,000 square kilometers, was the major cause of the short war in 1962 [91]. This virtually uninhabited plateau is a vital passage point between the Chinese autonomous regions of Tibet and Xinjiang [93]. China in turn claims 80,000 square kilometers of Arunachal Pradesh, and briefly occupied it during the 1962 war. Some speculate that China will accept the McMahon line as its border, if India waives or sharply modifies its claim to Aksai Chin [94, 95]. Other analysts believe that India wishes to freeze the status quo, a position for which China has little respect [96, 97].

GEOGRAPHICAL, POLITICAL, AND STRATEGIC ASPECTS OF THE CONFLICT

Territorial conflicts usually involve ethnic, geographic or economic conditions [98]. We survey several factors that may play a role in the conflict.

Geographical factors

The LAC is exceptionally long and the conditions along the border vary considerably. The borderland along the middle and eastern sectors is more accessible, fertile and densely populated than the Aksai Chin in the western sector, which is a barren plateau with a total population of less than 10,000. It is, however, of great economic importance to China, since Aksai Chin connects Tibet and Xinjiang. It is near the China-Pakistan Economic Corridor, a major project to connect Xinjiang to Pakistan's Gwadar port [99].

In the eastern sector, the Siliguri corridor is 130 km away from the Sikkim border. This narrow stretch of land is the only connection between India's North-Eastern states and the rest of the country. The Doklam standoff in 2017 was caused by intended Chinese road constructions that were perceived by India as a threat to this corridor [100].

The borderland is rich in mineral reserves, and there are several mines that are exploited or explored. The Aksai Chin has one of the largest zinc-lead deposits in the world, which is currently being prepared for exploitation [101]. Fifty kilometers north of the McMahon line, China launched large-scale investments into mining gold and silver in Lhünzê County. Another aspect is the future use of hydroelectric power. The McMahon line runs through the Brahmaputra river basin, where both China and India have plans for the construction of major hydropower plants [102].

Strategic factors

The People's Republic Army (PLA) is a dominant force. China's policy is increasingly assertive, employing a coercive policy against Taiwan, while staying in the gray zone below open conflict [103]. It is continually extending control over the South China Sea. Its dispute with Japan over the Senkaku/Diaoyudao islands shows the same rising tension as the dispute over the LAC [104].

According to Indian military strategists, the number of Chinese patrols in Indian territory is increasing each year [105]. The PLA has constructed military structures, and even entire villages, in disputed areas of the LAC [106–109]. The PLA strategy is often referred to as *salami slicing* by the Indian media. On the other hand, the terrain around the LAC is more accessible from the Indian side [88] and India's military bases are much nearer to the disputed areas than China's [100]. The balance of (military) power in the conflict is unclear.

Political factors

China and India have close economic ties and would benefit from a settlement of the border dispute, but they are also the two dominant powers in the region and political rivals. The dispute goes through a dynamic between cooperation and conflict, see Table 6.1, that is typical for the political relations between rival powers [110]. In recent years, India's prime minister Modi and China's President Xi Jinping established close personal relations [111]. After the Doklam standoff in 2017, they sought to overcome strategic differences through several informal summits. This was disrupted by the Galwan standoff in 2020, which was possibly triggered by India's decision to

dissolve the special status of the state of Jammu and Kashmir [112]. The incident has been a political setback for prime minister Modi, whose Bharatiya Janata Party (BJP) stands for India's territorial unity more strongly than any other party [113].

2005	Protocol on confidence building measures along the LAC.
2012	Agreement on a Working Mechanism for Consultation and Coordination on India-China Border Affairs.
2013	*Depsang standoff* followed by the Border Defence Agreement to "establish peace and tranquillity".
2014	*Chinese incursion in Chumur* just ten days before Xi visits India and signs a twenty billion dollar investment agreement.
2017	*Doklam Plateau standoff*
2018	Informal talks between Modi and Xi
2020	*Galwan River Valley standoff*

Table 6.1.: Timeline of the border conflict – a concatenation of military confrontations and bilateral agreements.

India's participation in the Quad, the security dialogue between the United States, India, Japan and Australia, may have served as a trigger for Chinese activity along the China–India border. The incursions in the Aksai Chin could be a statement from Beijing to both New Delhi and Washington, that it will continue to ensure its regional interests [90].

6.2. METHODS

DATA

We built a data-set of Chinese incursions into disputed areas from 2005-2020. We define incursions as unauthorized Chinese entries into areas that are internationally accepted as either Indian or disputed territories. We do not distinguish between foot patrols, motor patrols, or combat air patrols. We collected the data using journalistic and academic sources from the LexisUni database. It therefore is as much a study of the media attention as of the incursions. We rely on reports of Chinese incursions that are well documented by multiple independent media outlets and are reported

by major Indian newspapers or international media. We do not record incursions that are reported by the Indian government but not verified by a third party (India currently ranks 150 out of 180 on the World Press Freedom Index of Reporters without Borders (RSF), China ranks 175). The focus of this study is on Chinese incursions into India. We do not consider Indian incursions into China, as these there are few instances that can be verified across multiple independent sources. Most often, these incursions are reported only by the Chinese state media.

year	Gov India	Our data
2020	-	14
2019	663	3
2018	326	18
2017	426	16
2016	273	9
2015	290	5
2014	460	14
2013	411	14
2012	426	6
2011	213	6
2010	228	5
2009	270	6
2008	280	2
2007	140	1
2006	265	1
mean μ	334	8.0
stdev σ	132	5.6
σ/μ	0.40	0.70

Table 6.2.: **Validation of our data.** The Indian government publishes yearly numbers of border incidents (numbers of the Indo-Tibetan Border Police), which are compared to the numbers reported by the media in our data. The official numbers correlate well with our data. The official numbers peaked in 2014 and again in 2019. Remarkably, the number of media reports on incursions in 2019 was very low.

The Indian government publishes yearly numbers of border incursions and transgressions, with an average of 334 incursions per year over the period 2006-2019, see [104]. The number of incursions in 2020 has not been reported yet. The government numbers include minor incidents, such as finding cans of food consumed by Chinese patrols on Indian territory, that are not reported by the media. The official numbers are compared to our numbers in Table 6.2. The numbers reported in the media have a higher coefficient of variation (st.dev/mean) than the official numbers (0.70 versus 0.40). In other words, the numbers presented by the media are more volatile. It is likely that this higher volatility is a consequence of the self-reinforcing nature of media attention [114]. We should keep in mind that our data measures the number of incursions through a slightly distorted lens.

We found an average number of 8.0 incursions per year that were reported by the media (our data set). If we adjust the scales to compare the two time series, as illustrated in Fig 6.2, then they show the same trend. The number of incursions has been rising since 2006. There have been years in which the numbers were stable or even reduced, but they were invariably followed by a further increase.

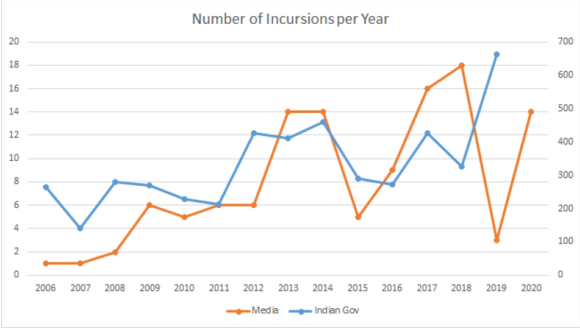

Figure 6.2.: **Comparison of our data and the official numbers on adjusted scales**. The upward trend over the entire period is the same in both data sets, but the numbers in our data are clearly more volatile than the official numbers.

The Indian government reported no less than 663 transgressions in 2019, but only 3 of these made it to the international media. Indian prime minister Modi and Chinese President Xi held several informal meetings at the time and reiterated their effort to ensure peace, in accordance with the 2005 protocol [115]. The chief of the Indo-Tibetan Border Police (ITBP) reported a peaceful situation [116]. These efforts to downplay the actual situation, with an all-time high number of transgressions, worked: the media reported an exceptionally low number of incursions that year. If we delete this outlier from our data set, the correlation between the government numbers and our data is 0.69. All things considered, our data agrees well with the official numbers of the Indian government.

A data set that is similar to ours, though much more restricted, has been assembled by the Observer Research Foundation [117]. This data set contains only biennial numbers of incursions over the years 2006-2014. The ORF data set is very close to ours (corr. coeff. 0.99).

DATA PROCESSING

Media reports rarely specify the exact time or location of the incursions. They specify the date and the name of a village, a military base, or a geographical landmark close to where the incursion took place. It is impossible to pinpoint the incursions with absolute precision in time or space. Our data contains the date of the incursion and a best estimate for its geographic coordinates. The LAC runs across mountain crests and only a few passes and valleys can be patrolled, so that these coordinates should

be approximately correct, within a few kilometers of the actual locations. A heat map of the incursions in Fig 6.3 clearly shows that the incursions are clustered in space.

Figure 6.3.: **A heat map of the incursions.** The media reports do not always give the exact coordinates and only mention a military base or village nearest to the incursion. It is impossible to pinpoint the precise locations of the incursions. However, it is clear that the incursions are clustered around hot spots where the border is not clearly defined. These are the so-called red-zones (USGS base map).

location (W)	coordinates	incursions	location (E)	coordinates	incursions
Depsang	35.3N, 78.0E	23%	Sikkim	27.6N, 88.8E	30%
Galwan	34.8N, 78.2E	6%	Tawang	27.7N, 91.8E	20%
Hotspring	34.3N, 79.0E	5%	Lhunze	28.5N, 93.3E	10%
Pangong	33.7N, 79.4E	26%	Bishing	29.1N, 95.0E	5%
Demchok	32.8N, 79.4E	16%	Anini	29.0N, 96.0E	10%
Chumur	32.7N, 78.6E	24%	Kibithu	28.3N, 97.2E	25%

Table 6.3.: **The incursions in the western and eastern sector.** The distribution is not even. In the western sector, almost all incursions occurred in Chumur, Demchok Depsang, and Pangong. In the eastern sector, three quarters of the incursions occurred in Sikkim, Tawang, and Kibithu.

The incursions in the middle sector are concentrated around the Barahoti military base. In the eastern sector there are six red-zones, one along the Sikkim border and five along the McMahon line. The data is more diffuse in the western sector, where the media reports incursions near six locations: Depsang, Pangong, Demchok, Chumur, Hot Springs, and Galwan Valley. The majority of the incursions occur in four locations, see Table 3 and the heat map in Fig 6.4.
We treat the locations of the incursions as categorical data, divided into thirteen locations, see Fig 6.5. The incursions in the middle sector are all in the Barahoti

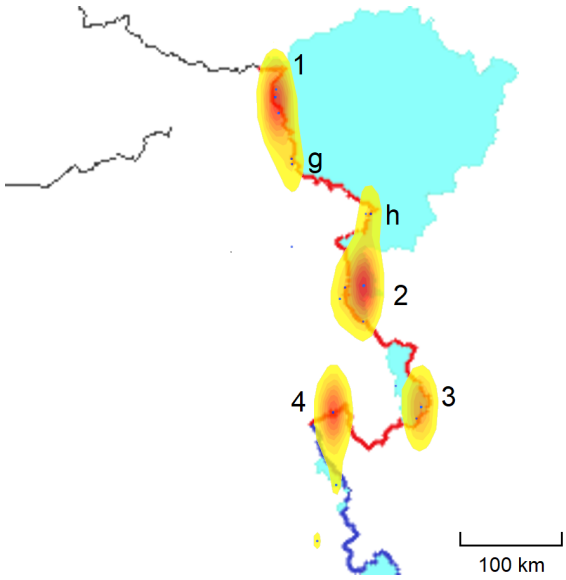

Figure 6.4.: **Heat map of the incursions in the western sector.** The majority of the incursions occur near four red-zones: 1 Depsang Plateau, 2 Pangong Lake, 3 Demchok, 4 Chumur. Some of the incursions are outside these four red zones: near the Galwan Valley (g) or near the Hot Springs border checkpost (h), which are relatively close to each other. Pangong Lake, which is patrolled by fast boats, is 134 km long, making the incursions very difficult to locate. Chumur is close to the middle sector and the incursions here take place over a larger area, with two incursions formally located in Uttarakhand (middle sector), but close to Chumur. We group all of these into this single red-zone.

area. They are more spread out in the other two sectors. In both the eastern sector and the western sector, there are six red-zones.

The meteorological conditions near the LAC are forbidding, with high altitudes (40 percent of the incursions occur above 5,000m) and sub-zero temperatures. As a consequence of this, the incursions are not only clustered in space, but also clustered in time, as can be seen in Fig 6.6. Half of the incursions (51 percent) take place during June–August, and almost none during December–February.

We remark that a detailed study of *when* incursions occur, in relation with socio-economic and political factors, was previously carried out in Greene et al. [118]

STATISTICAL METHODS

Border conflicts involve many different factors, which manifest themselves on different scales. They often involve totally scattered confrontations, which can spill

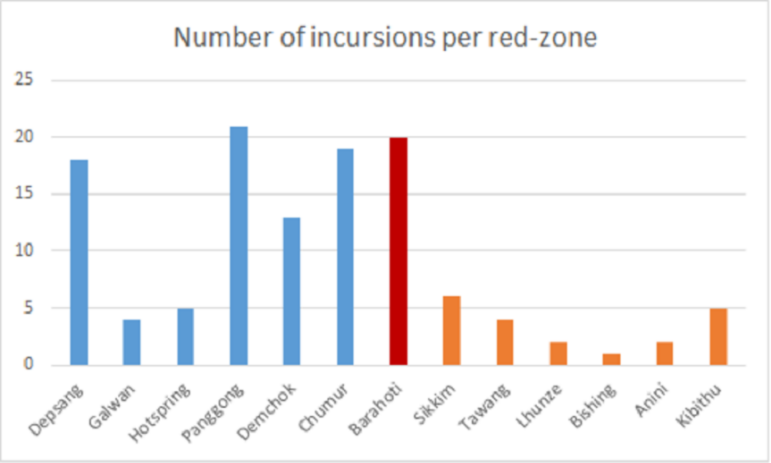

Figure 6.5.: **Grouping the incursions into thirteen red-zones**. The distribution of the incursions over the thirteen red-zones, colored by sector (west-middle-east).

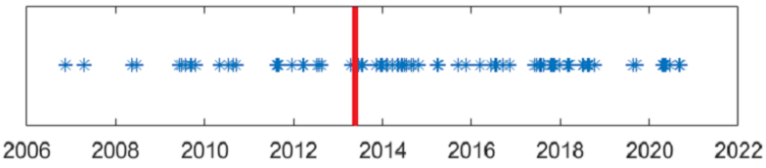

Figure 6.6.: **The incursions through time.** The red line marks the Depsang incursion, which has been a turning point in the conflict: the number of incursions doubled since then and remained at an elevated level. The events are clearly seasonally clustered.

over from one location to the next [119, 120]. The incursions themselves are local incidents, but may be part of military strategies that are played out on a larger scale. We therefore analyze the data at different spatial and temporal levels.

The length of the LAC is enormous, with a distance of well over a thousand kilometers between Indian-claimed Aksai Chin and Chinese-claimed Arunachal Pradesh. The western/middle sector and the eastern sector are separated by the independent countries of Nepal and Bhutan. We test if the incursions in these two parts of the border are statistically independent events by means of a Wald-Wolfowitz run test. To this end, we label the incursions as "E" and "W" to obtain a sequence of elements for which we count the number of runs, i.e., we count the number of segments of the sequence consisting of adjacent equal elements. If the incursions in these two parts of the LAC are statistically independent, then the number of runs is asymptotically normal with mean $\mu = \frac{2n_1n_2}{n_1+n_2} + 1$ and variance $\sigma^2 = \frac{(\mu-1)(\mu-2)}{n_1+n_2-1}$. Here n_1

is the number of incursions in the East and n_2 is the number of incursions in the West. We use this method to test the statistical dependence of the incursions in the three sectors. We also apply a multivariate Wald-Wolfowitz test for the number of runs in the western sector. There is no closed form formula for the number of runs in a multivariate test, but the expected number of runs and its standard deviation can be simulated [121, p 217].

Mathematically, the incursions along the LAC can be modelled by a point process, in which each location on the border has a probability intensity of incursion. In such models, it is customary to split a time series into a background process and an offspring process [122]. The offspring process contains the events that are triggered by the background process, as aftershocks of an earthquake. We therefore split the data set into primary incursions and secondary (triggered) incursions. We define an incursion as secondary if it occurs within 10 days in the same red-zone as an earlier incursion. The choice of 10 days is arbitrary, but the results are stable under a variation of plus or minus 3 days. It adjusts for the self-reinforcing nature of media attention, which is on a timescale of days only [123].

In the Wald-Wolfowitz test, we study incursions per sector. To understand the military strategy behind the Chinese incursions, the alleged salami-slicing, we study the incursions per red-zone. Game theory predicts that adversaries try to establish permanent control over a battleground (red-zone) by allocating more troops for a longer time than their opponents. Such a tactical allocation of troops and other military resources is a common phenomenon in border disputes [124, 125], which can be described by a Colonel Blotto game. This is a classical two-person constant sum game, in which the players allocate troops over several battlefields. A battlefield is won by the player that allocates more troops to that battlefield. The payoff is equal to the number of won battlefields. Of course, this game is a simplification of the actual situation. Blotto is a one-shot game in which the players can access the battlefields without constraint, while in reality the border conflict is an ongoing struggle and the accessibility differs per red zone. However, analysts have pointed out that China and India are engaged in a 'war of attrition' over the red-zones, in which they try to wear each other out, while avoiding a full confrontation [86]. We interpret the Chinese incursions as attempts to establish a temporary presence in a red-zone, which can be modelled by a Blotto game that is played over rounds. We compare the yearly incursions per red-zone to optimal strategy in a Blotto game.
A pure strategy in a Blotto game is an allocation $(x_1,\ldots,x_k)$ over k battlefields such that the x_i add up to the total total number of troops available to the player. An optimal mixed strategy selects an allocation and then assigns the numbers x_i uniformly at random to the battlefields [125]. We note that computing the specific x_i is non-trivial even for a limited number of battlefields [126]. Experimental game theorists have established that humans tend to play this game more aggressively and in a more targeted manner than predicted by the mathematical optimum [127]. In particular, the player with the least resources tends to follow a 'guerilla warfare' strategy, targeting a limited number of battlefields. To detect this targeting, we applied a k-means analysis and used silhouette scoring to determine incursion clusters on a yearly basis [128]. If a Blotto game is played over rounds, then the

cumulative allocation per battlefield evens out, because it is randomly assigned. We apply a chi-square test to determine if there is a significant difference between the cumulative allocation and the average.

The number of incursions has been rising since 2005, but this has not been a steady increase. There have been several major standoffs, which seem to have sparked subsequent incursions. The Doklam standoff in 2013 was a turning point in the conflict and led to a much more volatile situation and increased media attention. To take care of this, in our time-series analysis we mainly consider primary incursions. We compute its auto-correlation to detect cycles of rising and falling tension, and we compute the correlation between east and west to check if the tension is in sync along the LAC. Finally, we apply an auto-regressive model to forecast the future development of the conflict.

6.3. RESULTS AND DISCUSSION

INCURSIONS PER SECTOR

The center of gravity of the dispute is in the western sector, which has the largest number of incursions by far, see Table 6.4. The western sector and the middle sector are contiguous and the number of yearly incursions is weakly positively correlated (corr. coef. 0.26, 95% conf. int. (-0.28,0.81)). The eastern sector (Sikkim and the McMahon line) is disconnected from the western/middle sector, with the sovereign states of Nepal and Bhutan in between. The number of yearly incursions in the western sector and the eastern sector is uncorrelated (corr. coef. -0.11, 95% conf. int. (-0.57,0.41)). We first count the number of runs (a segment of consecutive incursions in the same sector) in the western sector versus the middle sector. It is equal to 25. The Wald-Wolfowitz run test (parameters $n_1 = 80, n_2 = 20$, cf. Table 6.4) predicts an average number of 33 runs with a standard deviation of 3.1. It rejects the hypothesis that the incursions in the western and middle sector are independent random events ($p = 0.005$). This supports the hypothesis that the western sector and the middle sector can be seen as one sector, which is in line with how China and India see it. They have described it as a single sector in their 2005 bilateral agreement.

If we partition the incursions into the western/middle sector versus the eastern sector, then the number of runs is 32. The Wald-Wolfowitz run test (parameters $n_1 = 100, n_2 = 20$) predicts 34.3 runs (st.dev 3.0), and returns a p-value of 0.22, which at the standard confidence level of five percent supports the hypothesis (or at least, does not refute it) that incursions in the east and west are independent random events. If we repeat this analysis for primary incursions, then the number of runs is 30 (down from 32). There are 68 primary incursions in the western/middle sector (down from 100) and 19 primary incursions in the eastern sector (down from 20). The Wald-Wolfowitz run test predicts of 30.7 runs (st. dev 2.7) and returns a p-value of 0.40. This supports the hypothesis that incursions in the west and in the east are independent events.

We conclude that both the correlation coefficient and the Wald-Wolfowitz test support the hypothesis that the incursions in the western/middle sector and in the eastern sector are statistically independent events. The border dispute can therefore

year	western	middle	eastern
2020	13	0	1
2019	1	0	2
2018	7	9	2
2017	8	4	4
2016	3	2	4
2015	4	0	1
2014	12	2	0
2013	12	1	1
2012	6	0	0
2011	5	0	1
2010	3	1	1
2009	5	1	0
2008	1	0	1
2007	0	0	1
2006	0	0	1
total	80	20	20
mean	5.3	1.3	1.3
std.dev.	4.4	2.4	1.2

Table 6.4.: **Yearly incursions in three sectors of the LAC.** The incursions in the western and middle sector are weakly correlated (corr. coef. 0.26) and the western and eastern sector are uncorrelated (corr. coef. -0.11).

be divided into two separate conflicts, centered around Aksai Chin and Arunachal Pradesh. This conclusion holds for the incursions, which are local and tactical events.

INCURSIONS PER RED-ZONE

In the previous section, we grouped the incursions per sector. We now consider a finer scale and consider incursions per red-zone. These are areas along the border, where the exact position of the LAC is contested. Almost all incursions are in these zones. We have identified thirteen red-zones, as given in Fig 6.5.

The majority of these incursions are in six red-zones in the western sector. A multi-variate Wald-Wolfowitz test rejects the hypothesis that the incursions in the western sector are independent. The number of runs in our data is 50 while the expected number of runs in a Wald-Wolfowitz test is 63.3 with standard deviation 3.4 ($p = 0.0001$). This implies that the incursions are not random events and that red-zones in the western sector are strategically targeted.

The number of incursions per red-zone in the western sector is given in Table 6.5. In at least 75% of the last nine years (a period of heightened tension), the PLA targeted a cluster (covering at most 2 locations) containing at least 3 times as many incursions as all other incursions in the western sector. If we compare the time-line of the incursions at both ends of the western sector in Depsang and Chumur, see Fig 6.7, then we see that the incursions there are clustered in time. The weather is

more severe at Depsang, which is at a higher altitude and on average is 5 degrees colder than Chumur. We find the same temperature difference for the dates of the incursions, which indicates that the local weather conditions do not influence the strategic allocation of the troops.

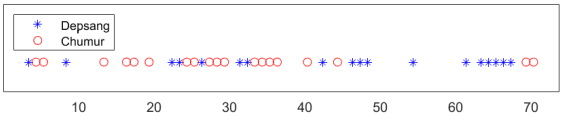

Figure 6.7.: **Incursions in Depsang and Chumur** The incursions in time in the two outermost points of the western sector, which are 300 km apart. The 37 incursions are numbered in following order. They are clearly clustered, indicating that one of the two zones is targeted at a time.

We compare the incursions in the six red-zones with optimal play in a Blotto game. Incursions are clustered using k-means (for k with the highest silhouette score) and color coded in Table 5. It demonstrates that the PLA almost always targets clusters (with 3 times the number of incursions with respect to the others) of 1 or 2 locations. In 2017 and 2018 the PLA targeted a single red-zone, and in 2013 it targeted two red-zones. If we test the maximum number of incursions in these years against a uniform distribution, then the p-values are respectively 0.0004, 0.002 and 0.10, which is another indication that these are not random encounters. Such a targeted strategy is consistent with an asymmetric Blotto game, in which the player with less resources assigns the troops to a limited number of battlefields and forfeits the others (guerrilla warfare strategy). Our model thus indicates that China adopts a weaker player strategy, which seems to contradict that it has a stronger military force and a better developed border infrastructure [129]. However, it has been observed that China's strength in numbers could be misleading and India's military position may be stronger than usually acknowledged by its military analysts [88, 130]. The Indian army has established new mountain divisions and improved its access to the red-zones, after the completion of the all weather Darbuk–Shyok–DBO Road in 2019. Indeed, this may have spurred an increase in Chinese activities [100, 131].

Game theory predicts that the number of incursions per red-zone averages out over time [125]. If we combine the relatively closely located Galwan valley and the Hotspring area into one, then the distribution of the incidents over the resulting five red-zones is $(0.23, 0.11, 0.26, 0.16, 0.24)$, while game theory predicts a distribution of 20% per red-zone. A chi-square test of the hypothesis that the incursions are drawn from a uniform distribution is inconclusive with a p-value of 0.09. The red-zones Galwan and Hotspring are relatively small and if we remove them altogether, then the p-value is 0.58. This indicates that the Chinese incursions in the Aksai Chin average out over time and that the four major red-zones in that area are of equal strategic importance to the PLA. Recent developments support this. In our data, the number of incursions in Demchok is below average, but the PLA is building up its presence there. In December 2020, it constructed a new housing colony in this

year	Depsang	Galwan	Hotspring	Pangong	Demchok	Chumur
2020	0	2	3	4	2	2
2019	0	0	0	1	0	0
2018	6*	0	0	0	1	0
2017	1	0	0	7*	0	0
2016	0	0	1	1	1	0
2015	3*	0	0	1	0	0
2014	1	1	0	3	2	5
2013	5	0	0	0	1	6*
2012	0	0	1	1	1	3*
2011	0	1	0	2	1	1
2010	1	0	0	1	1	0
2009	1	0	0	0	2	2
2008	0	0	0	0	1	0
total	18	4	5	21	13	19

Table 6.5.: **Yearly incursions in the western sector**. Clusters of incursions are colored red (high), blue (middle) and green (low). During at least 75% of the years between 2012-2022, the cluster with the most incursions contains at least 3 times as many incursions as the others. Yearly clusters are determined using k-means for k=2,3,4,5 and selecting k with the highest silhouette score. The asterisk marks battlefields which receive half or more of all incursions in that year. In the years 2013, 2017, and 2018 almost all incursions targeted a single battlefield.

red-zone [132]. Similar constructions have been observed all along the LAC, thanks to satellite imagery of Maxar Technologies [107, 130]. We conclude that a Blotto game models the military strategy of the PLA, and the incursions are strategically planned to gain control over the red-zones.

In the eastern sector, the conflict is much more controlled, see Table 6.6, although the number of incursions increased markedly in 2016, which is the year before the Doklam standoff. There has been a remarkable rise in the number of incursions in Kibithu, at the easternmost part of the border, close to Myanmar. The reason behind this is unclear, as this is not a region of strategic or economic importance. In the eastern sector, the number of incursions per red-zone is too low to draw any conclusions that are statistically meaningful.

The Chinese incursions in both the western and the eastern sector target a few red-zones at a time. In the western sector we can model the incursions by a Blotto game and our data matches the randomized allocation which is optimal in such a game. The incursions are clustered in time and space, but average out over time. This indicates that there is an ongoing competition for control of all the red-zones, in which the PLA has constructed semi-permanent fortifications. This may, however, not be a sign of strength as the strategy of the PLA is similar to that of a weaker

year	Sikkim	Tawang	Lhunze	Bishing	Anini	Kibithu
2020	1	0	0	0	0	0
2019	0	0	0	0	0	2
2018	1	0	0	0	1	0
2017	1	0	1	1	0	1
2016	0	2	0	0	0	2
2015	0	0	0	0	1	0
2014*	0	0	0	0	0	0
2013	1	0	0	0	0	0
2012*	0	0	0	0	0	0
2011	0	0	1	0	0	0
2010	0	1	0	0	0	0
2009*	0	0	0	0	0	0
2008	1	0	0	0	0	0
2007	0	1	0	0	0	0
2006	1	0	0	0	0	0
total	6	4	2	1	2	5

Table 6.6.: **Yearly incursions in eastern sector.** The number of incursions is comparatively small. During three years there were no incursions and eight years only had one incursion.

player in a Blotto game.

INCURSIONS OVER TIME

The majority of the incursions take place during the summer season. This is demonstrated in Fig 6.8, where we present the number of monthly incursions and extremal temperatures (observed min and max during 2007-2021). The red-zones are at high altitudes of over 4,000m and temperatures are extremely low in winter. The majority of the incursions take place at moderate temperatures of 5°C or above. The exception is Depsang, where 40% of the incursions took place at extreme temperatures of around −20°. Incursions at such temperatures have occurred in other red-zones, but only rarely. Due to the seasonality of the incursions and the modest size of our data set, we mainly consider the number of incursions per year.

The 21 day Depsang standoff in April 2013 was a decisive moment in the border dispute. It was followed by a sharp increase in incursions and a sequence of standoffs and skirmishes (Chumur 2014, 16 days; 2015 Burtse, 5 days; Doklam 2017, 73 days; Galwan 2020, 2 days). As a result of this, we cannot expect the time-series of incursions to be stationary. However, it clearly shows periodic fluctuations around an upward trend, as illustrated in Fig 6.9. The primary incursions show the same 4-year periodicity and the same upward trend. The periodic fluctuation around the trend is now also clearly visible in the incursions prior to 2013. According to the KPSS test (3 lags) the primary incursions are trend stationary (p-value 0.03).

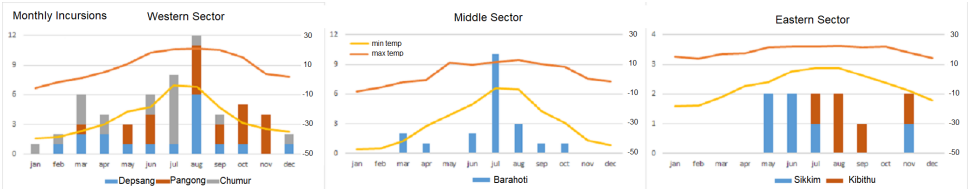

Figure 6.8.: **Incursions per month versus temperature.** Incursions per month in the three sectors (for selected red-zones) show that the majority occur in summer. In the western sector, the incursions in Pangong Lake occur mainly during August-November, while those in Chumur occur mainly in January-July. The weather in the eastern sector is less extreme than in the western/middle sector.

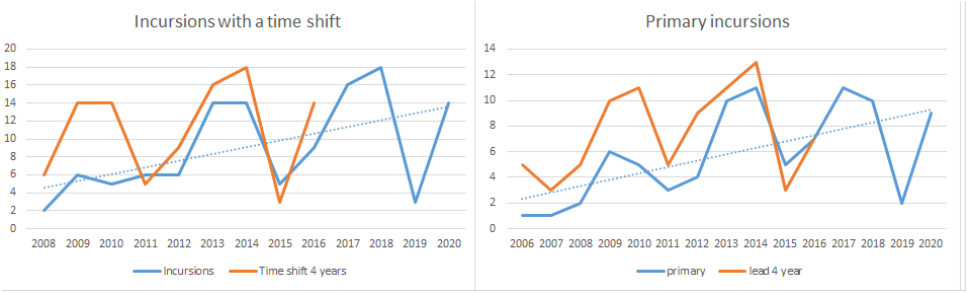

Figure 6.9.: **The periodicity of the conflict.** The number of incursions under a time shift of 4 years. The overlapping graphs illustrate the periodicity of the conflict (auto correlation 0.73). The graphs of primary incursions produce a similar overlap under a lead of 4 years (auto correlation 0.75) and upward trend.

We applied an ARIMA(3,1,0) model to the time-series of primary incursions as illustrated in Fig 6.10. Note that the model underpredicts the increase of 2013, which is the year of the Depsang standoff. It overpredicts the number of incursions in 2019, when the Indian media underreported Chinese incursions. The conflict is dominated by sudden military incidents or political developments, which are hard to pick up in an autoregression. However, the model shows the same periodicity as the data, but its fluctuation is more moderate. A forecast of the next four years predicts that this fluctuation persists.

The number of primary incursions in the western/middle sector and the eastern sector is uncorrelated (-0.02) but varies under a time shift, as shown in Table 6.7. As is to be expected, the maximum correlation occurs for a lead of 3 years, because of the periodicity of the time-series. In particular, a positive lead of 3 years for incursions in the west gives a high correlation (0.74). Again, this is as expected. The Depsang standoff, which is the first major incident in the west, preceded the Doklam standoff in the east by four years. In our analysis of incursions per sector,

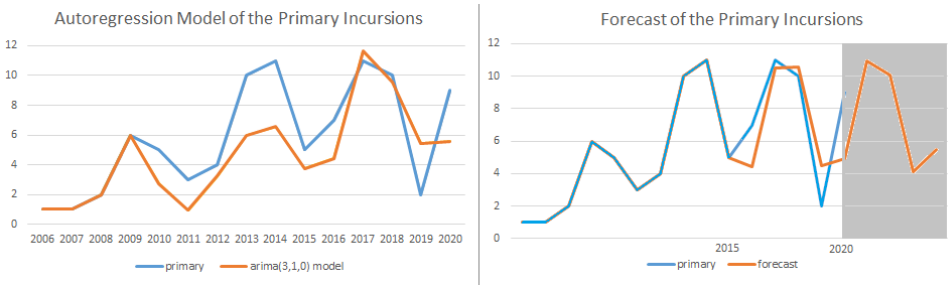

Figure 6.10.: **Autoregression of the primary incursions.** We applied an ARIMA(3,1,0) model to the time-series (lag 3, integration 1, moving average 0) and used it to forecast the period 2015-2024. It predicts that the cyclicity of the conflict will persist.

we found that these are independent events. However, if we compare the incursions under a time shift, then we observe that the tension of the conflict fluctuates in sync along the entire LAC.

lead (years)	-3	-2	-1	0.	1	2	3
corr. coef.	-0.10	0.04	0.17	-0.02	-0.02	0.40	0.74

Table 6.7.: **Correlation between the primary incursions in the west and the east.** We combine the western and eastern sector in one sector and apply varying leads between -3 and 3 years. A positive lead (predicting the incursions in the east) clearly increases the correlation. A negative lead (predicting the incursions in the west) has no significant effect.

6.4. CONCLUSION

We assembled a data set on incursions along the LAC that were reported in the media. From our analysis, we conclude that Chinese incursions in the west and in the east are independent. Militarily, the west and east can be seen as two different conflicts. Furthermore, the Chinese incursions do not seem to be random encounters, but are strategically planned in line with the optimal play in a Blotto game. However, the fluctuation of the tension (the number of yearly incursions) appears to be in sync in the west and the east. Tensions rise after major skirmishes or standoffs, which occur in the most contested red-zones of Depsang, Pangong, Chumur, Barahoti, and Doklam. Such standoffs are followed by bilateral talks to avoid further escalation of the conflict. The two countries remain at a constant state of high alertness. There are no signs that this situation will improve in the near future.

Our data set was built from media reports. In order to deal with the self-reinforcing nature of media attention, we considered incursions that were not preceded by

another incursion in the same red-zone. This adjusts for over reporting by the media. It does not adjust for under reporting, which happened in the year 2019. The fluctuation that we find in our analysis may be less strong in reality. The ability of the political leaders to downplay media attention could be an advantage for reaching an agreement. It could also be a disadvantage, if the media attention is drummed up. The future development of the conflict is in the hands of the political leaders.

China's foreign policy has become increasingly aggressive, stepping up its military exercises around Taiwan and extending its presence in the South China Sea. To counter China's expansive policies, Australia, the UK, and the USA have entered a partnership and one option for India is to align itself with the AUKUS countries. The military effort to step up its presence in the red-zones and counter the Chinese incursions, requires an enormous effort by India that can only be achieved through assistance by a strong partnership. This appears to be the approach that is favored by the Modi administration. It has strengthened its ties with Australia, Japan, and the USA ("the Quad") to counter Chinese expansion in the Indo-Pacific region.

Another option for India is a continued diplomatic approach, through ongoing bilateral talks with China. This may seem like a dead-end, since diplomacy has not made much progress over sixty years. On the contrary, Modi's efforts of rapprochements with China have failed, and India imposed economic sanctions against China after the Galwan incident. The best that bilateral talks have achieved so far is defusing conflicts to prevent further escalation. In spite of all this, there are several arguments that can be made in favor of a renewed diplomatic approach. The two countries are inextricably linked economically. A reduced military presence would reduce the ecological footprint. According to our analysis, only a few contested areas lie at the root of the conflict, and seem to generate incursions in other red-zones all over the LAC. The two countries could try to reach an agreement on only a limited part of the LAC. A good starting point would be an agreement on the border in the Sikkim sector and its nearby disputed zones on the border between China and Nepal or Bhutan. This would defuse the conflict in the eastern sector, and if our analysis is right, likely also in the western sector. This could be an important first step in a step-by-step resolution of the entire conflict.

Unfortunately, recent developments indicate that China is taking steps in the wrong direction. China and Bhutan have just signed a bilateral agreement to settle their dispute about the Doklam plateau, leaving India out of the equation. The Chinese media have presented this agreement as a snub to the Indian government [133], which does not bode well. If China pursues this approach, this could lead to a worsening of the conflict, leaving a strong military alliance with the AUKUS countires as the only option for India.

REFERENCES CHAPTER 6

[6] J.-T. Brethouwer, R. Fokkink, K. Greene, R. Lindelauf, C. Tornquist, and V. Subrahmanian. "Rising tension in the Himalayas: A geospatial analysis of Chinese border incursions into India". In: *PloS one* 17.11 (2022), e0274999.

[78] S. Biswas. "India-China clash: 20 Indian troops killed in Ladakh fighting". In: *BBC News* 16 (2020).

[79] C. Campbell. "China and India try to cool nationalist anger after deadly border clash". In: *Time* (2020).

[80] B. Zhang. "China and India: better jaw-jaw than war-war". In: *Singapore: Nanyang Technological University, RSIS Commentaries* 148 (2020).

[81] G. of India. *Joint press release of the 12th round of China- India commander level meeting*. 2021. URL: https://pib.gov.in/Pressreleaseshare.aspx?PRID=1741570.

[82] S. P. Westcott. "Seizing a window of opportunity? The causes and consequences of the 2020 Sino-Indian border stand-off". In: *Journal of Asian Security and International Affairs* 8.1 (2021), pp. 7–32.

[83] K. Kaushik. *India, China disengage at another friction point, troops return to permanent bases, Indian Express. 2021 Aug*. URL: https://indianexpress.com/article/india/india-china-disengage-at-another-friction-point-troops-return-to-permanent-bases-7442364/.

[84] G. of India and China. *Protocol on modalities for the implementation of confidence building measures in the military field along the Line of Actual Control in the China-India border areas*. 2005. URL: https://peacemaker.un.org/sites/peacemaker.un.org/files/CN%20IN_050411_Protocol%20between%20India%20and%20China.pdf.

[85] I. Rehman. "Keeping the dragon at bay: India's counter-containment of China in Asia". In: *Asian security* 5.2 (2009), pp. 114–143.

[86] Y. Joshi and A. Mukherjee. "From denial to punishment: The security dilemma and changes in India's military strategy towards China". In: *Asian Security* 15.1 (2019), pp. 25–43.

[87] T. Dalton, T. Zhao, and C. E. for International Peace. *At a Crossroads?: China-India Nuclear Relations After the Border Clash*. Carnegie Endowment for International Peace Washington, DC, 2020.

[88] F. O'Donnell and A. Bollfrass. *The strategic postures of China and India: A visual guide*. Harvard Kennedy School, Belfer Center for Science and International Affairs, 2020.

[89] A. E. Davis, R. Gamble, G. Roche, and L. Gawne. “International relations and the Himalaya: connecting ecologies, cultures and geopolitics”. In: *Australian Journal of International Affairs* 75.1 (2021), pp. 15–35.

[90] S. O. Wolf. “From Kashmir to Ladakh: the rationale behind Beijing’s border intrusions into India”. In: *Research Report, Brussels: South Asia Democratic Forum (SADF)*. Vol. 4. 2020.

[91] A. Lamb *et al. The Sino-Indian Border in Ladakh*. Australian National University Press, 1973.

[92] H. Zhang and M. Li. “Sino-Indian border disputes”. In: *ISPI Analysis* 181 (2013), pp. 1–9.

[93] D. Scott. “Sino-Indian territorial issues: The “razor’s edge””. In: *The Rise of China (part III, ch. 8)*. Cambridge University Press, 2012.

[94] T. Economist. *Indian, Pakistani and Chinese border disputes: Fantasy frontiers*. 2012. URL: https://www.economist.com/graphic-detail/2012/02/08/fantasy-frontiers.

[95] N. Maxwell. “Sino-Indian border dispute reconsidered”. In: *Economic and Political Weekly* (1999), pp. 905–918.

[96] R. M. Rossow, J. S. Bermudez, and K. Upadhyaya. *A Frozen Line in the Himalayas*. JSTOR, 2020.

[97] A. J. Tellis. “Hustling in the Himalayas: the Sino-Indian border confrontation”. In: *Carnegie Endownment* (2020).

[98] H. Buhaug and J. K. Rød. “Local determinants of African civil wars, 1970–2001”. In: *Political geography* 25.3 (2006), pp. 315–335.

[99] M. Ali. “China–Pakistan economic corridor: prospects and challenges”. In: *Contemporary South Asia* 28.1 (2020), pp. 100–112.

[100] T. Fravel. “China and the border dispute with India after 1962”. In: *Routledge handbook of China–India relations* (2020).

[101] H. Li, X.-W. Xu, G. Borg, H. A. Gilg, L.-H. Dong, T.-B. Fan, G. Zhou, R.-L. Liu, T. Hong, Q. Ke, *et al.* “Geology and Geochemistry of the giant Huoshaoyun zinc-lead deposit, Karakorum Range, northwestern Tibet”. In: *Ore Geology Reviews* 106 (2019), pp. 251–272.

[102] R. Gamble. “How dams climb mountains: China and India’s state-making hydropower contest in the Eastern-Himalaya watershed”. In: *Thesis Eleven* 150.1 (2019), pp. 42–67.

[103] H. Brands. “Paradoxes of the gray zone”. In: *Available at SSRN 2737593* (2016).

[104] S. Nagao. *Conflict Along the India-China Border: Can the Quad Make a Difference? Hudson Institute. 2021 Apr.* URL: https://www.hudson.org/foreign-policy/conflict-along-the-india-china-border-can-the-quad-make-a-difference.

[105] I. Rehman. “A Himalayan challenge: India’s conventional deterrent and the role of special operations forces along the Sino-Indian border”. In: *Naval War College Review* 70.1 (2017), pp. 104–142.

[106] R. Barnett. “China is building entire villages in another country’s territory”. In: *Foreign Policy* 7 (2021).

[107] J. Pollock. “Bhutan and the border crisis with China”. In: *South Asia@ LSE* (2021).

[108] I. A. Siddiqui. *LAC: China builds concrete towers with CCTV cameras to watch India*. 2021. URL: https://www.telegraphindia.com/india/lac-china-builds-concrete-towers-with-cctv-cameras-to-watch-india/cid/1822226.

[109] V. Som. *China Has Built Village In Arunachal, Show Satellite Images. New Delhi Television Ltd. 2021 Jan*. URL: https://www.ndtv.com/india-news/china-has-built-village-in-arunachal-pradesh-show-satellite-images-exclusive-2354154.

[110] M. D. Ward. “Cooperation and conflict in foreign policy behavior: Reaction and memory”. In: *International Studies Quarterly* 26.1 (1982), pp. 87–126.

[111] A. Acharya. “The myth of the “civilization state”: Rising powers and the cultural challenge to world order”. In: *Ethics & International Affairs* 34.2 (2020), pp. 139–156.

[112] S. Singh. “Experts Explain: What Triggered China’s Line of Actual Control (LAC) Moves?” In: *The Indian Express* (2020). URL: https://indianexpress.com/article/explained/china-india-line-of-actual-control-ladakh-6427647/.

[113] C. Wagner. “The Indian-Chinese Confrontation in the Himalayas”. In: *German Institute for International and Security Affairs, SWP Comment* 39 (2020).

[114] P. L. Vasterman. “Media-hype: Self-reinforcing news waves, journalistic standards and the construction of social problems”. In: *European Journal of Communication* 20.4 (2005), pp. 508–530.

[115] G. of India. *Report on the second China-India informal meeting*. 2019. URL: https://www.mea.gov.in/press-releases.htm?dtl/31938/2nd_IndiaChina_Informal_Summit.

[116] N. Chauhan. *Situation peaceful at India-China border, says ITBP chief. Hindustan Times. 2019 Oct*. URL: https://www.hindustantimes.com/india-news/situation-peaceful-at-india-china-border-says-itbp-chief/story-GG2ByMXWf2YbgUkPnaJ6oM.html.

[117] M. Bhonsale. “Understanding Sino-Indian border issues: An analysis of incidents reported in the Indian media”. In: *ORF Occasional paper* 143 (2018), p. 38.

[118] K. T. Greene, C. Tornquist, R. Fokkink, R. Lindelauf, and V. Subrahmanian. “Understanding the timing of Chinese border incursions into India”. In: *Humanities and Social Sciences Communications* 8.1 (2021), pp. 1–8.

[119] H. Buhaug and K. S. Gleditsch. “Contagion or confusion? Why conflicts cluster in space”. In: *International studies quarterly* 52.2 (2008), pp. 215–233.

[120] L. Hadley. “Borders and the Feasibility of Rebel Conflict”. In: *Borders in Globalization Review* 1.1 (2019), pp. 66–82.

[121] P. Sprent and N. C. Smeeton. *Applied nonparametric statistical methods*. CRC press, 2016.

[122] A. Reinhart. “A review of self-exciting spatio-temporal point processes and their applications”. In: *Statistical Science* 33.3 (2018), pp. 299–318.

[123] P. Lorenz-Spreen, B. M. Mønsted, P. Hövel, and S. Lehmann. “Accelerating dynamics of collective attention”. In: *Nature communications* 10.1 (2019), p. 1759.

[124] F. Caselli, M. Morelli, and D. Rohner. “The geography of interstate resource wars”. In: *The Quarterly Journal of Economics* 130.1 (2015), pp. 267–315.

[125] E. O. Kimbrough, K. Laughren, and R. Sheremeta. “War and conflict in economics: Theories, applications, and recent trends”. In: *Journal of Economic Behavior & Organization* 178 (2020), pp. 998–1013.

[126] A. Ahmadinejad, S. Dehghani, M. Hajiaghayi, B. Lucier, H. Mahini, and S. Seddighin. “From duels to battlefields: Computing equilibria of Blotto and other games”. In: *Mathematics of Operations Research* 44.4 (2019), pp. 1304–1325.

[127] S. M. Chowdhury, D. Kovenock, and R. M. Sheremeta. “An experimental investigation of Colonel Blotto games”. In: *Economic Theory* 52 (2013), pp. 833–861.

[128] P. J. Rousseeuw. “Silhouettes: a graphical aid to the interpretation and validation of cluster analysis”. In: *Journal of computational and applied mathematics* 20 (1987), pp. 53–65.

[129] R. P. Rajagopalan and R. Prakash. “Sino-Indian border infrastructure: An update”. In: *ORF Occasional Paper* 42 (2013).

[130] H. Boyd and M. Nouwens. “Understanding the military build-up on the China–India border”. In: *News and Analysis. The International Institute for Strategic Studies* (2020).

[131] D. T. Ahmed, S. Ali, M. Shahid Ali, W. Rehman, and S. Amir. “Face-off between India and China in galwan valley: an analysis of Chinese incursions and interests”. In: *Electronic research journal of social sciences and humanities* 2 (2020), pp. 38–50.

[132] T. Statesman. *China builds temporary houses for soldiers in Demchok across LAC*. 2020. URL: https://www.thestatesman.com/india/china-builds-temporary-houses-for-soldiers-in-demchok-across-lac-1502941796.html.

[133] A. Brar. *China sees ‘snub’to India in Bhutan agreement. And Chinese are mocking Chinascope. The Print. 2021.*

7

SEARCH AND RESCUE ON A POSET

A Search and Rescue game (SR game) is a new type of game on a graph that has quickly found applications in scheduling, object detection, and adaptive search. In this chapter, we broaden the definition of SR games by putting them into the context of ordered sets and Bayesian networks, extending known solutions of these games and opening up the way to further applications.

7.1. INTRODUCTION

A search-and-rescue game, or SR game, is a two-player win-lose game that which is played on a *finite* set X of locations. Hider chooses $h \in X$ and Searcher chooses a permutation σ of X, which we call a *search*. If $\sigma(j) = h$ then $\{\sigma(i) : i \leq j\}$ is the set of *searched locations*. For each $x \in X$ there is a Bernoulli random variable β_x with known distribution to both players. Searcher wins (rescues) if the product of β_x over the searched locations is equal to one, and otherwise she loses. In particular, the search halts as soon as $\beta_x = 0$. Searcher's payoff $\Pi(\sigma, h)$ is the probability that she wins, which we call the *rescue probability*. Hider wins if he is not rescued, i.e., we have a suicidal Hider.

SR games were first defined by Lidbetter in [134] and quickly proved to be a fruitful avenue of new study. They have been applied to scheduling problems [135, 136], object detection [137], rendezvous problems [138], and adaptive search [139]. For such applications, it is natural to impose an order on the set of locations, as some jobs can be performed only if other jobs have finished. In our paper, we therefore consider SR games on a partially ordered set X. A search now has to respect the order and is only allowed if $\sigma(i) < \sigma(j)$ implies $i < j$. For instance, if $m \in X$ is a maximal element for which $x < m$ for all $x \neq m$, then a search halts in m. We call this an ordered search-and-rescue game, or simply an OSR game. We also consider the stronger restriction that σ is only allowed if $i < j$ implies $\sigma(i) < \sigma(j)$. A function with this property is called a *chain* [140] and we say that this game is a chained SR game, or simply a CSR game. If we represent the partial order by a Hasse diagram,

Parts of this chapter have been submitted to Naval Research Logistics [7].

then we get a search game on a (directed) graph, which is a topic of its own [141]. A search is a path on the Hasse diagram in which Searcher may skip some vertices but is not allowed to backtrack. She can either search a node or skip it without turning back. This appears to be a new game on a graph.
The original SR game as defined by Lidbetter is a game on an (undirected) graph. Searcher chooses a path and Hider chooses a vertex h. Searcher's payoff is the product of all β_v over all vertices v in the path prior to h. More specifically, let the path be a walk along the vertices $v_1, v_2, \ldots, v_n$ and let v_j be the first vertex that is equal to h. Then Searcher's payoff is the expected value of

$$\prod_{x \in \{v_1, \ldots, v_j\}} \beta_x,$$

i.e., the product of the success probabilities. Note that $\{v_1, \ldots, v_j\}$ is a multi-set. Searcher is allowed to backtrack. Even if x occurs twice or more in the multi-set, then still β_x is only sampled once. If the graph is a rooted tree and if Searcher can only start from the root, then Hider selects a leaf because all internal nodes of the tree are dominated. Lidbetter proves that an optimal search consists of a mix of depth-first searches. For instance, consider the following example from [134] of a rooted tree with three leaves a, b, c and one internal node. The depth first searches in terms of arrivals at the leaves are abc, bac, cab, cba. If $h = a$ and the depth-first

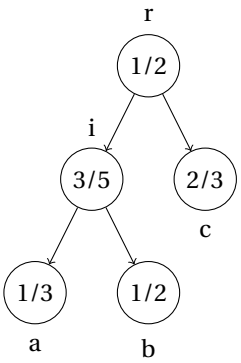

Figure 7.1.: A tree with three leaves a, b, c, root r and internal node i. Success probabilities displayed in the nodes.

search is abc then Searcher's payoff is $\frac{1}{10}$. If the depth-first search is bac then the payoff is $\frac{1}{20}$.
In our approach, this SR game on a tree in Fig. 7.1 can be defined as an OSR game on the unordered set $X = \{a, b, c\}$ with correlated random variables $\beta_a, \beta_b, \beta_c$. The nodes r, i correspond to events that determine whether or not Searcher rescues. For instance, let r be the event "no storm" and let i be the event "high visibility". A rescue in a and b requires no storm and high visibility. A rescue in c only requires no storm. On top of that, the locations a, b, c each have particular rescue probabilities, dependent on these events r, i. In this approach the tree is

a *Bayesian network* [142, 143] in which r, i are latent variables. More formally, let $Pr(x) = Pr(\beta_x = 1)$ be the probability of a *successful search* of location x. If we put $Pr(a) = \frac{1}{10}, Pr(b) = \frac{3}{20}, Pr(c) = \frac{1}{3}$ and we put the conditional probabilities $Pr(b|a) = \frac{1}{2}, Pr(c|a) = Pr(c|b) = Pr(c|b,a) = \frac{2}{3}$, then the probability distribution is determined. We retrieve Lidbetter's game on a tree, in which Searcher can only search the leaves. The probabilities of the internal nodes correspond to the correlations between the events a, b, c.

What happens to Lidbetter's depth-first search theorem if we replace the Bernoulli random variables by other random variables? Can we find effective bounds on the value of the game? What happens if the search is ordered? These are the motivating questions for this study.

The paper is organized as follows. We first introduce notation and terminology. We then solve the CSR and OSR games on a poset for uncorrelated Bernoulli random variables. Surprisingly, despite having a more restricted strategy space, the CSR game is more difficult to solve. We then consider correlated random variables, extending the work of Lidbetter in [134] and linking the SR game to Bayesian networks. We are able to give bounds on the value of the SR game, but we can only solve it for simple posets under restrictions on the probability distribution of the Bernoulli random variables. In the final section, we discuss some further generalizations of SR games.

7.2. DEFINITIONS AND NOTATION

In this paper we consider games on a partially ordered set (poset) $(X, <)$ with an associated collection of Bernoulli random variables β_x indexed by X. An SR game is an example of a *search game* between an immobile hider and a mobile searcher on a finite set of locations [144, Ch 3]. The strategy space of player II (Hider) is the set of locations X and the strategy space of player I (Searcher) are permutations of subsets of X. Usually, in a search game the payoff is measured in duration or costs and Hider is the maximizer. In an SR game, payoff is measured in probability and Hider is the minimizer.

Throughout this work, we need some basic notions and results on posets, for which [140] is a standard reference. The set $\{1, \ldots, n\}$ with its standard total order is denoted $[n]$. A function $f\colon [n] \to X$ is order-reflecting if $f(i) < f(j)$ implies $i < j$. We consider injective functions only. Locations can be searched only once. The function is a chain if $i < j$ implies $f(i) < f(j)$, in which case the image $f([n])$ is a totally ordered subset of X. We associate functions with searches and denote them by σ instead of f.

We have a collection of Bernoulli random variables β_x with $x \in X$. These random variables may be *dependent*. We write $Pr(S)$ for the probability that $\beta_x = 1$ for all $x \in S$. If S contains just one or two elements, we write $Pr(x)$ or $Pr(x, y)$. $Pr(X)$ is the probability that all searches are successful.

Hider selects a single element $h \in X$. Searcher selects an order-reflecting function σ. Let k be the minimal number such that $h \in \sigma([k])$. If there is no such k then

Searcher receives 0 and Hider receives 1. Otherwise, Searcher's payoff is

$$\Pi(\sigma, h) = Pr(\sigma([k])) \tag{7.1}$$

and Hider's payoff is the complementary probability. There is an abundance of P's: Π is payoff and Pr is probability. We say that this is an *OSR game*. It models a process of progressive search. Once x is searched, all unsearched $y < x$ become inaccessible. We have a *CSR game* if Searcher is limited to chains. It models a process of urgently progressive search. Once x is searched all $y < x$ and all y that are unrelated to x become inaccessible. We denote the value of an SR game by $V(X)$. It will be clear from the context what type of SR game we consider.

Both players face a decision problem in which they weigh their options. Ratios of probabilities play a role, and therefore it is convenient to consider the *odds* of events. For $x \in X$ we denote the odds of failure by

$$o_x = \frac{1 - Pr(x)}{Pr(x)}.$$

If $Pr(x) = 0$ then Hider will hide in x and cannot be rescued. We require that $Pr(x) > 0$ for all $x \in X$ so the odds are well-defined. For $S \subset X$ we denote the sum of the odds by

$$O_S = \sum_{x \in S} o_x.$$

It is a quantity that often turns up in decision problems [145].

Lidbetter proved that an optimal search and rescue on a tree can be described by weighed coin tosses, as in a behavior strategy [146]. It goes as follows. Suppose i is an internal node with children a and b. Let $S \subset X$ be the leaves that are descendants of i and let A and B be the descendants of a and b. In particular, $S = A \cup B$. Let $V(A)$ be the value of the subgame on the tree with root a, and let $V(B)$ be the value for b. Searcher flips a coin with odds

$$\frac{1}{V(A)} - \frac{Pr(B)}{V(B)} : \frac{1}{V(B)} - \frac{Pr(A)}{V(A)} \tag{7.2}$$

to decide between a and b. After reaching a leaf, Searcher continues by backtracking as in depth-first search. Note that $V(A)$ is the probability of rescue in subgame A, which is greater than or equal to $Pr(A)$, the probability of successful search of all locations. Therefore, $\frac{1}{V(A)} \geq 1$ and $\frac{Pr(B)}{V(B)} \leq 1$, so these odds are well-defined. Also note that the odds favor the subgame with the smaller rescue probability. An optimal search is most likely to start in the most difficult subset first.

Hider can also select h optimally by tossing coins and going down the tree. At node i the odds of choosing between A and B are

$$\frac{1 - Pr(A)}{V(A)} : \frac{1 - Pr(B)}{V(B)}. \tag{7.3}$$

A suicidal Hider obviously has a preference for the set with the least rescue probability and the largest probability of failure of the search.

7.3. UNCORRELATED SEARCH AND RESCUE

In this section, the random variables β_x are uncorrelated.

Lemma 7.1. *Suppose $(X,\prec)$ is an extension of $(X,<)$, i.e., $x<y$ implies $x\prec y$. Then $V(X,\prec)\le V(X,<)$ for the OSR game and $V(X,\prec)\ge V(X,<)$ for the CSR game.*

Proof. If a map is order-reflecting for $\prec$, then it also is order-reflecting for $<$. In the OSR game, the strategy space for Searcher does not decrease if we replace $\prec$ by $<$. Therefore, the value of the OSR game does not decrease if we replace $\prec$ by $<$. If a map is a chain for $<$, then it also is a chain for $\prec$. By the same argument, the value of the CSR game does not decrease if we replace $<$ by $\prec$. □

Unordered X. Suppose that the partial order on X is trivial, i.e., the only order relation is $x=x$. Chains are singletons and in the CSR game Searcher can only search a single location. The payoff matrix is diagonal, with probabilities $Pr(x)$ on the diagonal. It is optimal for both players to select x with probability inversely proportional to $Pr(x)$. The value of the CSR game can be expressed neatly in terms of the cardinality of X plus the sum of the odds of failure:

$$\frac{1}{|X|+O_X}. \tag{7.4}$$

In the OSR game, every search is allowed. This game is one of the motivating examples that led Lidbetter to define SR games. It is related to single machine scheduling, see [134]. Hider chooses x with probability proportional to o_x. Searcher starts a search in x with probability proportional to o_x, and continues randomly. The value of the OSR game is equal to

$$\frac{1-Pr(X)}{O_X}. \tag{7.5}$$

In the degenerate case, when $Pr(X)=1$ the rescue is always successful and the odds of failure add up to zero. In this case, the value of the game is equal to 1.

Totally ordered X. If X is totally ordered, then an order-reflecting function is a chain, which means that the CSR game and the OSR game are the same. We can identify X with $\{1,\dots,n\}$. A search halts as soon as it reaches the greatest element n. Suppose Searcher limits herself to searches in which she starts in i and searches the remaining locations in increasing order. Then Hider and Searcher both have n pure strategies and the payoff matrix M is triangular.

$$M=\begin{bmatrix} p_1 & p_1p_2 & p_1p_2p_3 & \cdots & p_1p_2p_3\cdots p_n \\ 0 & p_2 & p_2p_3 & \cdots & p_2p_3\cdots p_n \\ 0 & 0 & p_3 & \cdots & p_3\cdots p_n \\ \vdots & \vdots & \vdots & \ddots & \vdots \\ 0 & 0 & 0 & \cdots & p_n \end{bmatrix} \tag{7.6}$$

The optimal Searcher strategy in this restricted game is to start from $i>1$ with probability proportional to o_i and to start from 1 with probability inversely

proportional to p_1. The optimal Hider strategy is to choose location $i < n$ with a probability proportional to o_i and location n with a probability inversely proportional to p_n. The value of the game with matrix M is equal to

$$\frac{1}{1+O_X}. \tag{7.7}$$

Now we limited Searcher's strategies, but notice that Hider's strategy remains the same if we reorder the locations $1,\dots,n-1$ in a random way. Hider's strategy remains optimal in the full game, and therefore we have solved the game.

Lemma 7.2. *The value of the OSR game on a poset $(X,<)$ with uncorrelated Bernoulli random variables is contained in the interval $\left[\frac{1}{1+O_X}, \frac{1-Pr(X)}{O_X}\right]$. The value of the CSR game is contained in the interval $\left[\frac{1}{|X|+O_X}, \frac{1}{1+O_X}\right]$.*

Note that $Pr(X)$ is small and O_X is large for large X. The bounds on the value of the OSR game produce a narrow interval if X is large. We will return to this lemma in the next section for correlated random variables.

Proof. The value of the OSR game on an unordered X is equal to $\frac{1-Pr(X)}{O_X}$, which by Lemma 7.1 puts an upper bound on the value. For the lower bound, consider any extension of $(X,<)$ to a total order. This restricts Searcher and gives the lower bound. For the CSR game, the same argument works in the opposite direction by Lemma 7.1. □

7

The multi-stage OSR game. Let $X = X_1 \cup \cdots \cup X_n$ be a union of disjoint sets and put $x < y$ if and only if $x \in X_i$ and $y \in X_j$ for $i < j$. In other words, X is an ordinal sum of unordered subsets, see [140, p 100]. We say that X_j is *stage j*. Once a search enters a stage, it cannot continue in an earlier stage. The game on this poset is very similar to the game on a total order. Note that it is optimal to end with a full search of the final stage. Searching an extra location cannot decrease the rescue probability. Let V_j be the value of the OSR game restricted to X_j, which is unordered. We write $P_j = Pr(X_j)$ and $O_j = O_{X_j}$. By Equation (7.5) we have $V_j = \frac{1-P_j}{O_j}$. As in the game on a total order, suppose Searcher limits herself to searches of consecutive stages $j, j+1,\dots,n$. Within each X_i her search is optimal for the restricted game on this set. Under this restriction, Searcher essentially only selects the initial stage j and therefore has n strategies. In response, Hider also selects a stage and applies his optimal strategy, so he essentially has n strategies as well. The payoff matrix L is very similar to the matrix for the total order.

$$L = \begin{bmatrix} V_1 & P_1V_2 & P_1P_2V_3 & \cdots & P_1P_2P_3\cdots V_n \\ 0 & V_2 & P_2V_3 & \cdots & P_2P_3\cdots V_n \\ 0 & 0 & V_3 & \cdots & P_3\cdots V_n \\ \vdots & \vdots & \vdots & \ddots & \vdots \\ 0 & 0 & 0 & \cdots & V_n \end{bmatrix}$$

The solution of this restricted game is similar to that of the total order. Hider chooses stage $j < n$ with probability proportional to $\frac{1-P_j}{V_j} = O_j$ and stage n with probability proportional to $\frac{1}{V_n} = \frac{O_n}{1-P_n}$. Note that $V_n = 1$ if $P_n = 1$. Searcher starts in stage $j > 1$ with probability proportional to $\frac{1}{V_j} - \frac{P_{j-1}}{V_{j-1}}$ and starts in stage 1 with probability inversely proportional to V_1. In this way, Searcher makes sure that she searches stage j with probability proportional to $\frac{1}{V_j}$. The value of the game with matrix L is

$$\frac{1}{\frac{P_n O_n}{1-P_n} + O_X}. \tag{7.8}$$

We need to argue that Searcher cannot do better than this. Suppose we combine $X_{j-1} \cup X_j$ for $j < n$, then the number of stages goes down by one which gives more freedom to Searcher, but we argue that Hider's optimal strategy does not change. In the game with n stages, Hider selects stage $j < n$ with probability proportional to O_j. He then selects $x \in X_j$ with probability proportional proportional to o_x. This is the same as first selecting stage $X_{j-1} \cup X_j$ with probability proportional to $O_{j-1} + O_j$ and then tossing a coin with odds $O_{j-1} : O_j$ to select from X_j. We can combine or split up stages without affecting the optimal Hider strategy. The game is equivalent to the two-stage game on the ordinal sum $(X \setminus X_n) \cup X_n$. All searches that start in $X \setminus X_n$ and end with a full search of X_n have expected probability of rescue given by Equation (7.8).

An element $m \in X$ is a *maximum* if there are no $x > m$. Let $M \subset X$ be the subset of maxima. An optimal search always ends in M. If σ does not end in M, then it can be extended by some $m \in M$ without decreasing the probability of rescue. Since there is no order relation between different elements of M, an optimal search ends with a full search of M.

Theorem 7.3. *Let $M \subset X$ be the subset of maxima. Let P_M be the product of all success probabilities over $m \in M$ and let O_M be the sum of the odds over M. The value of the OSR game on X is equal to*

$$\frac{1}{\frac{P_M O_M}{1-P_M} + O_X}. \tag{7.9}$$

Proof. Let $(X \setminus M) \cup M$ be the ordinal sum of two unordered subsets. The value of the OSR game on this poset is given by Equation (7.9). By Lemma 7.1 this puts an upper bound on the value of the OSR game on X. Conversely, extend the partial order of $X \setminus M$ to a total order and consider the OSR game on the resulting poset. By Lemma 7.1 the value of the game on this poset puts a lower bound. This is a multi-stage game that ends in M such that all previous stages are singletons. The value of this game is again given by Equation (7.9) and the lower bound equals the upper bound. □

This theorem settles OSR games, and we now turn our attention to CSR games. Our next lemmas sharpen the bounds of Lemma 7.2.

Lemma 7.4. *Let $M \subset X$ be the subset of maxima. If Hider hides in $m \in M$ with probability inversely proportional to $Pr(m)$ and in $x \in X \setminus M$ with probability proportional to o_x, then the rescue probability is at most*

$$\frac{1}{|M| + O_X}$$

for any search. This puts an upper bound on the value of the game.

Proof. For any chain $x_1, x_2, \ldots, x_k$ that ends in $x_k \in M$, the expected rescue probability is

$$\frac{(1 - Pr(x_1)) + Pr(x_1)(1 - Pr(x_2)) + \cdots + Pr(x_1) \cdots Pr(x_{k-1})}{|M| + O_X} = \frac{1}{|M| + O_X}.$$

If the chain does not end in a maximum, then the rescue probability is less. □

An antichain is a subset $S \subset X$ such that any two elements of S are incomparable. The *width* of X is the size of its largest antichain. By Dilworth's theorem [147], it equals the minimum number of disjoint chains into which the set can be partitioned

Lemma 7.5. *Let w be the width of X. There exists a mixed Searcher strategy with rescue probability at least*

$$\frac{1}{w + O_X}.$$

This puts a lower bound on the value of the game.

Proof. Consider the following strategy for Searcher. She decomposes X into w disjoint chains and selects a random $x \in X$ to start the search. The search proceeds along the unique chain that contains it. Searcher selects initial elements x with probability inversely proportional to $Pr(x)$ and all other elements with probability proportional to o_x. Suppose Hider selects h and let $S = \{x_1, \ldots, x_k\}$ be the chain that contains h with $x_j = h$. Within this subset S we have the game on a total order in which Searcher applies the optimal strategy. The rescue probability is the same for all elements. Hider is indifferent between all elements of X. □

In particular, we have solved the game if M is a maximal antichain of X. For instance, if the Hasse diagram is a tree. The upper bound on the game depends on $|M|$ which can be computed in linear time by depth-first search. The lower bound on the game depends on w which can be computed in polynomial time [148].

The multi-stage CSR game. We reconsider the ordinal sum $X = X_1 \cup \cdots \cup X_n$ of unordered subsets, this time for the CSR game, in which Searcher can only search one location from each X_i. In the OSR game, Searcher can search all locations from X_i. As before, we write O_j for the sum of the odds over the elements in the stage X_j for i and we write $O_{\leq j}$ for the sum of the odds over all stages $\leq j$. Let k be such that $|X_k| + O_{\leq k}$ is *maximal*. By Lemma 7.4 Hider can limit the rescue probability to

$$\frac{1}{|X_k| + O_{\leq k}}$$

by choosing h from the first j stages only. We show that Searcher can actually achieve this rescue probability.

We add an initial node s at stage zero and a terminal node t at stage $n+1$ with $Pr(s) = Pr(t) = 1$. This does not change the game as s and t can be searched for free and therefore Hider will not select these nodes. We represent the search strategy as a network flow on the Hasse diagram of this order, which has a single source s and a single sink t. Searcher starts from s with probability one. We need to prove that Searcher achieves a rescue probability $\geq \frac{1}{|X_k|+O_{\leq k}}$ at each node. Instead of probability one, we give Searcher a total weight of $|X_k| + O_{\leq k}$ at node s. Now she needs to make sure that the rescue probability is ≥ 1 for each node. The inflow I_x at each node x has to be $\geq \frac{1}{Pr(x)}$ which is needed to achieve rescue probability one. Excess flow can skip the node. The rescue fails with probability $1 - Pr(x)$ and therefore takes away o_x from the flow. The outflow is $I_x - o_x$. The entire stage j takes away O_j from the flow. After $j < k$ stages, the total flow is reduced to $O_{\leq k} - O_{\leq j} + |X_k|$. The next stage requires an inflow of $O_{j+1} + |X_{j+1}|$ which can be satisfied since

$$O_{\leq k} - O_{\leq j} + |X_k| \geq O_{j+1} + |X_{j+1}|$$

by the fact that $O_{\leq i} + |X_i|$ is maximal at k. After k stages, the outflow is equal to $|X_k|$. The required inflow for a stage $j > k$ is equal to $O_j + |X_j|$ and this stage takes away O_j from the flow. Since we have

$$|X_k| - O_{k+1} - \ldots - O_j \geq |X_j|$$

the required inflow can always be met. This guarantees a rescue probability ≥ 1 for each node, and if we normalize the probability, then we find that the value of the game is $\frac{1}{O_k+|X_k|}$.

An antichain $A \subset X$ is *maximal* if for every $x \in X$ there is an $a \in A$ such that either $a \leq x$ or $x \leq a$. A maximal antichain partitions the poset X into $A^- = \{x \colon \exists a \in A, x \leq a\}$ and $A^+ = \{x \colon \exists a \in A, a < x\}$. In other words, A is a cut. The elements of A are maximal in the poset A^- with the order inherited from X. Hider can guarantee a rescue probability $\leq O_{A^-} + |A|$ by hiding in $x \in A^-$ with probability o_x if $x \notin A$ and probability inversely proportional to $Pr(x)$ if $x \in A$.

Theorem 7.6. *Let A be a maximal antichain that maximizes $O_{A^-} + |A|$. The value of the CSR game on X is equal to*

$$\frac{1}{O_{A^-} + |A|}.$$

Proof. Hider can achieve this rescue probability. We need to prove that Searcher can achieve it as well. We add a source s and a sink t with rescue probability one, with $s < x < t$ for all $x \in X$. Searcher's task is to find a network flow such that the inflow $I_x \geq \frac{1}{Pr(x)}$ for all nodes. Each node reduces the flow by o_x. We have a network flow problem but unlike the standard max-flow min-cut problem it is max-cut min-flow and the flow is dissipative. However, it is possible to modify the proof of the max-flow min-cut theorem for this problem. We have adapted the proof given by Trevisan [149, Ch 15].

Let E be the edge set and let f_{xy} be the flow on $(x,y) \in E$. There are two constraints at each $x \in X$: inflow at least $\frac{1}{Pr(x)} = o_x + 1$ to guarantee rescue probability one, and dissipation (inflow minus outflow) is at least o_x to guarantee a full search of the node.

$$\begin{aligned} \text{minimize} \quad & \sum_{(s,x)\in E} f_{sx} \\ \text{subject to } \forall x \in X \quad & \\ & \sum_{(v,x)\in E} f_{vx} \geq o_x + 1, \\ & \sum_{(v,x)\in E} f_{vx} - \sum_{(x,w)\in E} f_{xw} \geq o_x, \end{aligned}$$

where all $f_{xy} \geq 0$. The dual problem has two variables for the two constraints at each $x \in X$ and has one constraint for each $(v,x) \in E$.

$$\begin{aligned} \text{maximize} \quad & \sum_{x\in X} (o_x+1)g_x + o_x h_x, \\ \text{subject to} \quad & \\ & g_x + h_x \leq 1, \qquad \forall (s,x) \in E, \\ & g_x + h_x - h_v \leq 0, \qquad \forall (v,x) \in E,\ v \neq s, \end{aligned}$$

where all $g_x, h_x \geq 0$. If we put $g_a = 1$ for all $a \in A$ a maximal antichain and $h_b = 1$ for all $b < A$, and zero elsewhere, then the constraints of the dual problem are satisfied. This choice is feasible and in this case

$$\sum_{x\in X} (o_x+1)g_x + o_x h_x = O_{A^-} + |A|.$$

7

We need to show that this is a solution of the dual problem for some antichain, because then the minimax theorem implies that Searcher has a feasible flow that achieves the required rescue probability.

Let g_x and h_x be a feasible solution of the dual problem. Pick $0 \leq T \leq 1$ uniformly at random and put $\bar{h}_x = 1$ if $h_x \geq T$ and $\bar{g}_x = 1$ if $h_x + g_x \geq T > h_x$. For all other x we set $\bar{h}_x = \bar{g}_x = 0$. This implies that $\bar{h}_x + \bar{g}_x \leq 1$ and if $\bar{h}_x + \bar{g}_x = 1$ then $\bar{h}_v = 1$ for all $(v,x) \in E$. Therefore, $\bar{g}_x$ and $\bar{h}_x$ are feasible. We claim that $A = \{x\colon \bar{g}_x = 1\}$ is a (random) antichain. In other words, there is no path between any $a, b \in A$. To see this, notice that $h_a < T$ and by the second constraint $g_x + h_x < T$ for all successors of a. If $g_b + h_b \geq T$ then b is not a successor of a and A is indeed an antichain.

The value of $\sum_{x\in X} (o_x+1)\bar{g}_x + o_x\bar{h}_x$ is equal to $O_{A^-} + |A|$, since all $x \in A^-$ either have $\bar{g}_x = 1$ or $\bar{h}_x = 1$ and all $x \in A$ have $\bar{g}_x = 1$. The expected value is equal to

$$\sum_{x\in X} (o_x+1)Pr(g_x + h_x \geq T > h_x) + \sum_{x\in X} Pr(h_x \geq T) = \sum_{x\in X} (o_x+1)g_x + \sum_{x\in X} h_x,$$

which is maximal. Therefore, there must be an antichain such that $O_{A^-} + |A|$ equals the solution of the dual problem, as required. □

The optimal Searcher strategy is a feasible solution of an LP problem and can therefore be computed in polynomial time in terms of $|X|$. The optimal Hider strategy can also be computed in polynomial time, by solving the dual problem and random rounding.

7.4. CORRELATED SEARCH AND RESCUE

In this section, the random variables β_x are correlated. This makes the games much more difficult to solve. We are only able to solve the games for simple posets under strong restrictions on the distribution of the Bernoulli random variables.

We first consider the OSR game on an unordered X: any permutation of X is an admissible search. If there are only two locations $X = \{a, b\}$ we have a simple symmetric matrix game

$$\begin{pmatrix} Pr(a) & Pr(a,b) \\ Pr(a,b) & Pr(b) \end{pmatrix},$$

which is easy to solve. For three locations the game is already much more elaborate.

Definition 7.7. *For three locations x, y, z we say that x and y are* conditionally independent *with respect to z if*

$$Pr(x, y|z) = Pr(x|z)Pr(y|z).$$

It is denoted $(x \perp\!\!\!\perp y|z)$.

The common way to define conditional independence is for events, which in our case are successful searches of locations. We note that if A, B, C are three events such that $A \perp\!\!\!\perp B|C$, then it does not necessarily hold that $A \perp\!\!\!\perp B|\overline{C}$, where $\overline{C}$ denotes the complementary event of C.

Conditional independence is often interpreted in terms of learning [143]. An equivalent way to define $(x \perp\!\!\!\perp y|z)$ is $Pr(x|z, y) = Pr(x|z)$. In terms of learning: if we learn that z has happened, then the probability of x gets a Bayesian update $Pr(x|z)$, but if we then learn that y has also happened, we learn nothing new. In the SR game on three locations $\{a, b, c\}$ in Fig. 7.1 we have that $Pr(c|a) = Pr(c|b) = Pr(c|b, a)$ and therefore both $a \perp\!\!\!\perp c|b$ and $b \perp\!\!\!\perp c|a$.

The OSR game on three unordered locations. Let $X = \{a, b, c\}$ and suppose that both $a \perp\!\!\!\perp c|b$ and $b \perp\!\!\!\perp c|a$. We build a graphical model of this probability distribution in Fig. 7.2 in analogy of the SR game on a tree in Fig. 7.1.

The three leaves of the graphical model are labeled by the three locations. Contrary to Fig 7.1, the internal nodes q, r do not necessarily correspond to events. The edge weights are *ratios* of conditional probabilities, which may be larger than one, which is why we say this is a *pseudo-Bayesian network*. In Bayesian networks, nodes correspond to events and edge weights are conditional probabilities, which are at most one. To compute the rescue probability of a leaf, multiply the edge weights of the path to that leaf. More generally, to compute $Pr(S)$ for $S \subset \{a, b, c\}$ multiply the edge weights of its spanning tree. For instance,

$$Pr(a, c) = \frac{Pr(c)}{Pr(c|b)} \cdot \frac{Pr(b|c)}{Pr(b|a)} \cdot Pr(c|b) \cdot Pr(a|b) = \frac{Pr(b, c) \cdot Pr(a)}{Pr(b)}$$

which is equal to $Pr(c|b) \cdot Pr(a) = Pr(c|a) \cdot Pr(a)$, for this tree. This is indeed equal to $Pr(a, c)$.

In this setup, searching a leaf requires the probabilities of the path leading up to it, as in Lidbetter's SR game. If all edge weights are bounded by one, then we

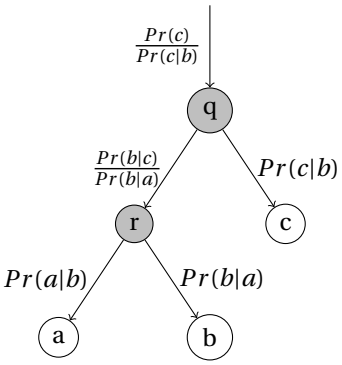

Figure 7.2.: The tree of Fig. 7.1 revisited as a network with events a, b, c and internal nodes q, r. The events a, b, c represent successful rescue in these three locations. The weights of the directed edges are ratios of conditional probabilities.

are back at the original SR game on a tree. In fact, there is no need to bound the weight $\frac{Pr(c)}{Pr(c|b)}$ of the first incoming edge. It is a common divisor of all rescue probabilities. It is a sunk cost that can be replaced by one, without changing the optimal strategies of the players. Then we multiply all payoffs by $\frac{Pr(c|b)}{Pr(c)}$ and the game remains essentially the same.
Suppose Searcher first successfully searches b. The probabilities of the two remaining locations are now updated to $Pr(a|b)$ and $Pr(c|b)$. The Bayesian factors for these updates satisfy

$$\frac{Pr(c|b)}{Pr(c)} \leq \frac{Pr(a|b)}{Pr(a)}$$

because the paths of a and b have more edges in common than the paths of c and b. The weights of these edges are taken out by the update, which is why the Bayes factor for a is larger, and hence the incentive to now search a is stronger. This is a Bayesian interpretation of depth-first search.

In order to extend this example from three to more locations, we need some further terminology. First of all, conditional independence extends from three events as in Definition 7.7 to collections of random variables. It is a central topic of study in probabilistic learning [150]. We will need a rather special notion that is tailored to SR games.

Definition 7.8 (co-independence)**.** *Let $X = A \cup B$ be a partition into disjoint sets such that for any $A' \subset A, B' \subset B$ and any $a \in A, b \in B$ it holds that $Pr(A'|B') = Pr(A'|b)$ and $Pr(B'|A') = Pr(B'|a)$. Furthermore, $Pr(A'|a,b) = Pr(A'|a)$ and $Pr(B'|a,b) = Pr(B'|b)$. Then we say that A and B are* co-independent*, denoted $X = A \| B$ or simply $A \| B$.*

Informally speaking, each element of A teaches us the same about B and any element from B teaches us more about B than all of A.

Definition 7.9. *Let X be a set of two locations or more. We say that X is* reducible *if it admits a partition $X = A \cup B$ into disjoint non-empty subsets $A \| B$. We say that it is* completely reducible *if every subset $Y \subset X$ containing two elements or more is reducible.*

In particular, if X is completely reducible then $X = A_0 \| A_1$, which can be partitioned into $A_0 = A_{00} \| A_{01}$ and $A_1 = A_{10} \| A_{11}$ etc. In the SR game on a tree, the probability distribution on the leaves is completely reducible. For instance, in the SR game of Fig. 7.1 we have $\{a, b\} \| c$ and $\{a\} \| \{b\}$.

Lemma 7.10. *If $X = A \| B$ then the Bayes factor*

$$\frac{Pr(A'|B')}{Pr(A')}$$

is the same for any nonempty $B' \subset B$ and $A' \subset A$.

Proof. Let $a \in A$ and $b \in B$. By co-independence and the properties of conditional probability

$$\frac{Pr(A'|B')}{Pr(A')} = \frac{Pr(A'|b)}{Pr(A')} = \frac{Pr(b|A')}{Pr(b)} = \frac{Pr(b|a)}{Pr(b)},$$

which does not depend on A' and B'. □

Theorem 7.11. *Suppose that X is completely reducible such that $X = A_0 \| A_1$ and each subsequent $A_w = A_{w0} \| A_{w1}$ for a binary word w. Then the probability distribution can be represented by a pseudo-Bayesian tree with nodes A_w and root X, which has an incoming edge without an initial node. Each A_w has sibling $A_{\bar{w}}$, such that w and $\bar{w}$ have common prefix v and only differ in the last digit. In particular, A_v is the parent of A_w. The incoming edge of A_w has weight*

$$\frac{Pr(a_{w0}|a_{\bar{w}})}{Pr(a_{w0}|a_{w1})},$$

for arbitrary elements $a_w \in A_w$. The incoming edge of the root has weight $\frac{Pr(a_0)}{Pr(a_0|a_1)}$, because the root has no sibling. If T is the spanning tree of $S \subset X$ then $Pr(S)$ is the product of the weights of the edges in T.

Proof. By induction, the conditional distribution $Pr(\cdot|a_i)$ on A_i for $i \in \{0, 1\}$ can be represented by pseudo-Bayesian trees. These are the two subtrees that spring from the root X. Let $S_i = S \cap A_i$ for $i \in \{0, 1\}$. Then

$$Pr(S) = Pr(S_1|S_0)Pr(S_0) = Pr(S_1|a_0)Pr(S_0).$$

By induction, $Pr(S_1|a_0)$ equals the product of the weights for its spanning tree T_1 in the pseudo-Bayesian subtree for A_1. By Lemma 7.10

$$Pr(S_0) = Pr(S_0|a_1) \cdot \frac{Pr(a_0)}{Pr(a_0|a_1)}$$

the right-hand side of which is equal to the product of the weights over the spanning tree T_0 and the weight of the incoming edge at X. □

Note that we may switch the labels 0 and 1 and therefore $\frac{Pr(a_{w0}|a_{\tilde{w}})}{Pr(a_{w0}|a_{w1})} = \frac{Pr(a_{w1}|a_{\tilde{w}})}{Pr(a_{w1}|a_{w0})}$. Indeed, this is a consequence of co-independence, since

$$\frac{Pr(a_{w0}|a_{\tilde{w}})}{Pr(a_{w1}|a_{\tilde{w}})} = \frac{Pr(a_{\tilde{w}}|a_{w0})Pr(a_{w0})}{Pr(a_{\tilde{w}}|a_{w1})Pr(a_{w1})} = \frac{Pr(a_{w0})}{Pr(a_{w1})} = \frac{Pr(a_{w0}|a_{w1})}{Pr(a_{w1}|a_{w0})}.$$

If all weights are bounded by one (with the possible exception of the incoming edge of the root, which is a sunk cost), then we have a proper Bayesian network of events. In this case, the game is equivalent to an SR game on a tree.

Corollary 7.12. *Lidbetter's solution of the SR game on a tree extends to the OSR game for a completely reducible distribution on an unordered X provided that all Bayesian factors $\frac{Pr(a_{w0}|a_{\tilde{w}})}{Pr(a_{w0}|a_{w1})} \leq 1$.*

Corollary 7.13. *Let X be unordered and completely reducible such that all weights on the pseudo-Bayesian network are ≤ 1 including the weight on the incoming edge at the root. The OSR game on X has value $V(X) \leq \frac{1-Pr(X)}{O_X}$.*

Proof. Let the decomposition of X begin with $A \| B$ and let w be the weight of the incoming edge at the root. Searcher either starts with an exhaustive search of A followed by B, or vice versa. Hider hides in A or in B. Essentially we have a 2×2 payoff matrix

$$\begin{pmatrix} wV(A) & wPr(A)V(B) \\ wPr(B)V(A) & wV(B) \end{pmatrix},$$

where $V(A), V(B)$ are the values of the subgames on the two trees that spring from the root and $Pr(A), Pr(B)$ are the products of the weights of these two trees. Searcher incurs the cost w and flips a coin as in Equation (7.2). The value of the game is

$$\frac{w(1 - Pr(A)Pr(B))}{\frac{1-Pr(A)}{V(A)} + \frac{1-Pr(B)}{V(B)}}.$$

By induction the denominator is $\geq O_A + O_B = O_X$. We also have $Pr(X) = w \cdot Pr(A) \cdot Pr(B)$. Therefore, the denominator is $w - Pr(X) \leq 1 - Pr(X)$ by our assumption that $w \leq 1$. □

Lidbetter showed that depth-first search is optimal. Searcher starts at the root and continues until it reaches a leaf and backtracks, continuing at an unsearched node that is closest to the leaf. What can be said if all Bayesian factors are ≥ 1? A search is *backjumping* [151] if it continues at an unsearched node that is closest to the root. It is a common method in AI and automatic theorem proving [152] to prevent a search more dispersive. To specify this, suppose that a node x has two children a and b with offspring A and B. If a search first visits a leaf in A then it does not re-enter A before visiting a leaf of B. Backjumping search is the opposite of backtracking search It is a natural procedure if all Bayesian factors are ≥ 1, when it is unlikely that a search of a nearby leaf will be successful. Numerical experiments show that it is not true that the optimal search is a mix of backjumping searches if all Bayesian factors are ≥ 1. They do indicate that the following weaker statement is true.

Conjecture 7.14. *Consider the OSR game with a completely reducible distribution with all Bayesian factors* ≥ 1. *An optimal Searcher strategy contains a pure strategy that is backjumping.*

Definition 7.15. *We say that the probability distribution on* X *is* positively correlated *if* $Pr(A|B) \geq Pr(A)$ *for all* $A, B \subset X$. *We say that it is* negatively correlated *if* $Pr(A|B) \leq Pr(A)$.

This property extends to arbitrary random variables for which it is known as positive or negative *association* [153]. Note that a completely reducible distribution on X with all weights ≤ 1 is positively correlated. It is negatively correlated if all weights are ≥ 1. For positively correlated X the search gets progressively easier, which is a general assumption in search games [154]. For negatively correlated X it gets progressively more difficult, which may be a more natural assumption for a rescue operation.

Lemma 7.16. *The value of the OSR game on a positively correlated poset* X *is* $\geq \frac{1}{1+O_X}$. *The value of the CSR game on a negatively correlated poset* X *is contained in the interval* $[\frac{1}{|X|+O_X}, \frac{1}{1+O_X}]$.

In particular, the value of the OSR game on a completely reducible X with all weights ≤ 1 is contained in the interval $[\frac{1}{1+O_X}, \frac{1-Pr(X)}{O_X}]$.

Proof. For a positively correlated distribution we have that

$$Pr(A) = Pr(A \setminus \{a\}|a) \cdot Pr(a) \geq Pr(A \setminus \{a\})P(a)$$

for any $a \in A$. By induction, $Pr(A \setminus \{a\}) \geq \prod_{b \in A \setminus \{a\}} Pr(b)$. Therefore, the payoff matrix is bounded from below by the matrix for the uncorrelated SR game. By Lemma 7.2 we conclude that $V(X) \geq \frac{1}{1+O_X}$ for the OSR game. For a negatively correlated distribution, we have the opposite signs, and we conclude that $V(X) \leq \frac{1}{1+O_X}$ for the CSR game. The worst case CSR game is an unordered X in which Searcher can only search one location. The payoff matrix is diagonal with entries $Pr(a)$. This game has value $\frac{1}{|X|+O_X}$. □

So far, we mainly considered unordered X, which is the least restrictive for Searcher in the OSR game. A total order is most restrictive, and we are only able to solve that game in a limited case. Before doing that, we first exhibit some examples to show that the solution of the OSR game is not trivial.

The OSR game on a total order. Let $X = \{a, b, c\}$ be a total order $a < b < c$. The payoff matrix of the game is

$$\begin{pmatrix} Pr(a) & Pr(a,b) & Pr(a,b,c) \\ Pr(a) & 0 & Pr(a,c) \\ 0 & Pr(b) & Pr(b,c) \\ 0 & 0 & Pr(c) \end{pmatrix}.$$

7

We write $\bar{x}$ for the event that the search in x is unsuccessful. A straightforward but tedious computation shows that the solution of the game depends on the Bayes factor

$$\frac{Pr(a|\bar{b},c)}{Pr(a|b)}. \tag{7.10}$$

If it is more than one, Searcher's optimal strategy mixes the searches in rows 2,3,4. If it is less than one, she mixes the searches in rows 1,3,4.

The CSR game on a star. Let $X = U \cup \{*\}$ where U is unordered and $u < *$ for all $u \in U$. The Hasse diagram of this poset is a star graph. A search either consists of $*$ or of $\{u,*\}$. Suppose that $*$ is independent of U, i.e., $Pr(u,*) = Pr(u) \cdot Pr(*)$. If Searcher selects $\{u,*\}$ with probability proportional to $\frac{1}{Pr(u)}$, then Hider is indifferent between all locations in U. The rescue probability in $*$ is proportional to $|U| \cdot Pr(*)$. If $Pr(*) > \frac{1}{|U|}$ then Hider does not hide in $*$. The game reduces to the CSR game on U with value $\frac{1}{O_U+|U|}$. Not all Hider strategies are active.
If $Pr(*) < \frac{1}{|U|}$ then Searcher includes the search $\{*\}$ with probability proportional to $\frac{1}{Pr(*)} - |U|$ to make Hider indifferent. Under this strategy, the rescue probability is $\frac{1}{O_X+1}$ for all locations. If Hider hides in u with probability proportional to $\frac{1-Pr(u)}{Pr(u)}$ and in $*$ with probability proportional to $\frac{1}{Pr(*)}$, then the rescue probability is $\frac{1}{O_X+1}$. This is the value of the game.
The CSR game on a star falls apart in two separate cases. Now consider an OSR game on a total order $X = \{1,2,\dots,n\}$. such that $Pr(A) = 0$ for all sets of cardinality > 1 except for sets $A = \{j,n\}$. This is the CSR game on a star, again illustrating that the OSR game on a total order falls apart into different cases.

7

Theorem 7.17. *Let $X = \{1,2,\dots,n\}$ be a negatively correlated total order such that n is independent of the other locations, i.e., $Pr(A|n) = Pr(A)$ for all $A \subset X \setminus \{n\}$, and such that $Pr(n) \leq \frac{1}{n-1}$. Then the value of the game is $V(X) = \frac{1}{O_X+1}$.*

Proof. By Lemma 7.16 we know that $V(X) \leq \frac{1}{O_X+1}$. It suffices to find a Searcher strategy that guarantees this rescue probability. Suppose Searcher limits herself to a search of only one or two locations, one of which is n. Then we have the SR game on a star with uncorrelated random variables, which by the example above has the required value. □

7.5. FURTHER GENERALIZATIONS OF SR GAMES

There are several ways to generalize SR games that may deserve further study. We discuss some of them here, without going into a full analysis.

General random variables. The most straightforward generalization is to replace the $\{0,1\}$-valued random variables by arbitrary non-negative random variables. Let's denote the set of locations by $[n] = \{1,\dots,n\}$ with partial order $\prec$ so that we can denote the random variable of location i by X_i. A possible interpretation of X_i is that the rescue comes with a certain (random) reward that depends on the location. For example, an adversarial Hider that is out to do damage can be more or less

detrimental, depending on the location. In this setting, it is natural to replace $\{0,1\}$-valued variables by weighted variables. In analogy of Equation (7.1) we now have a zero-sum game with payoff equal to the expected value of the product over the visited locations:

$$\Pi(\sigma,h)=\mathbf{E}[X_{i_1}\cdot X_{i_2}\cdots X_{i_k}],$$

where $i_1,i_2,\ldots,i_{k-1}$ are the searched locations before arriving at the hideout $h=i_k$. If the random variables are independent and the expected values are ≤ 1, then the payoff matrix for this game is equivalent to a payoff matrix for Bernoulli random variables. Our results from section 2 carry over to this case.
If the expected values are not bounded by one, then the game gets more difficult to solve. We illustrate that for the OSR game on a total order $[n]$ with expected values $e_i=E[X_i]$. If we limit Searcher to searches of consecutive locations, then we get the payoff matrix of Equation (7.6):

$$A=\begin{bmatrix} e_1 & e_1e_2 & e_1e_2e_3 & \cdots & e_1e_2e_3\cdots e_n \\ 0 & e_2 & e_2e_3 & \cdots & e_2e_3\cdots e_n \\ 0 & 0 & e_3 & \cdots & e_3\cdots e_n \\ \vdots & \vdots & \vdots & \ddots & \vdots \\ 0 & 0 & 0 & \cdots & e_n \end{bmatrix}$$

We say that a subset of consecutive locations $i,i+1,\ldots,j$ is a *run* if all cumulative products $e_i,e_ie_{i+1},\ldots,e_ie_{i+1}\cdots e_j$ are ≥ 1. For a run, we have that row i of the matrix dominates the following rows from $i+1$ up to $j+1$. We can delete these rows from the matrix. If j happens to be the final location n, then we only delete rows up to j. Columns i up to $j+1$ (or n) in the remaining matrix are multiples of column i by factors $1,e_{i+1},e_{i+1}e_{i+2},\ldots,e_{i+1}e_{i+2}\cdots e_{j+1}$. The column with the minimum multiple dominates the others, which can be deleted, so that the resulting matrix is again triangular. Let k be the location of the remaining column. If Searcher searches k, then she also searches the locations from i up to k, so we can replace X_k by $X_i\cdots X_k$. Similarly, we can replace X_{j+2} by $X_{k+1}\cdots X_{j+2}$. Essentially, we have an OSR game on a total order, with a reduced number of locations. By removing the runs, we end up with a game in which only the final location possibly has expected value >1. The previous solution of the OSR game with uncorrelated Bernoulli random variables carries over to this situation.

Random rescue sets. Let X denote the poset of locations, as before. A draw from $\{0,1\}$-valued random variables β_x corresponds to a random subset $R\subset X$, which we call the *rescue set*. It is selected by Nature. The players do not know which R is drawn, but they do know Nature's probability distribution on the family of subsets 2^X. For instance, weather conditions could limit the search to k out of n locations, but it is impossible to predict which locations will have bad weather. In this example, Nature draws uniformly from the subsets of cardinality k. If $k=1$ then we have the special case of a CSR game on an unordered X in which every location has rescue probability $\frac{1}{n}$. If $k=n$ then all locations can be searched and the only restriction is the order. This is an example of the hypergraph incidence game [155].

In an SR game, the search halts once it reaches a location $x \notin R$. Bad weather may prevent a successful rescue in a certain location, but it does not stop the operation. A search can continue even if it visits a location that is not in R. Let $S \subset X$ be the set of searched locations, i.e., the image of σ. Then the payoff is one if $h \in R \cap S$ and zero otherwise. This is an extension of the hypergraph incidence game, in which Searcher chooses an edge S, Hider chooses a location h, and Searcher wins if $h \in S$.

Search and Recovery. In 2009 Air France Flight AF 447 disappeared on its way from Rio to Paris over the middle of the Atlantic. After several unsuccessful search operations, the wreckage was recovered two years later using Bayesian search [156]. In this approach, the probability distribution of the location of the wreckage (the prior) is updated after a search by a Bayesian factor that compensates for the probability of detection. We can easily adapt SR games to this situation, by interpreting β_x as the probability of detection instead of the probability of successful search. As in the case of rescue sets in the previous example, a search is allowed to continue if β_x is equal to zero. This is Bayesian search against a worst-case prior distribution. If Hider can move once a search is over and before a new search begins, then the game models a manhunt or a hunt for prey. Similar games have been studied by Owen and McCormick [157] and Gal and Casas [158].

7.6. CONCLUSION

We have presented a new type of Search and Rescue game on partially ordered sets. We were able to solve the game in polynomial time in terms of the number of locations for uncorrelated random variables. We showed that the SR game on a tree can be interpreted as a game with correlated random variables, for which the distribution is completely reducible. This game was solved by Lidbetter under the restriction that Bayesian factors are bounded by one from above. If they are bounded by one from below, the solution appears to be more difficult. We conjecture that an optimal search involves a backjumping search. A full solution of the game for general Bayesian factors seems to be out of reach, but we did find general bounds on the value of the game. We hope that SR games on posets and Bayesian networks provide a fruitful avenue of further research and applications.

REFERENCES CHAPTER 7

[7] J.-T. Brethouwer and R. Fokkink. “Search and Rescue on a Poset”. In: *preprint, arXiv:2312.06622, submitted to Naval Research Logistics* (2023).

[134] T. R. Lidbetter. “Search and rescue in the face of uncertain threats”. In: *European J. Oper. Res.* 285.3 (2020), pp. 1153–1160.

[135] A. Agnetis, B. Hermans, R. Leus, and S. Rostami. “Time-critical testing and search problems”. In: *European J. Oper. Res.* 296.2 (2022), pp. 440–452.

[136] A. Agnetis and T. R. Lidbetter. “The Largest-Z-ratio-First algorithm is 0.8531-approximate for scheduling unreliable jobs on m parallel machines”. In: *Oper. Res. Lett.* 48.4 (2020), pp. 405–409.

[137] A. Balaska and J. Rife. “Defining Time-Varying Metrics of Task Conflict in Human/Robot Teams Using Simulated Agents”. In: *2022 IEEE International Symposium on Technologies for Homeland Security (HST)*. IEEE. 2022, pp. 1–7.

[138] P. Leone, J. Buwaya, and S. Alpern. “Search-and-rescue rendezvous”. In: *European J. Oper. Res.* 297.2 (2022), pp. 579–591.

[139] T. R. Lidbetter and Y. Xie. “The search and rescue game on a cycle”. In: *Theor. Comput. Sci.* (2023), p. 114016.

[140] R. P. Stanley. *Enumerative combinatorics*. Cambridge, UK: Cambridge University Press, 1999.

[141] S. Gal. “Search games: a review”. In: *Search theory: a game theoretic perspective* (2013), pp. 3–15.

[142] S. L. Jensen and T. D. Nielsen. *Bayesian Networks and Decision Graphs*. Berlin: Springer, 2007.

[143] J. Pearl. *Probabilistic reasoning in intelligent systems: networks of plausible inference*. Morgan kaufmann, 1988.

[144] S. Alpern and S. Gal. *The theory of search games and rendezvous*. Vol. 55. Springer Science & Business Media, 2006.

[145] F. T. Bruss. “Sum the odds to one and stop”. In: *Ann. Probab.* (2000), pp. 1384–1391.

[146] M. Maschler, S. Zamir, and E. Solan. *Game theory*. Cambridge University Press, 2020.

[147] R. P. Dilworth. “A decomposition theorem for partially ordered sets”. In: *Classic papers in combinatorics* (1987), pp. 139–144.

[148] S. Felsner, V. Raghavan, and J. Spinrad. “Recognition algorithms for orders of small width and graphs of small Dilworth number”. In: *Order* 20 (2003), pp. 351–364.

[149] L. Trevisan. “Combinatorial optimization: exact and approximate algorithms”. In: *Stanford University* (2011).

[150] M. Studeny. *Probabilistic conditional independence structures*. Springer Science & Business Media, 2006.

[151] P. Van Beek. “Backtracking search algorithms”. In: *Foundations of Artificial Intelligence*. Vol. 2. Elsevier, 2006, pp. 85–134.

[152] A. Ramos, P. Van Der Tak, and M. J. Heule. “Between restarts and backjumps”. In: *Theory and Applications of Satisfiability Testing-SAT 2011: 14th International Conference, Ann Arbor, MI, USA*. Springer. 2011, pp. 216–229.

[153] J. D. Esary, F. Proschan, and D. W. Walkup. “Association of random variables, with applications”. In: *Ann. Math. Stat.* 38.5 (1967), pp. 1466–1474.

[154] R. Fokkink, K. Kikuta, and D. Ramsey. “The search value of a set”. In: *Ann. Oper. Res.* 256.1 (2017), pp. 63–73.

[155] E. R. Scheinerman and D. H. Ullman. *Fractional graph theory: a rational approach to the theory of graphs*. Courier Corporation, 2011.

[156] L. D. Stone, C. M. Keller, T. M. Kratzke, and J. P. Strumpfer. “Search for the wreckage of Air France Flight AF 447”. In: *Stat. Sci.* 29.1 (2014), pp. 69–80.

[157] G. Owen and G. H. McCormick. “Finding a moving fugitive, a game theoretic representation of search”. In: *Comput. Oper. Res.* 35.6 (2008), pp. 1944–1962.

[158] S. Gal and J. Casas. “Succession of hide–seek and pursuit–evasion at heterogeneous locations”. In: *J. R. Soc. Interface* 11.94 (2014), p. 20140062.

ACKNOWLEDGEMENTS

The PhD journey is a long road, with many ups and downs. I had the privilege to spend the last four years studying the mathematics I am passionate about, and I look back on many great memories and experiences. In this section, I want to thank the people who helped me create this thesis, either by contributing directly or by making the last four years more enjoyable.

Robbert, I am deeply grateful for your support and guidance throughout my PhD journey. For this thesis, we worked with mathematics from several diverse disciplines, and your wide breadth of knowledge was always both impressive and invaluable. Your own way of approaching academia, infused with humor, has always resonated with me. A good example is when you started a conference talk with an unrelated puzzle. While unconventional, this certainly captured the attention of the entire audience and led to several conversations with other attendees afterwards. It was just one of the many instances where you caused me to reevaluate my perspectives on the established conventions of academia. I am indebted to you for everything you taught me, for the times you advocated on my behalf, and for our thought-provoking discussions on mathematics and academia, often during our journeys to and from Breda. I hope you enjoyed our time tackling intriguing mathematical problems together as much as I have.

Roy, this PhD would not have existed without you setting up the project. Furthermore, your intriguing and motivating ideas seemed unending. You provided many inspiring projects and facilitated countless interesting conversations with people from your extensive network. I am grateful for the opportunity you provided me to visit Northwestern University in Chicago, a trip I thoroughly enjoyed. Additionally, I appreciate you organising a dinner at your house for everyone involved in the project, a gesture that made me feel welcomed and valued. Your ideas and support have been fundamental to this thesis.

Frank, while you were not involved on a daily basis, I always valued your feedback during our yearly progress meetings. Furthermore, I appreciate your awareness and understanding of the challenges faced by PhD students, perhaps best demonstrated in your talk on “what is a good PhD trajectory”. This talk offered a well-thought-out and insightful perspective about the experiences, struggles and personal growth a PhD student undergoes. Your empathy and consideration contributes significantly to the positive and welcoming atmosphere within the applied probability group.

The other members of my committee: Cor Kraaikamp, Henk Schuttelaars, Marie Postma, Herman Monsuur and Martin van Gijzen. Thank you for reading and judging my thesis and for the helpful comments.

All of my coauthors: Bart, Arnout, Anne and the others. Thanks for the enjoyable and fruitful collaborations. Mathematics is better if you can share your passion with other people.

All my fellow PhDs, with whom I walked the PhD road together: Ardjen, Francesco, Hidde, Jasper, Jonathan, Lasse, Marc, Michal, Serena, Vicente, Yanyan. Thank you for the fun PhD events and board game nights. Sharing our PhD stories provided a sense of relief, reminding us that we all face similar challenges. I remember many nice conversations, coffee breaks, lunches and after-work drinks we had. My time at TU Delft would not be half as fun without you.

All my friends outside of academia, both old and new. Thank you for the countless fun times, much-needed distractions, and enjoyable evenings we have shared. Nils, thanks for our numerous late evenings filled with intriguing discussions concerning anything at all. Mitchel, you have been basically part of my family since we were seven. The many friends I made at Abacus, and in particular Dennis, Wietske, Koen, Hidde and Daan. And all those friend groups I have spent evenings online with during the lockdown during COVID-19, when social contact was very limited, thank you for helping me maintain my sanity.

Everyone part of the Twentse Thestrals and the quidditch community, and in particular Boyd, Lies, Anouk, Wouter and Alex. I have always enjoyed our times together on and off the pitch, especially our international tournaments. It always provided great distractions whenever work felt overwhelming. Practicing a sport is a great way to clear your head in times of stress, and it was always fun to meet up with my quidditch buddies again.

My family, I am grateful for you all. Mama, Fred, thank you for all the support you gave me over the years, and always providing a warm and welcoming place to come back home to. Willemien, Anne-Petra, Christa, I am thankful for all the hugs, the enthusiastic conversations about Formula 1 and the mutual help we offer whenever it may be needed. Thessa, Marleen, my nieces who are still too young to read my words of thanks to them, it fills me with joy to see you grow up and learn about the world around you. Papa, thank you for always being interested in my research. It never ceases to amaze me how you seem to actually understand the work I do, which is quite an achievement for someone who did not study mathematics.

And finally, and most importantly, I am profoundly grateful for all the love and support from my partner, Christel. The PhD journey is not always easy, and you were there for me whenever it was needed. Life is better shared with you, and I look forward to our future, together.

Curriculum Vitæ

Jan-Tino Brethouwer was born in Deventer, the Netherlands, on June 22, 1994. He completed his high school education cum laude in 2012 at Baudartius College in Zutphen. During his time in high school, Jan-Tino participated in the Mathematics Olympiad twice, sparking his interest in mathematical puzzles. This led him to decide to study Applied Mathematics at the University of Twente. He acquired his bachelor's degree cum laude in 2016 and his master's degree at the end of 2018. During his master's program, he developed an interest in game theory and wrote his master's thesis in this field. This interest led him to seek a PhD position. In January 2020, he began his PhD research in the Applied Probability group at the Delft University of Technology, which resulted in this thesis.

List of Publications

The following publications underlie this thesis:

- **J.F. Brethouwer**, A. Buijsrogge, and R. Fokkink. "On an equidistribution problem of De Bruijn and Erdős". *Paper in preparation* (2024)
- **J.F. Brethouwer**, B. Van Ginkel, and R. Lindelauf. "General Lotto Games with Scouts: Information versus Strength". *arXiv:2404.05841, submitted to Dynamic Games and Applications* (2024)
- **J.F. Brethouwer** and R. Fokkink. "Search and Rescue on a Poset". *arXiv:2312.06622, submitted to Naval Research Logistics*, (2024)
- M. A. Golden, T. Slough, H. Zhai, A. Scacco, M. Humphreys, E. Vivalt, A. Diaz-Cayeros, K. Y. Dionne, S. KC, E. Nazrullaeva, P. M. Aronow, **J.F. Brethouwer**, A. Buijsrogge, J. Burnett, S. DeMora, J. R. Enríquez, R. Fokkink, C. Fu, N. Haas, S. V. Hayes, H. Hilbig, W. R. Hobbs, D. Honig, M. Kavanagh, R. H. A. Lindelauf, N. McMurry, J. L. Merolla, A. Robinson, J. S. Solís Arce, M. ten Thij, F. F. Türkmen, and S. Utych. "Gathering, Evaluating, and Aggregating Social Scientific Models". *Submitted to Political Analysis* (2023)
- A. Buijsrogge, R. Lindelauf, A. van de Rijt, and **J.F. Brethouwer**. "Self-Organized Social Distancing". *Submitted to the Journal of Mathematical Sociology* (2023)
- **J.F. Brethouwer**, R. Fokkink, K. Greene, R. Lindelauf, C. Tornquist, and V. Subrahmanian. "Rising tension in the Himalayas: A geospatial analysis of Chinese border incursions into India". In: *PloS one 17.11* (2022), e0274999
- **J.F. Brethouwer**, A. van de Rijt, R. Lindelauf, and R. Fokkink. ""Stay nearby or get checked": A Covid-19 control strategy". In: *Infectious Disease Modelling 6* (2021), pp. 36–45

List of Conference Presentations

- *General Lotto Games with Scouts: Information versus Strength*, 2023 LSE-Warwick Workshop on Search Games and Patrolling, London School of Economics, Londen, July 3-4 2023
- *The Value of Information on the Opponent's Strategy: Two-stage asymmetric General Lotto games with Partial Information*, 13th ISDG Workshop, University of Naples "Parthenope", Naples, June 7-9, 2023
- *Understanding the timing of Chinese border incursions into India*, Poster presentation, Conference on AI & National Security, Northwestern Roberta Buffett Institute for Global Affairs, Chicago, Oktober 20, 2022

- *Learning in a Game of Search and Pursuit*, 19th International Symposium on Dynamic Games and Applications, University of Porto, Porto, July 25-28, 2022
- *Stay nearby or get checked: Sociale netwerk analyse als middel tegen Covid-19*, Lunch-colloquia NLDA, December 10, 2020